INVESTIGATION ON MICROSTRUCTURE, MECHANICAL AND DURABILITY CHARACTERISTICS OF RECYCLED AGGREGATE CONCRETE WITH NON-TRADITIONAL SUPPLEMENTARY CEMENTITIOUS MATERIALS

MOHAMMED F. E. ALNAHHAL

FACULTY OF ENGINEERING
UNIVERSITY OF MALAYA
KUALA LUMPUR

2017

INVESTIGATION ON MICROSTRUCTURE, MECHANICAL AND DURABILITY CHARACTERISTICS OF RECYCLED AGGREGATE CONCRETE WITH NON-TRADITIONAL SUPPLEMENTARY CEMENTITIOUS MATERIALS

MOHAMMED F. E. ALNAHHAL

DISSERTATION SUBMITTED IN FULFILMENT OF THE REQUIREMENTS FOR THE DEGREE OF MASTER OF ENGINEERING SCIENCE

FACULTY OF ENGINEERING
UNIVERSITY OF MALAYA
KUALA LUMPUR

2017

UNIVERSITY OF MALAYA

ORIGINAL LITERARY WORK DECLARATION

Name of Candidate: **Mohammed F. E. Alnahhal**

Matric No: **KGA150051**

Name of Degree: **Master of Engineering Science**

Title of Project Paper/Research Report/Dissertation/Thesis ("this Work"):

Investigation on Microstructure, Mechanical and Durability Characteristics of Recycled Aggregate Concrete with Non-Traditional Supplementary Cementitious Materials

Field of Study: **Structural Engineering & Materials**

I do solemnly and sincerely declare that:

(1) I am the sole author/writer of this Work;
(2) This Work is original;
(3) Any use of any work in which copyright exists was done by way of fair dealing and for permitted purposes and any excerpt or extract from, or reference to or reproduction of any copyright work has been disclosed expressly and sufficiently and the title of the Work and its authorship have been acknowledged in this Work;
(4) I do not have any actual knowledge nor do I ought reasonably to know that the making of this work constitutes an infringement of any copyright work;
(5) I hereby assign all and every rights in the copyright to this Work to the University of Malaya ("UM"), who henceforth shall be owner of the copyright in this Work and that any reproduction or use in any form or by any means whatsoever is prohibited without the written consent of UM having been first had and obtained;
(6) I am fully aware that if in the course of making this Work I have infringed any copyright whether intentionally or otherwise, I may be subject to legal action or any other action as may be determined by UM.

Candidate's Signature Date:

Subscribed and solemnly declared before,

Witness's Signature Date:

Name:

Designation:

ABSTRACT

The use of supplementary cementitious materials (SCMs) from industrial and agricultural by-products as a partial replacement for conventional cement and recycled materials by concrete industry is viable alternative to sustainable development. The utilization of SCMs has become more intense in the concrete industry due to their better long-term properties. Thus, the increasing awareness and usage of traditional SCMs, such as fly ash, silica fume and ground granulated blast-furnace slag in concrete have pressured the construction industry to look for alternatives to overcome the concerns over their availability in the future. This research evaluates the performance of concrete that was developed using a high amount of recycled aggregate (RA) incorporated with non-traditional SCMs from agricultural wastes, namely rice husk ash (RHA), palm oil fuel ash (POFA) and palm oil clinker powder (POCP) as alternative sources of SCMs. Unlike previous investigations, that only concentrated on the effect of RA on performance of the concrete, this research presents the mechanical and durability properties of the RHA, POFA and POCP in RA-based concrete as well as their physical and chemical characteristics to draw meaningful relationships between SCMs properties and performance of RA-based concrete. The physical and chemical characteristics of these non-traditional SCMs were measured using techniques such as particle size analysis, scanning electron microscopy (SEM) imaging and x-ray fluorescence (XRF). In addition, SEM imaging and X-ray diffraction (XRD) analysis were used to characterize the microstructure of RA-based concrete containing SCMs. The variables investigated include different percentages of RHA, POFA and POCP at 10%, 20% and 30% cement replacement levels to investigate their effect on fresh and hardened concrete properties, as well as their ability to mitigate degradation resulting from different aggressive media like water absorption, acid attack, sulfate attack, penetration of chloride ions and elevated temperatures. In terms of fresh and hardened properties, the results showed that the 10%

replacement level of cement by RHA produced the highest strength at all ages tested. Although POFA and POCP were found to negatively affect the strengths at an early age, the hardened properties showed improvement after a relatively long curing period of 90 days. However, the 90-day compressive strength of 30 MPa was achieved by using SCMs at levels up to 30%. In terms of durability properties, the results showed that the incorporation of RHA, POFA and POCP up to 30% minimizes concrete deterioration and loss in compressive strength and mass when the specimens were exposed to HCl acid solution. Further, less propagation of micro-cracks caused by expansive ettringite was observed in the case of $MgSO_4$ attack. The RA-based concrete incorporated with sustainable SCMs exhibited significant benefits in terms of depletion of natural resources as well as reduction in CO_2 emissions up to 30% compared to conventional concrete. Overall, the cement required for concrete production can be reduced using agricultural by-products, which are considered as waste materials and thus, the concrete produced using up to 30% of SCMs as a replacement for cement could be considered as more environmentally-friendly concrete.

ABSTRAK

Penggunaan bahan-bahan bersimen tambahan (SCMs) daripada bahan sampingan perindustrian sebagai pengganti separa simen konvensional dan juga penggunaan bahan-bahan kitar semula, khususnya bahan konkrit guna semula sebagai agregat, dalam industri konkrit adalah teknik yang kian berkembang dan mampu menyumbang kepada pembangunan mampan. Penggunaan SCMs yang kini semakin pesat dalam industri konkrit adalah kerana sifat jangka panjangnya yang lebih baik. Oleh itu, kesedaran yang semakin meningkat dan penggunaan SCMs yang konvensional, seperti abu terbang, wasap silika dan 'sanga relau bagas berbutir dalam konkrit telah memberi tekanan kepada industri pembinaan bagi mencari alternatif untuk mengatasi kebimbangan terhadap kebolehdapatan bahan tersebut pada masa hadapan. Kajian ini menilai prestasi konkrit yang telah dibangunkan menggunakan bahan kitar semula beragregat tinggi (RA) yang dipadankan dengan SCMs konvensional dari bahan sampingan perindustrian, iaitu abu sekam padi (RHA), abu bahan api kelapa sawit (POFA) dan serbuk klinker minyak sawit (POCP) sebagai sumber alternatif SCM. Tidak seperti kajian sebelum ini yang hanya tertumpu pada kesan prestasi konkrit berasaskan RA, kajian ini telah mengukur sifat-sifat mekanikal dan ketahanlasakan RHA, POFA dan POCP dalam konkrit berasaskan RA serta ciri-ciri fizikal dan kimianya untuk menghasilkan hubungan yang berfaedah di antara sifat-sifat SCMS dan prestasi konkrit berasaskan RA. Ciri-ciri fizikal dan kimia SCMs konvensional ini diukur meggunakan teknik analisis saiz zarah, pengimejan imbasan mikroskop elektron (SEM) dan x-ray pendarfluor (XRF). Di samping itu, analisis pengimejan SEM dan pembelauan X-ray (XRD) telah digunakan untuk mencirikan mikrostruktur konkrit yang berasaskan RA yang mengandungi SCMs. RHA, POFA dan POCP telah digunakan sebagai SCMs masing-masing pada peratusan 10%, 20% dan 30% tahap penggantian simen bagi mengkaji kesan ke atas sifat-sifat konkrit segar dan keras, serta keupayaan bahan tersebut dalam mengurangkan degradasi yang

disebabkan oleh media agresif yang berbeza seperti penyerapan air, pendedahan kepada asid, pendedahan kepada sulfat, penembusan ion klorida dan suhu yang tinggi. Tambahan pula, kajian perbandingan ke atas pengeluaran CO_2 disebabkan oleh pembuatan bahan-bahan konkrit utama telah dijalankan bersama-sama dengan eko-kecekapan untuk semua campuran. Dari segi sifat segar dan keras, hasil kajian menunjukkan bahawa tahap penggantian 10% daripada simen oleh RHA memberikan kekuatan tertinggi pada semua peringkat masa yang diuji. Walaupun POFA dan POCP didapati memberikan kesan negatif terhadap kekuatan pada masa yang singkat, sifat-sifat kekerasan menunjukkan peningkatan selepas pengawetan masa yang agak lama iaitu 90 hari. Walau bagaimanapun, kekuatan mampatan pada 30 MPa telah dicapai dengan menggunakan SCMs pada tahap 30%. Dari segi sifat-sifat ketahanlasakan pula, hasil kajian menunjukkan bahawa penambahan RHA, POFA dan POCP dapat mengurangkan kemerosotan kekuatan konkrit dan kekuatan mampatan sehingga 30% apabila spesimen didedahkan kepada larutan asid HCl. Seterusnya, didapati kurang berlakunya mikro-retak disebabkan oleh pengembangan ettringite apabila didedahkan kepada $MgSO_4$. Konkrit yang berasaskan RA digabungkan dengan SCMs yang mampan memberikan manfaat yang besar dalam mengurangkan kekurangan sumber asli serta pengurangan pelepasan CO_2 sehingga 30% berbanding dengan konkrit konvensional. Secara keseluruhan, simen yang diperlukan bagi pengeluaran konkrit boleh dikurangkan menggunakan bahan sampingan perindustrian, yang dianggap sebagai bahan buangan; dengan itu, konkrit yang dihasilkan menggunakan sehingga 30% SCMs sebagai pengganti simen boleh dianggap sebagai konkrit mesra alam.

ACKNOWLEDGEMENTS

To my life-coach, my father Dr. Fouad Alnahhal: because I owe it all to you. To my mother, this work could not have happened without your prayers and inspiration. Many thanks for your endless love, support and encouragement!

I would like also to take this opportunity to express gratefulness and thankfulness to my supervisor, Associate Professor Dr. Ubagaram Johnson Alengaram. I sincerely appreciate all the advice, support and invaluable views that he has provided. A special thanks is also extended to my supervisor, Professor Ir. Dr. Mohd Zamin Bin Jumaat for his support. I sincerely wish to thank Associate Professor Dr. Mamoun Alqedra for his precious advice in the research program at its very beginnings. The friendly cooperation and assistance from Dr. Kim Hung Mo is highly appreciated. The financial support provided by University of Malaya under the Equitable Society Research Cluster in the form of a Grant for a study, in which this research forms a part, is gratefully acknowledged.

And finally, but by no means least, a word of thanks also goes to all laboratory technicians for their assistance in ensuring the successful completion of the experiments.

May God Bless You All

TABLE OF CONTENTS

LIST OF FIGURES

LIST OF TABLES

LIST OF SYMBOLS AND ABBREVIATIONS

RA	:	Recycled Concrete Aggregate
$Ca(OH)_2$	:	Calcium Hydroxide
C–S–H	:	Calcium Silicate Hydrate
SCMs	:	Supplementary Cementitious Materials
FA	:	fly ash
SF	:	Silica Fume
GGBS	:	Ground Granulated Blast Slag
OPC	:	Ordinary Portland Cement
RHA	:	Rice Husk Ash
POFA	:	Palm Oil Fuel Ash
POC	:	Palm Oil Clinker
POCP	:	Palm Oil Clinker Powder
CO_2	:	Carbon Dioxide
C&D	:	Construction and Demolition
NA	:	Normal Aggregate
AAV	:	Aggregate Abrasion Value
ACV	:	Aggregate Crushing Value
SEM	:	Scanning Electron Microscopy
XRF	:	X-ray Fluorescence
XRD	:	X-ray Diffraction
LOI	:	Loss on ignition

LIST OF APPENDICES

CHAPTER 1: INTRODUCTION

1.1 Background

In today's fast growing urbanization, environmental sustainability is a significant factor that cannot be ignored by architects, engineers, researchers and, above all, by the construction industry; one of the means to achieve the balance in sustainable development is through the utilization of locally available waste or recyclable materials. The alarming rate of concrete production that consumes a vast amount of natural resources around the world signifies the need for sustainability through the use of alternate materials. Typically, the main ingredients in concrete, namely binders and aggregates constitutes about 10–15% and 60–80% of the total volume, respectively (Wang et al., 2015). By considering these figures for a typical concrete mix proportion, 3.3 billion tonnes of cement and the 22 billion tonnes of aggregates are being consumed annually (Celik et al., 2015), which results in 11 billion cubic meters of ready mixed concrete worldwide, or about four tonnes of concrete per person per year, and this makes concrete one of the largest consumers of natural resources. To put these figures in perspective, a wall of 4 m-width × 70 m-height could be built along the equator using 11 billion cubic meter of concrete that is consumed annually. And, while the construction materials are resource- and energy-intensive in addition to the detrimental impact on environment and sustainability, concrete industry is essential to the nation's civilization.

The quarrying activities around the world to produce coarse aggregates have drastically changed the ecological balance, and hence, it is indispensable to search for sustainable alternatives to replace both the binder and the aggregates that are being used in concrete to reduce the adverse effects due to excessive use of virgin materials. On the contrary, many waste materials are dumped in open fields and underutilized; one such waste, recycled concrete aggregate (RA), obtained from construction and demolition

wastes could be considered a potential recyclable material to replace conventional coarse aggregates.

RA is available in many developed and developing countries due to the demolition of aged buildings and structures; further, in many war-torn countries, many structures have been the target of bombing, and structures have become redundant. In recent years, the utilization of RA from construction and demolition wastes has drawn the attention of researchers as a sustainable and feasible technique to replace the conventional aggregate in concrete (Yuan & Shen, 2011). Nevertheless, many studies concluded that utilization of RA in concrete will affect the hardened and durability properties negatively (Kou & Poon, 2015; Malešev et al., 2010; Sheen et al., 2013). However, the current trend involves using locally available industrial and agricultural waste ashes from the residues of rice and palm oil industries as SCMs to enhance the mechanical and durability performance of RA concrete. A previous investigation showed that the properties of RA can be enhanced by reducing the adhered mortar content and improving its quality (Shi et al., 2016).

The excessive use of natural resources could be significantly reduced through the use of SCMs and this would ensure its sustainability for future needs. It is anticipated that in future, due to concerns over the availability of the traditional SCMs, the utilization of other sustainable sources as SCMs is essential. The use of waste materials as SCMs in RA concrete would be an interesting area to be explored. The abundantly available waste materials can be utilized in concrete as a replacement for cement or filler materials to achieve industrial ecology. In most of the cases, this method does pave the way for systematic waste treatment and disposal method to avoid environmental pollutions.

1.2 Problem statement

The disposal of construction and demolition wastes is one of the challenges faced by many developed and developing nations due to the scarcity of open lands and the limited size of municipal dumping sites to accommodate large quantities of debris and unprocessed construction wastes. The random and uncontrolled disposal of construction and demolition wastes create several environmental impacts. The RA constitutes the major portion of the construction and demolition wastes, with over 900 million tonnes generated annually in the United States, Europe and Japan (Sadati et al., 2016). This results in huge quantities of RA being heaped as piles of rocks, and thus, RA has a role to play in sustainable development; RA has become increasingly important in the field of construction as an alternative to primary (natural) aggregates.

On the other hand, the practice of using SCMs has become more intense in the concrete industry due to their better long-term properties. Hence, concerns over the plentiful availability of the traditional SCMs led to contemplation about other sustainable sources as pozzolanic materials. For instance, the total amount of fly ash that can be used as SCM is about 800 million tonnes, which is less than half of the amount needed annually around the world (Celik et al., 2015). And, while concrete industry is expected to expand at a faster rate over time, the current trend involves using locally available industrial and agricultural waste ashes from the residues of rice and palm oil industries as alternative SCMs.

The rice industry generates millions of tonnes of rice husk during milling of paddy rice, which comes from the fields. It was estimated that about 156 million tonnes of rice husk are generated globally, of which 2.14 million tonnes in Malaysia annually; it is estimated that 18–22% of rice husk by weight will be converted into RHA after burning in boilers (FAOSTAT, 2012; Rozainee et al., 2008; USDA, 2014). Thus, rice husk has

the potential to produce 26–34 million tonnes of RHA containing over 90% (up to 95%) amorphous silica that could be used as an alternative SCM (Gursel et al., 2016). The commercial viability of RHA is not prevalent, and hence, dumping of RHA in the vicinity of the agricultural lands is a considerable threat to the environment. Hence, research works needed on the utilization of RHA as sustainable SCM in different types of concrete. Furthermore, the amount of palm oil residues produced globally per year is about 184 million tonnes, with 53 million tonnes in Malaysia, the world's second largest producer and exporter of palm oil; and it is estimated that the expansion of palm oil plants would increase by 5% every year (Mohammed et al., 2011; Yusoff, 2006). The resulting ash after combustion, i.e., POFA, is 5% by weight of the original solid materials. According to these statistics, the annual production of POFA is about 10 million tonnes around the world.

From another perspective, concrete industry accounts for 5-7% of all man-made carbon dioxide (CO_2) emissions (Benhelal et al., 2013). Consequently, the problem is likely to get worsened by 2025 as about 3.5 billion tonnes of CO_2 is expected from the manufacturing of cement (Shi et al., 2011). Further, it is predicted that by 2050 the concrete production will reach four times the level as that of 1990 (Damtoft et al., 2008). This progressive emissions of CO_2 have reached to an alarming level and are expected to be expanded even at a faster rate. According to Collins (2010), about 820 kg of CO_2 is being emitted for every 1000 kg of cement manufactured. Around half of these emissions are from decarbonation process in which CO_2 is lost from the limestone ($CaCO_3$) to produce calcium oxide (CaO) and the remaining is from the fuel used to fire the kiln at temperature of 1500 °C (Cao et al., 2016).

From technical point of view, there are some problems related to the incorporation of RA into new concrete represented by reduction in strength and durability properties.

Moreover, there is a consensus by researchers that the broad use of RA in concrete is hindered by its ability to withstand different aggressive environments, such as water absorbency, chemical attacks and exposure to seawater (Debieb et al., 2010; Somna et al., 2012). The relatively higher porosity of RA compared with normal aggregate makes the RA-based concrete more susceptible to damage when exposed to aggressive solutions. Hence, the capability of concrete members to resist various aggressive environments is a key durability issue that affects the life cycle performance of concrete structures. On the other hand, the incorporation of SCMs was found to improve the mechanical and durability properties of RA-based concrete significantly due to the pozzolanic mechanism.

In view of that, the worldwide changes are causing considerable uncertainty for the future availability and quality of materials needed for concrete. Thus, there is an essential need to search for sustainable alternatives of the main ingredients that are being used in concrete in order to achieve a sufficient reduction level of CO_2 emissions along with the depletion of natural resources.

1.3 Research objectives

This research was conducted with the long-term aim of developing sustainable and high-quality materials for use as alternative SCMs. The study focuses on the microstructure, mechanical and durability properties of concrete made of 100% recycled concrete aggregate incorporated with locally available non-traditional supplementary cementitious materials obtained from by-products of two different industries.

The main objectives were:

1. To evaluate the effect of recycled concrete aggregate (RA) as coarse aggregate on the engineering performance of concrete.
2. To study the effect of three supplementary cementitious materials, namely RHA, POFA and POCP on the fresh and hardened properties of RA-based concrete.
3. To assess the durability performance of RA-based concrete incorporated with supplementary cementitious materials and exposed to aggressive environments.
4. To investigate the microstructure characteristics of RA-based concrete containing supplementary cementitious materials.

1.4 Scope of the work

This experimental investigation evaluates the effect of non-traditional SCMs, namely RHA, POFA and POCP on concrete made from 100% RA. Using a total of 11 concrete mixes, the effect of these SCMs on the fresh and hardened properties including, workability, compressive strength, ultrasonic pulse velocity, splitting tensile strength, flexural strength and modulus of elasticity of RA-based concrete was determined. Moreover, SCMs-RHA, POFA and POCP, were utilized as partial substitution of cement to enhance the resistance of RA-based concrete against aggressive chemical attacks. The

ability of RA-based concrete to withstand the natural aggressive environments was simulated using hydrochloric acid (HCl) and magnesium sulfate ($MgSO_4$) solutions. Moreover, microanalysis was considered, since the durability properties are related to the microstructure of concrete. Further, the influence of abovementioned SCMs on water absorption, chloride-ion penetration and electrical resistivity of RA-based concrete was determined. Furthermore, as a principle of the research, a comparative study on CO_2 emissions due to the manufacture of the major concrete materials was carried out along with the eco-strength efficiency among all mixtures based on the CO_2 emissions and compressive strength.

The variables investigated in this research include the percentage of cement replacement by RHA, POFA and POCP (0%, 10%, 20%, and 30%), in addition to the whole replacement of crushed granite aggregate by RA. Further, the tests were conducted for a period up to 120 days, since the use of SCMs is commonly associated with concrete properties at later ages.

1.5 Research significance

The incorporation of sustainable SCMs could reduce cement production and consequently this would further reduce the energy consumption and greenhouse gas emissions; as such, the natural resources would be saved and this opens up avenue for more sustainable construction materials and method. Sustainable sources of SCMs including RHA, POFA and POCP have been utilized by researchers in development of normal, high-strength and lightweight concretes (Ahmmad et al., 2017; Chao-Lung et al., 2011; Mo et al., 2017); however, the utilization of these SCMs has been limited to some properties and very few literatures are available. Moreover, previous investigations dealt with the effect of traditional SCMs, such as fly ash and silica fume on the durability properties of RA-based concrete (Corinaldesi & Moriconi, 2009; Kou & Poon, 2013;

Lima et al., 2013), and there is a limited study on the properties of RA-based concrete incorporating POFA (Tangchirapat et al., 2012); however, there are no research works carried out on the behavior of RA-based concrete incorporating RHA and POCP as SCMs for chemical attacks. Hence, this research work is significant as the utilization of non-traditional SCMs in the development of RA-based concrete is attempted and various properties on materials, concrete, durability and micro-structure have been investigated and reported.

CHAPTER 2: LITERATURE REVIEW

2.1 Introduction

Studies were carried out on the utilization of waste materials, construction and demolition waste management, engineering and mechanical properties of RA concrete, durability features of RA concrete and the effect of supplementary cementitious materials in concrete. These aspects are important to detail out the required scope of study for this research.

2.2 Sustainability in concrete industry

Sustainability and sustainable development have become key issues in engineering profession. The most widely accepted definition of sustainable development was developed in 1987 by the World Commission on Environment and Development, and defined it as, "meeting the needs of the present without compromising the ability of future generations to meet their own needs" .

One of the main goals in achieving sustainable construction materials is to reduce the overuse of virgin materials used to produce cement, coarse and fine aggregates. Every year, millions of tons of agricultural wastes are being returned to the environment in the form of harmful solid, liquid, and gaseous waste materials, and most of these wastes are unutilized or underutilized; these wastes cause environmental issues due to storage problem and pollution to the surrounding field. In recent years, there is an increasing awareness on the quantity and diversity of solid waste generation and its impact on the human health. Consequently, the increasing concern about the environmental consequences resulting from waste disposal has led researchers to investigate the utilization of the wastes as potential construction materials. Among the possible solutions favoring greater environmental sustainability in the construction industry is through the

utilization of the construction and demolition wastes alongside the use of agricultural by-products to produce new concrete.

2.3 Construction and demolition waste management

The growth in the utilization of construction and demolition (C&D) wastes, especially after the World War II, is quite impressive (Khalaf & DeVenny, 2004). Since then, the investigation works on the demolition of aged structures and the construction of new ones has become a frequent phenomenon in a large part of the world due to change of purpose, structural deterioration, rearrangement of a city and natural disasters. According to statistical data, C&D wastes normally make up to 10–30% of the waste received at landfill sites around the world. In many densely populated countries of Europe, where disposal of debris is becoming more and more difficult, only 50 million tonnes (28%) is reused or recycled from the 180 million tonnes of C&D wastes that generated in the European Union annually, and the remaining 130 million tonnes (72%) sent to the landfills, as shown in Table 2.1 (Matias et al., 2013).

In the United States, approximately 200–300 million tons of building-related C&D debris is generated every year, out of which only 20–30% is recycled. In United Kingdome, it was reported that every year around 70 million tons of C&D materials ended up as wastes. In Australia, C&D wastes account for 16–40% of the total solid waste generated. In Hong Kong, about 2900 tons of C&D wastes were received at landfills per day in 2007. China produces 29% of the world's municipal solid wastes each year, of which construction activities contribute for nearly 40% (Meyer, 2009; Yuan & Shen, 2011).

Table 2.1: Volume of C&D wastes and recycling (Matias et al., 2013)

Member state	C&D wastes in million ton	% Reused or recycled	% Landfilled
Germany	59	17	83
United Kingdom	30	45	55
France	24	15	85
Italy	20	9	91
Spain	13	<5	>95
Netherlands	11	90	10
Belgium	7	87	13
Austria	5	41	59
Portugal	3	<5	>95
Denmark	3	81	19
Greece	2	<5	>95
Sweden	2	21	79
Finland	1	45	55
Luxembourg	1	<5	>95
Total	**180**	**28**	**72**

According to the statistics, there is about 1.55 billion tonnes of C&D wastes generated in China every year (Li et al., 2017). In Hong Kong, the construction industry produces about 37,000 tonnes of construction and demolition (C&D) waste every day, which is roughly four times higher than that of municipal solid waste. But the shortage of land for new landfills and the end of major land reclamation projects in the near future have setup alarm in Hong Kong to find alternative uses of the C&D waste (Poon et al., 2004a).

In Malaysia, the construction industry generates a lot of construction waste which cause significant impacts on the environment and increasing public concern in the local community. Thus, the minimization of construction waste has become a pressing issue.

In the Malaysian construction industry, there is limited data on the current amount of solid waste generation. In 2005, the total solid waste generated in Malaysia was around 7 million tonnes at a rate of 19,100 tons per day (Siwar, 2008). Moreover, Hassan et al. (1998) reported that the C&D waste forms about 28% of the total solid waste in the Central and Southern region of Malaysia. These data reveal that the C&D wastes cause significant impacts on the environment and increasing concern in the local community due to the generation of substantial construction wastes (Mahayuddin et al., 2008). A study done by Begum et al. (2006) of the project sites in Malaysia, construction waste materials contain a large percentage of reusable and recyclables. Estimated 73% of the waste materials in the project site is reused and recycled. Table 2.2 shows the amount of reused and recycled waste materials on the site. The highest amount of reused and recycled materials is concrete and aggregate, comprising 67.64% of the total reused and recycled material. The practice reuse and recycling of construction waste materials is common on the site of one of the project sites. Furthermore, reuse and recycling of waste have been promoted in order to reduce waste and protect the environment.

Table 2.2: Amount of reused and recycled construction waste materials on the site in Malaysia (Begum et al., 2006)

Construction waste material	Amount of waste generated (tons)	Amount of reused and recycled	
		Tonnage	Percentage
Soil and sand	7,290	5,400	27.33
Brick and blocks	315	126	0.64
Concrete and aggregate	17,820	13,365	67.64
Wood	1,350	810	4.0
Metal products	225	54	0.27
Roofing materials	54	5.4	0.03
Total	**27068.4**	**19760.4**	**100**

Adverse impacts of generation of C&D wastes are multiple, including running up a large amount of land resources for waste landfilling and harming the surroundings by hazardous pollution. As C&D wastes are unavoidable and ‘‘zero waste’’ is not practical, research pursuing solutions to reuse the C&D wastes has been conducted in the past few decades.

2.4 Recycled aggregate from C&D wastes

Recycled concrete aggregate (RA) constitutes the major portion of the C&D waste. RA is available in many developed and developing countries due to demolition of aged buildings and structures; further in many war torn countries, many structures have been target of bombing and structures have become redundant. In recent decades, significant contribution by researchers has been conducted concerning the utilization of RA as a sustainable and feasible technique to replace the normal aggregate (NA) in concrete (Yuan & Shen, 2011). Nevertheless, there are technical problems related to the incorporation of RA into new concrete represented by reduction in strength and durability properties (Kou & Poon, 2015; Malešev et al., 2010; Sheen et al., 2013).

2.4.1 Properties of recycled concrete aggregate

The RA consists of two phases: the original stone particles and the attached mortar, as shown in Figure 2.1 (De Juan & Gutiérrez, 2009; Thomas et al., 2013). The original stone particles were the aggregate that used in the parent concrete; the attached mortar is comprised of fine aggregate and cement paste. RA is generally angular in shape because of the crushing process required to make the proper sizes for use as an aggregate. The attached mortar also results in the RA being more porous than normal aggregate (NA). The quality of RA mainly depends on the strength of the parent concrete from which it is obtained (Kou & Poon, 2015). Generally, the volume of the residual mortar in RA varies according to the size of aggregate. De Juan and Gutiérrez (2009) applied different

methods to determine the adhered mortar content. They concluded that the old mortar content vary depending on the test applied; it was 25 – 70% for treatment with hydrochloric acid solution and 40 – 55% for thermal treatment. In addition, they revealed that the amount of mortar attached to fine fraction is higher than to coarse fraction: wide ranges of 33 – 55% for 4/8 mm fraction and 23 – 44% for 8/16 mm fraction have been obtained. Poon et al. (2004b) reported that RA extracted from waste concrete consists of 65 – 70% aggregates and 35 – 30% of cement paste by volume. The latter is more porous than the former. Consequently, RA is mostly inhomogeneous, less dense and has more voids as compared to NA. Typical crushed granite aggregate has a density of approximately 2600 – 2650 kg/m^3 and a water absorption capacity of approximately 1%. For RA, due to the presence of a large amount of adhered mortar, their density may vary from 2200 to 2400 kg/m^3 and the water absorption capacity may vary from 5 to 15%. The variations in density and water absorption capacity are due to the differences in properties of the parent concrete from which the RA is derived.

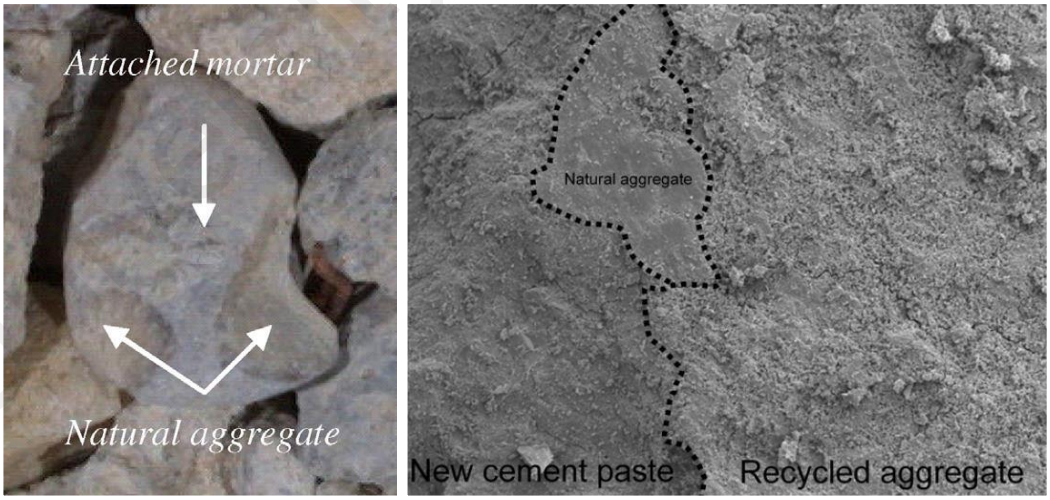

Figure 2.1: The original stone particles and the attached mortar in RA (Thomas et al., 2013)

Table 2.3 shows the basic physical properties of RA compared to NA (Safiuddin et al., 2013). It can be seen that the physical properties of RA are generally worse than those of NA due to the presence of weak and loose attached mortar on its surface, which makes it

porous. NA generally has low water absorption due to low porosity, but the attached mortar on RA has greater porosity, which allows the aggregate to hold more water in its pores than NA. McNeil and Kang (2013) reported water absorption values of 0.5 – 1 % for NA and 4 – 4.7 % for RA in the saturated surface dry condition. However, the magnitude of the effects varies with the quality of the parent concrete as well as the amount of old mortar found in RA (Andreu & Miren, 2014). It was reported that the water absorption of RA increases with the decrease in strength of parent concrete from which the RA is derived, while it decreases with the increase in maximum size of aggregate (Padmini et al., 2009).

Table 2.3: Basic physical properties of NA and RA (Safiuddin et al., 2013)

Physical property	Normal coarse aggregate	Recycled concrete aggregate
Shape and texture	Well rounded, smooth (gravels) to angular and rough (crushed rock)	Angular with rough surface
Specific gravity (saturated surface-dry based)	2.4 – 2.9	2.1 – 2.5
Bulk density (compacted) (kg/m^3)	1450 – 1750	1200 – 1425
Absorption (weight %)	0.5 – 4	3 – 12
Pore volume (volume %)	0.5 – 2	5.0 – 16.5

The mechanical properties of RA are, generally, inferior compared to those of NA. For instance, the aggregate abrasion value (AAV) of RA ranging from 20% to 45%, which are higher than those of NA (López-Gayarre et al., 2009). Moreover, the aggregate crushing value (ACV) provides an indication of the aggregate strength. The lower the value, the stronger is the aggregate. According to Yehia et al. (2015), the ACV of RA was found to be in the range of 20-30% which is worse than the value of NA. In addition, the

results by Jain et al. (2015) showed that the crushing and impact values of RA were 43-48% and 9-20% higher than NA, respectively.

2.4.2 Effect of recycled concrete aggregate on concrete properties

Extensive works have been conducted on the mechanical properties of concrete made with RA. In general, it was found that the mechanical properties of RA-based concrete are not as high as concrete made with NA. Figure 2.2 illustrates the schematic diagrams of NA- and RA-based concretes, showing the basic difference of matrix in between two concrete (Behera et al., 2014). The cement matrix is responsible for limiting the properties of RA-based concrete. Therefore, it needs more attention regarding the performance of concrete when RA is to be used. The results obtained by Akça et al. (2015) showed that utilization of concrete made from 100% RA is limited, due to the reduction in the hardened strength ranging from 15 – 25%. Moreover, after reviewing the effect of RA on concrete, Safiuddin et al. (2013) found that the reduction in the strength of concrete made from RA and attributed it to the existing porous mortar that is adhered on its surface, which has higher water absorption.

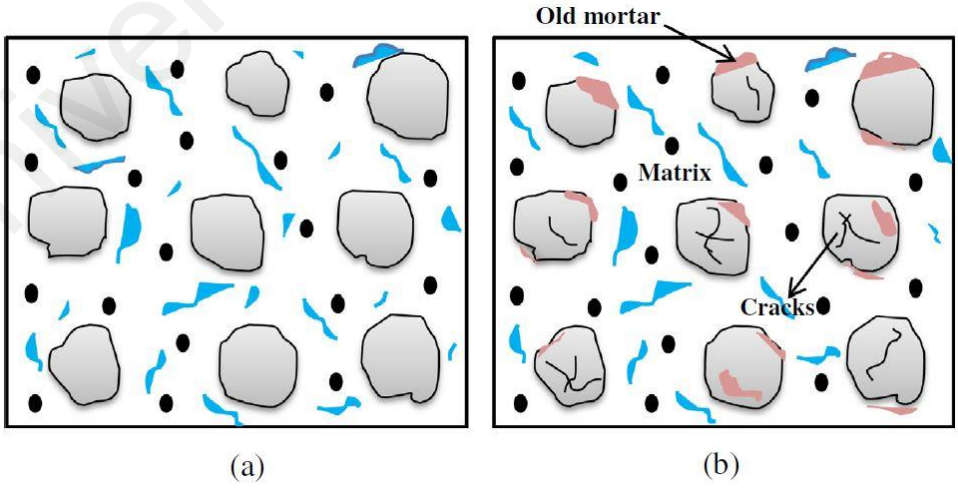

Figure 2.2: Difference between matrices of (a) NA-based concrete and (b) RA-based concrete (Behera et al., 2014)

2.4.2.1 Fresh properties

The high water absorption of RA is a main factor affecting the fresh properties and the workability of concrete mixture. A study by Akça et al. (2015) revealed that the slump of concrete composed of RA is lower than conventional concrete composed of NA, and the variation in slump depends on the ratio of replacement. Malešev et al. (2010) concluded that concrete with 100% RA requires about 20% more water quantity to obtain same workability in comparison to conventional concrete. Safiuddin et al. (2011) showed that the decrease in slump was higher at a greater RA content. Matias et al. (2013) revealed that the use of aggregate with rounder shape and texture has indeed influence on the concrete's workability, by comparison with angular particles, which the latter require more cement paste and water to achieve an adequate workability.

2.4.2.2 Mechanical properties

The previous studies showed a consensus on the mechanical properties of RA-based concrete; the higher the level of substitution, the lower the strength. The effect of RA on the mechanical properties of concrete depends considerably on its source, content and physical properties. As a general principle, up to 30% of NA could be replaced by RA without significantly affecting the mechanical properties of concrete. Further, the reduction in the strength of concrete made of RA attributed to the existing porous old mortar found in RA particles, which has inferior properties than NA (Safiuddin et al., 2013). Moreover, the results obtained by Akça et al. (2015) concluded that utilization of 100% RA to produce new concrete is limited, due to the reduction in the hardened strength ranging from 15% to 25%.

In terms of compressive strength, the investigation done by Seara-Paz et al. (2014) showed that the use of RA at replacement levels of 20%, 50% and 100% decreases the compressive strength by 11%, 18% and 31%, respectively. However, Andreu and Miren

(2014) concluded that the fully replacement of NA by RA would be possible when RA produced from original concrete with a minimum compressive strength of 60 MPa. Similar concept observed by Etxeberria et al. (2007), when they reported that the weakest point in RA-based concrete made from parent concrete with a strength of 45–60 MPa is determined by the strength of the RA itself.

Investigation into long-term mechanical properties of concrete performed by Kou and Poon (2013) compared NA- and RA-based concrete with 100% RA replacement level. They observed that the compressive strength gain of RA-based concrete over 5 years of curing produced a 62% increase in compressive strength compared to only a 34% increase in compressive strength of NA-based concrete. A 65% splitting tensile strength increase in RA-based concrete over 5 years was also reported, compared to only a 37% increase in NA-based concrete, as shown in Table 2.4. This increase in strength was attributed to the possible long-term hydration of un-hydrated cement in the RA particles.

Table 2.4: Long-term mechanical properties of RA-based concrete (Kou & Poon, 2013)

Mechanical property	Mixture type	28 days (MPa)	5 years (MPa)	Gain from 28 days to 5 years (%)
Compressive Strength	100% NA	43.8	58.9	34
	100% RA	34.3	55.4	62
Splitting Tensile Strength	100% NA	2.43	3.32	37
	100% RA	2.26	3.64	65

The results obtained by Thomas et al. (2013) showed that concretes prepared with 20%, 50% and 100% of RA have relative tensile strength values of 90%, 85% and 80%, respectively, compared to corresponding normal concrete. Moreover, Tabsh and Abdelfatah (2009) summarized that the RA-based concrete made from parent concrete

with compressive strength of 50 MPa or higher is as strong as the normal concrete in terms of splitting tensile strength. Sheen et al. (2013) reported 10–23% reduction in the flexural strength for the specimens prepared with RA when compared to control specimens with NA. The lower flexural values attributed to the weak nature of the RA, which allow the aggregate to fail faster compared to the NA.

It was reported that the modulus of elasticity of RA-based concrete is typically 10 – 33% lower than that of normal concrete (Anderson et al., 2009). The relatively lower modulus of elasticity of the attached mortar compared to the original stone particles caused the reduction in the modulus of elasticity. Table 2.5 summarizes the effect of RA on the properties of concrete (Safiuddin et al., 2013).

Table 2.5: Effect of RA on concrete properties (Safiuddin et al., 2013)

Property	Range of changes
Dry density	5 – 15% less
Compressive strength	0 – 30% less
Splitting tensile strength	0 – 10% less
Flexural strength	0 – 10% less
Bond strength	9 – 19% less
Modulus of elasticity	10 – 45% less
Porosity	10 – 30% more
Permeability	0 – 500% more
Water absorption	0 – 40% more
Chloride penetration	0 – 30% more
Drying shrinkage	20 – 50% more
Creep	30 – 60% more
Thermal expansion	10 – 30% more

2.4.2.3 Durability properties

The durability of concrete is defined as the ability of concrete to withstand chemical attack, and external environmental and physical actions. The durability of concrete is greatly influenced by its permeability behavior. A concrete with low permeability has better durability performance. Lower permeability means lower content of voids in concrete, and therefore water and some other corrosion agents cannot penetrate easily into concrete.

While the durability of RA-based concrete has not been as extensively studied as the mechanical properties, there have been efforts put forth to evaluate the long term durability properties of the RA-based concrete, such as water absorption, chloride-ion penetration, acid attack and sulfate attack.

(a) ***Water absorption***

The water absorption capacity of concrete is an important property, which provides data on the water accessible porosity of concrete; concrete with high water absorption capacity is less durable in aggressive environmental conditions. Since the water absorption capacity of RA is higher than that of NA, concrete containing RA has higher water absorption capacity than conventional concrete. The water absorption is evaluated by an immersion test, which measures the open porosity of concrete specimens, and by capillarity test, which measures the capillary water absorption due to a difference in pressure occurred between the liquid on the concrete's surface and inside the capillary pores of concrete (De Brito & Saikia, 2013).

Kwan et al. (2012) observed an increase in water absorption capacity of concrete as the replacement level of NA by RA increased, as shown in Figure 2.3. They state that the replacement of 30 % by weight of NA by RA led to a water absorption capacity below 3 %, i.e. a concrete considered to have low water absorption capacity. For an 80 %

replacement, the water absorption capacity of concrete was 2.2 times higher than that of conventional concrete. Rao et al. (2011) also observed a gradual increase of water absorption capacity of concrete with the incorporation of RA to replace NA due to the higher water absorption capacity of RA, which was about 3.5 times higher than that of NA.

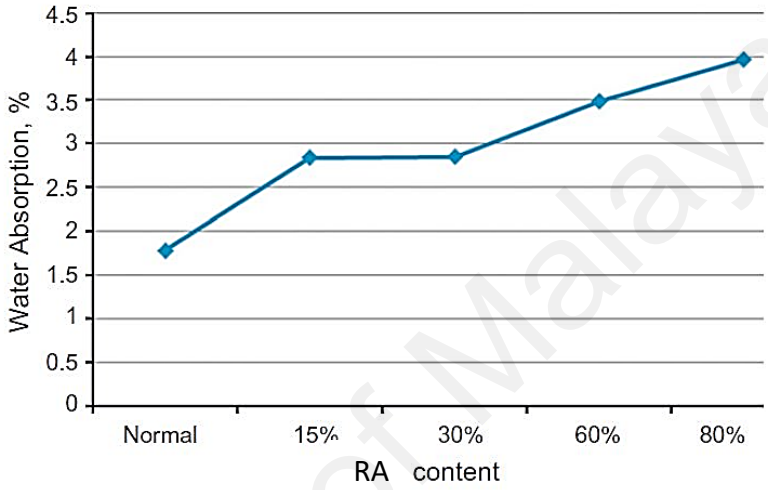

Figure 2.3: Water absorption of concrete at various percentages of the RA (Kwan et al., 2012)

(b) ***Chloride permeability***

The ingress of chloride ions is considered as one of the most common form of aggressive attacks on reinforced concrete, which leads to corrosion of reinforcing steel and subsequent reduction in strength, serviceability, and aesthetics of the structure (Shi et al., 2012). Thus, the ability of concrete members to withstand the transport of chloride ions into the level of the rebar depends on the interconnectivity of the concrete pore structure. It is interesting to know that the pH stability of hydration products, e.g. $Ca(OH)_2$ and C–S–H, is ranging from 10-13 (Kutchko et al., 2011). At this pH level, the rate of the corrosion reaction will be negligible. However, penetration of chloride ions through capillary pores at the rebar level promotes the formation of hydrochloric acid and amplifies decalcification by forming soluble calcium chloride, which in turn leads to fall

in pH to a level at which the oxidation reaction for corrosion may occur (Wong et al., 2010). Therefore, this suggests that the use of pozzolanic materials could be effective to block the ingress path of chloride ions.

The determination of diffusivity of chloride ions through concrete can provide data on the permeability performance of concrete. Lower chloride permeability is desirable for durable concrete structures. Several studies were undertaken to understand the chloride permeation performance of concrete containing RA (Corinaldesi & Moriconi, 2009; Kou & Poon, 2012). In several researches, it was reported that the incorporation of RA in concrete increases the chloride permeability of concrete; however, some results also indicate negligible influence of RA incorporation on the chloride permeability performance of concrete (De Brito & Saikia, 2013). Andreu and Miren (2014) studied the chloride ion penetration at replacement levels of 20, 50 and 100% for three types of recycled concrete (RC) produced from parent concrete with compressive strength of 40, 60, and 100 MPa. They showed that the resistance to chloride ion penetration decreases as the RA content increases. In addition, they classified the results following the ASTM C1202 corrosion ranges between very low and moderate risk of corrosion, as shown in Figure 2.4. The reference conventional concrete (CC) allowed for the lowest passing of chloride ions through the specimens, while the concrete produced with 20% and 50% of RA obtained results on the limit of very low corrosion range, the total replacement of series 60 MPa and 40 MPa achieved values of low and moderate corrosion limit, respectively.

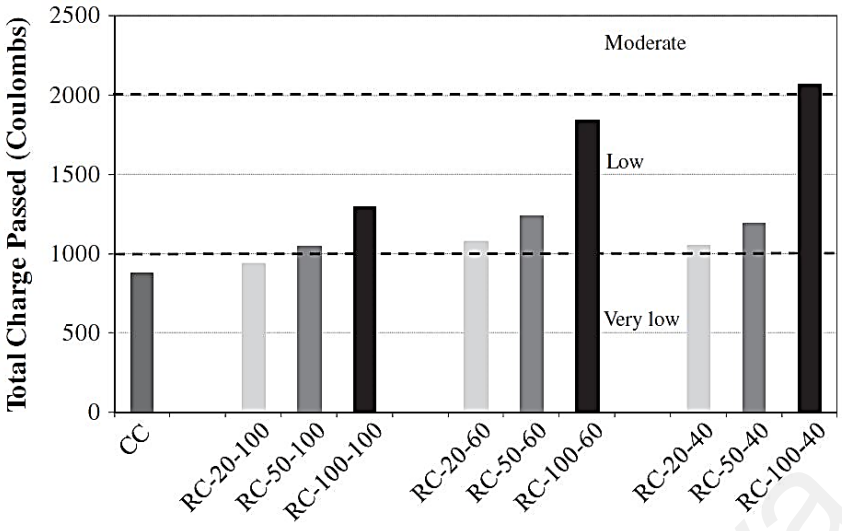

Figure 2.4: Chloride-ion penetration of RA-based concrete and ASTM corrosion ranges (Andreu & Miren, 2014)

(c) ***Acid resistance***

The alkaline nature of Portland cement concrete renders it more susceptible to acid attack (Pacheco-Torgal et al., 2008). The mechanism of HCl acid attack can be explained by the progressive neutralization of the alkaline nature of the cement matrix via the decomposition of hydration products, e.g. $Ca(OH)_2$ and C–S–H, forming soluble calcium chloride ($CaCl_2$) salt and water, as explained in Equation 2.1 and Equation 2.2 (Donatello et al., 2013). According to Beddoe and Dorner (2005), the pH-stabilities of $Ca(OH)_2$ and C–S–H found in the deteriorated zones were about 12.6 and 10.5, respectively. These compounds will be successively decomposed until a silica gel residue is obtained at pH of below 2 (Yuan et al., 2013). Thus, the decalcification of C–S–H could proceed after the depletion of $Ca(OH)_2$.

$$HX + Ca(OH)_2 \rightarrow CaX + H_2O \quad (2.1)$$

(Acid) + (Calcium Hydroxide) → (Calcium Salt) + (Water)

$$HCl + C\text{–}S\text{–}H \rightarrow CaCl_2 + Si(OH)_4 + H_2O \quad (2.2)$$

Nuaklong et al. (2016) revealed that the RA-based concrete has lower acid resistance than that of NA-based concrete. This was due to the high water absorption, volume of permeable voids, and sorptivity of RA-based concrete compared to those of NA-based

concrete. In addition, the calcium compound in RA particles reacted with acid solution and resulted in more deterioration. The permeable voids found in the old adhered mortar on the RA particles allow the entry of acid ions, which in turn degrade the concrete and decrease its mechanical properties due to chemical reactions between acid ions and hydration products (Nuaklong et al., 2016; Yuan et al., 2013).

(d) ***Sulfate resistance***

The $MgSO_4$ attack mechanism normally starts with the reaction between hydration products and $MgSO_4$ ions that penetrate by absorption property from external sources to form $Mg(OH)_2$, magnesium silicate hydrate and gypsum ($CaSO_4 \cdot 2H_2O$), as shown in Equation 2.3 (Heikal et al., 2015). The increased concentration of gypsum promotes the conversion of tricalcium aluminate (C_3A) to ettringite, as shown in Equation 2.4 (Li et al., 2014). The progressive formation of ettringite, which is inherently expanding, leads to generate stresses beyond the capability of the tensile strength of the cement matrix (Müllauer et al., 2013), which in turn causes subsequent cracks and reduction in the strength (Bizzozero et al., 2014).

$$MgSO_4 + Ca(OH)_2 + 2H_2O \rightarrow Mg(OH)_2 + CaSO_4 \cdot 2H_2O \text{ (gypsum)} \quad 2.3$$

$$\text{Tricalcium aluminate } (C_3A) + \text{gypsum} \rightarrow \text{ettringite} \quad 2.4$$

A few research are available on the evaluation of the resistance of RA-based concrete to sulfate attack. Limbachiya et al. (2012) reported that expansions in mortar bars due to sulfate attack increased as the replacement ratio of RA increased. Dhir et al. (1999) showed that expansions of concrete containing RA up to 30% were similar to that without RA. However, about 52% increase in expansion recorded for 50% replacement level and a 68% increase in expansion recorded for 100% replacement level. Moreover, the voids found in RA allow the ingress of sulfate ions in to the pore structure and react with the

hydration products to form gypsum and ettringite, which are expansive in nature, leading to the deterioration of concrete's surface (Hwang et al., 2013; Somna et al., 2012).

2.5 Supplementary cementitious materials (SCMs)

2.5.1 Historical background

The roots of current widespread use of SCMs in the construction industry return to the Antique world, especially to the ancient Greeks between 750 B.C. and 600 B.C., where the volcanic ash materials incorporated with hydraulic lime to create a cementitious mortar. The Greeks passed this knowledge to the Romans, who constructed engineering marvels, such as the Roman aqueducts and the Coliseum, which still stand today (Cultrone et al., 2005). SCMs contribute to the properties of hardened concrete through hydraulic or pozzolanic activity. The word "pozzolan" was actually derived from a large deposit of Mount Vesuvius volcanic ash located near the town of Pozzuoli, Italy.

2.5.2 Classification of SCMs

SCMs can be used either as an addition to the cement or as a replacement for a portion of the cement. Most often, the SCMs is used to replace a portion of the cement content for economical or property-enhancement reasons. In addition, SCMs can be divided into two categories based on their type of reaction: hydraulic or pozzolanic, as shown in Figure 2.5. Hydraulic materials react directly with water to form cementitious compounds. On the other hand, the ASTM C125 defines the pozzolanic material as 'a siliceous or siliceous and aluminous material that itself possess little or no cementitious value but will, in finely divided form and in the presence of water, chemically react with calcium hydroxide at ordinary temperatures to form compounds possessing cementitious properties'.

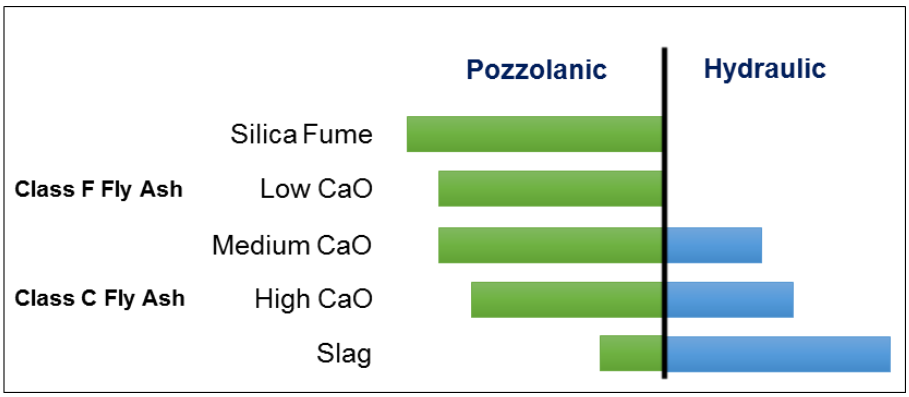

Figure 2.5: Types of reactions of various types of SCMs

From another perspective, SCMs can be classified based on: (i) origin, (ii) chemical compositions and (iii) particle properties. The first mentioned, namely basing the classification on the origin, provides a good way of creating a classification system. It should be noted that the term 'origin' does not refer to the geological location of the material, but rather the way it is obtained or how it forms. Therefore, SCMs can be divided into two broad classes: natural and artificial SCMs, as shown in Figure 2.6 (Snellings et al., 2012).

Natural occurring SCMs can be further divided into two classes: volcanic materials and sedimentary materials. Volcanic materials, such as tuffs, zeolites and pumice, can exhibit pozzolanic properties if the cooling of the molten material is at a fast enough rate. The cooling rate is required to be relatively fast in order to ensure that the silica is in its reactive form. Sedimentary materials, which includes diatomaceous earth, clay and shale, are deposits of high-silica rocks.

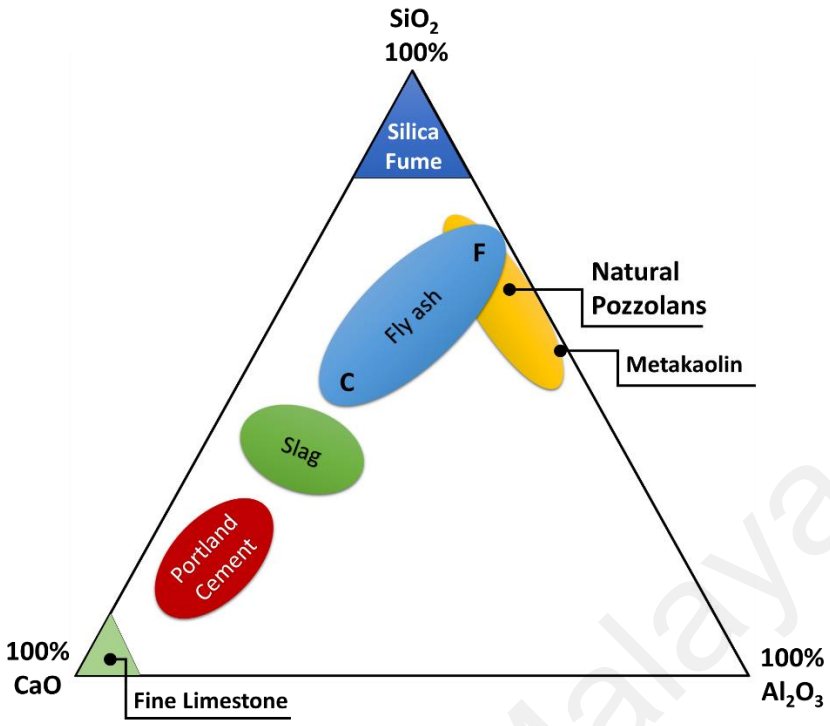

Figure 2.6: Classification of SCMs (Lothenbach et al., 2011)

Artificial SCMs are classified mostly as waste materials. Examples of materials within this category include the industrial and agricultural by-products. The most common products include silica fume (from the production of ferrosilicon alloys), fly ash (from the combustion of coal), slag (from the production of iron), rice husk ash (from rice industry) and palm oil fuel ash (from palm oil industry).

2.5.3 Effect of SCMs on concrete properties

More recently, the usage of SCMs from industrial and agricultural wastes, such as silica fume, slag, fly ash, rice husk ash and palm oil fuel ash has become more intense in concrete industry due to their contribution to the reduction of cement content, strength improvement and durability enhancement. The use of such by-products in concrete industry not only prevents these products from being land-filled but also enhances the properties of concrete. For instance, the investigation by Cordeiro et al. (2009) showed that the concrete incorporated with up to 20% of RHA as SCMs increased the mechanical

behavior and improved the resistance against chloride-ion penetration compared to the corresponding normal concrete.

The use of SCMs in concrete affects the strength development by three known phenomena: (i) filler effect, (ii) dilution and (iii) the reactivity of SCM (Juenger & Siddique, 2015). Equally as important, replacement level, fineness and type of SCM also have an impact on the rate of strength attainment of concrete. These factors are interdependent to some extent, as for example, replacement of cement leads to the dilution, which in turn reduce hydration rate at the early age. In terms of filler effect, it relates to the decrease of voids present in a concrete mix. The presence of voids causes an overall decrease in strength and durability of concrete. In addition, SCMs tend to have smaller particle size ranges compared to that of cement. Therefore, the addition of SCMs increases the packing capacity and effectively reduces the volume of voids.

If SCM is used as an additional material, an improvement in concrete properties is expected due to the reduction in water-to-binder ratio (Kou & Poon, 2012). In contrast, when SCM is used as a cement replacement material, a reduction in development of the strength occurs, more noticeable at early ages due to the effect of cement dilution as well as the slow nature of the pozzolanic reaction (Juenger & Siddique, 2015). In terms of dilution effect, if cement is replaced with a SCM of relatively lower reactivity, the total amount of hydration products that can form is reduced and as a result, it affects the pozzolanic reaction at the early ages. The pozzolanic reaction is affected by the presence of an alkaline environment and with a reduction in cement, and inadvertently a reduction in hydration products associated with its hydration, the rate at which the required alkaline environment is achieved is decelerated, therefore, hindering the pozzolanic reaction. Despite the possible adverse effects at early ages, the strength of concrete containing SCMs can potentially be equal to or even exceed the strength of reference mixtures at

later ages. For example, Chao-Lung et al. (2011) indicated that RHA is highly pozzolanic material and can be used up to 20% as SCM without negatively affecting the strength and durability properties of concrete. In addition, Johari et al. (2012) concluded that utilization of POFA tends to reduce the early mechanical properties, while the strength at later age was comparable to the control specimens due to the pozzolanic mechanism of POFA. Further, Bamaga et al. (2013) revealed that concrete containing 20% POFA has a compressive strength that is equivalent to those without POFA at the age of 28 days and beyond. Furthermore, Corinaldesi and Moriconi (2009) concluded that the incorporation of fly ash and silica fume in concrete proved to be very effective in improving the pore structure of the cement matrix, causing enhancement in terms of mechanical performance, such as compressive, tensile and bond strengths. This improvement in the strength is attributed to the pozzolanic reaction in which SCMs are capable of taking part in a hydration reaction mainly due to the presence of the reactive components, e.g. SiO_2. When cement is hydrated, portlandite is produced which in turn creates an environment with a relatively high alkalinity in the cementitious paste and also acts as a reactant in the pozzolanic reaction, as shown in Equation 2.5 and Equation 2.6 (Snellings et al., 2012).

$$\underset{\text{(Belite)}}{2Ca_2SiO_4} + \underset{\text{(Water)}}{4H_2O} \rightarrow \underset{\text{(C–S–H phase)}}{3CaO{\cdot}2SiO_2{\cdot}3H_2O} + \underset{\text{(Portlandite)}}{Ca(OH)_2} \quad (2.5)$$

$$2SiO_2 + 3Ca(OH)_2 \rightarrow 3CaO{\cdot}2SiO_2{\cdot}4H_2O \quad (2.6)$$

The pozzolanic reaction utilises the portlandite as a reactant to produce C–S–H, where the latter contribute to gain more strength. Furthermore, the continual depletion of portlandite refines the concrete pores and enhances particle packing. Therefore, concrete containing SCMs are sensitive to curing due to the moisture required to facilitate the pozzolanic reaction.

The type of SCM incorporated also affects the strength gain and can be related to the reactivity, morphological and physical properties. Sata et al. (2007) investigated the effect of SCMs made from various by-products on mechanical properties of high-strength concrete. Ground pulverized coal combustion fly ash (FA), ground fluidized bed combustion fly ash (FB), ground rice husk ash (RHA) and ground palm oil fuel ash (POFA) were used to partially replace Portland cement. They found that concretes containing 10–40% FA or FB and 10–30% RHA or POFA exhibited higher compressive strengths than that of the control concrete. In addition, it was reported that, due to its highly pozzolanic nature, RHA can be used up to 20% as SCM without affecting the strength and durability properties of concrete (Chao-Lung et al., 2011). One of the latest additions that could be considered as a potential SCM is POFA, a by-product obtained from palm oil mills. It is produced by burning of oil palm shell, fibers and empty fruit bunches at temperatures between 800 and 1000 °C for electricity generation during the palm oil extraction process (Nagaratnam et al., 2016). The investigation on the potential use of POFA as SCM concluded that POFA is a good pozzolanic material since it has a high amount of silica content (50–70%) (Ranjbar et al., 2016). Palm oil clinker (POC) is another by-product from the palm oil industry. The difference between POFA and POC is that POFA is collected in the form of ash, while POC is collected as large chunks. Attempts have been made by Kanadasan and Abdul Razak (2015) to utilize the POC powder (POCP) as a cement replacement material in self-compacting mortar; they found that the replacement of 50% of POCP with a similar particle size as that of cement could produce compressive strength of about 70% as that of control specimens.

The optimum replacement level can be explained by the achievement of an optimum particle packing state as well as the effect of cement dilution. When very fine SCMs are added to concrete, the particle packing increases, resulting in a decrease of the overall voids. However, if too much fines are added, the particle packing is disturbed and the

packing density decreases again (Jaturapitakkul et al., 2011). The dilution of cement can also affect the strength development at the early ages such that the increase of replacement level leads to reduce the cement content, thus less hydration products will be produced namely C–S–H, where C–S–H is the main component that contributes to the strength of concrete (Alsubari et al., 2016).

2.5.4 Recycled aggregate concrete with SCMs

While the RA-based concrete in its beginnings only designed using conventional cement (Sagoe-Crentsil et al., 2001), later it was developed using blended cement with traditional SCMs. Researchers showed that in spite of the reduction in the mechanical and durability performance of RA-based concrete, the concrete could attain considerable enhancement by utilization of traditional SCMs with high pozzolanic activity, such as fly ash (FA), silica fume (SF) and ground granulated blast slag (GGBS) (Kou et al., 2011; Lima et al., 2013; Limbachiya et al., 2012). The incorporation of SCMs was found to improve the impermeability of RA-based concrete due to two possible mechanisms: (a) the ability of SCM particles to penetrate into the pores of RA leading to enhance the interfacial transition zone (ITZ) bonding between RA and cement matrix (Çakır, 2014), (b) the pozzolanic reaction between SiO_2 and $Ca(OH)_2$ to form extra C–S–H gel, which in turn densifies the microstructure of cement matrix and prevents the ingress of aggressive solutions into the inner part of concrete (Somna et al., 2012). Thus, the use of conventional SCMs such as metakaolin (Kou et al., 2011), silica fume (Dilbas et al., 2014), fly ash (Corinaldesi & Moriconi, 2009; Lima et al., 2013; Limbachiya et al., 2012) and GGBS (Hwang et al., 2013) was found to enhance the mechanical and durability properties of RA-based concrete.

2.6 Summary

Though the negative impact of concrete on the environment has been clearly explained by several researchers, yet the use of cement and aggregates is linked to both economic and social growth and development. The literature review focused on the use of RA in concrete and the associated behavior. In addition, the effect of SCMs on concrete properties has been reviewed. This clearly indicates that the use of SCMs in concrete is more beneficial in terms of both mechanical and durability aspects.

Moreover, it can be stated that the addition of SCMs in concrete enhances the strength development and it depends on the incorporation method. If it is used as additional material, the outcome is generally seen through early age development. Moreover, the secondary hydration reactions also aid to the strength development, as well as the fact that the water-to-binder ratio is effectively reduced. However, on the basis of cement replacement, the early age strength tends to be affected. This is dependent on the replacement level and reactivity of the SCM used. The use of SCMs leads to concrete with better pore structures. The pore refinement is as a result of enhanced particle packing and the pozzolanic hydration products. The pozzolanic reaction utilizes the calcium hydroxide from cement hydration to form more C-S-H. The calcium hydroxide typically only generates an alkaline environment and is associated with weaker structural properties. Hence, replacing it with C-S-H is beneficial as the microstructure is refined and the strength can be increased. The early age compressive strength of SCM-based concrete is lower than a 100 % OPC concrete mixture due to the dilution and lower reactivity. However, the concrete containing SCMs is typically greater to or equal compressive strength to that of the reference at later ages.

Finally, the use of SCMs has some pitfalls, yet the lucrative properties, in terms of performance and economics, cannot be ignored. Hence, studying the effects of using

SCMs provides valuable knowledge in the way of greening the concrete industry and increasing its sustainability for future use.

CHAPTER 3: MATERIALS AND TEST METHODS

3.1 Introduction

An extensive experimental program was meticulously planned in order to achieve the objectives of this study. Figure 3.1 illustrates the experimental program undertaken to assess the suitability of SCMs and RA for use in concrete. The suitability was assessed from the basis of the extent of replacement of natural aggregates with RA and its effect on concrete containing SCMs. A brief introduction of the constituent materials for producing concrete along with an explanation of the test methods are also provided in this chapter.

3.2 Materials

3.2.1 Cement

A commercial ordinary Portland cement (OPC) with strength grade of 42.5 MPa conforming to ASTM C150 was used throughout this research.

3.2.2 Supplementary cementitious materials (SCMs)

Three types of SCMs, RHA, POFA and POCP from the by-products of two agricultural industries, namely rice and palm oil were utilized in this study. Both the physical and chemical characteristics of the binders were determined including: (i) the particle size distribution, (ii) visualization of the morphology via scanning electron microscopy (SEM) imaging, and (iii) the chemical composition via X-ray fluorescence (XRF).

Both POFA and POCP collected from palm oil mill were ground to 30,000 cycles in Los Angeles abrasion machine, whilst RHA was purchased from supplier and directly used in the concrete. Figure 3.2 shows the SEM image of OPC and RHA at the same magnification factor.

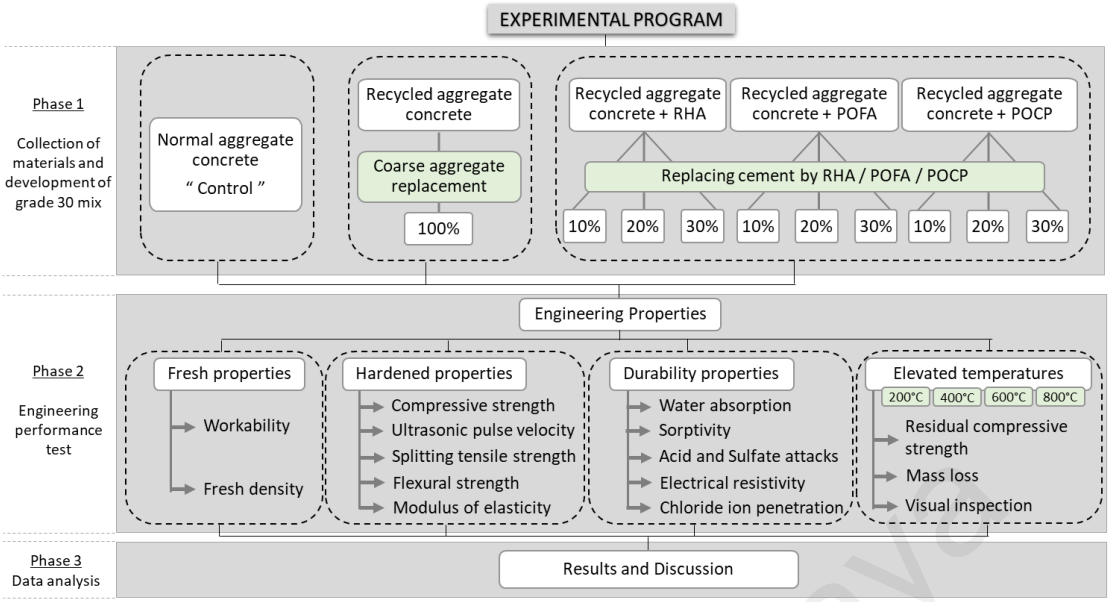

Figure 3.1: Experimental program details

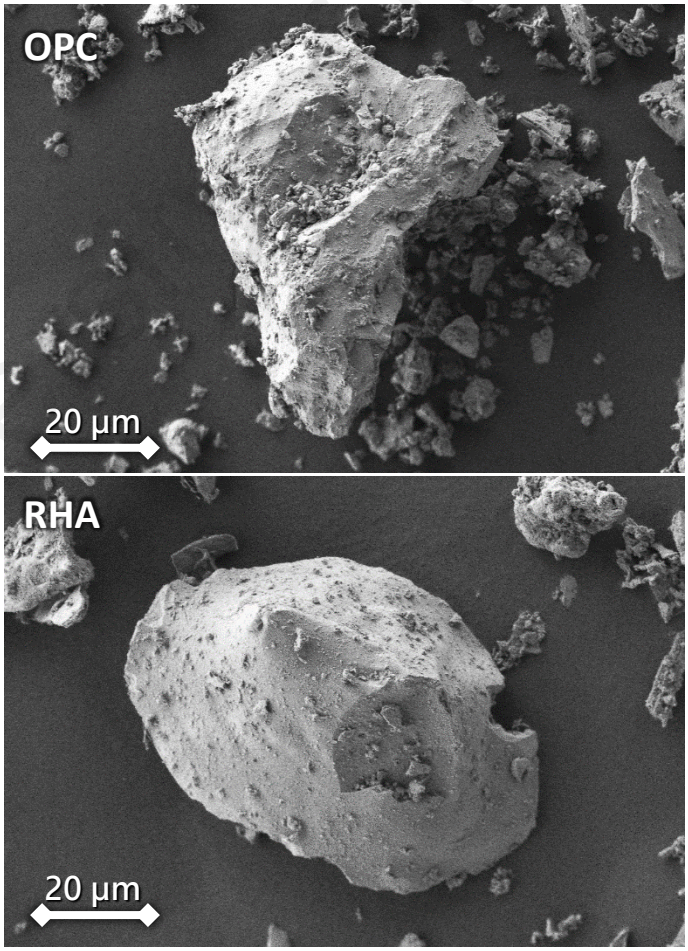

Figure 3.2: Scanning electron microscopy image of OPC and RHA

POFA is available in ash form with relatively coarse particles. Therefore it was further processed in order to achieve a sufficient fineness and to improve its reactivity to be able to react with $Ca(OH)_2$ to produce calcium silicate hydrate (C-S-H). Firstly, the collected POFA was dried in an oven at 105 ± 5 °C for 24 h to remove the moisture content, as this raw material is kept in an open area in the vicinity of the factory. Secondly, the dried POFA was sieved through 300-μm sieve to eliminate the coarse particles and impurities. Finally, the POFA was ground using a Los Angeles abrasion machine with a speed of about 33 revolution per minute for 30,000 cycles. Figure 3.3 shows the SEM image of POFA before and after grinding process at the same magnification factor.

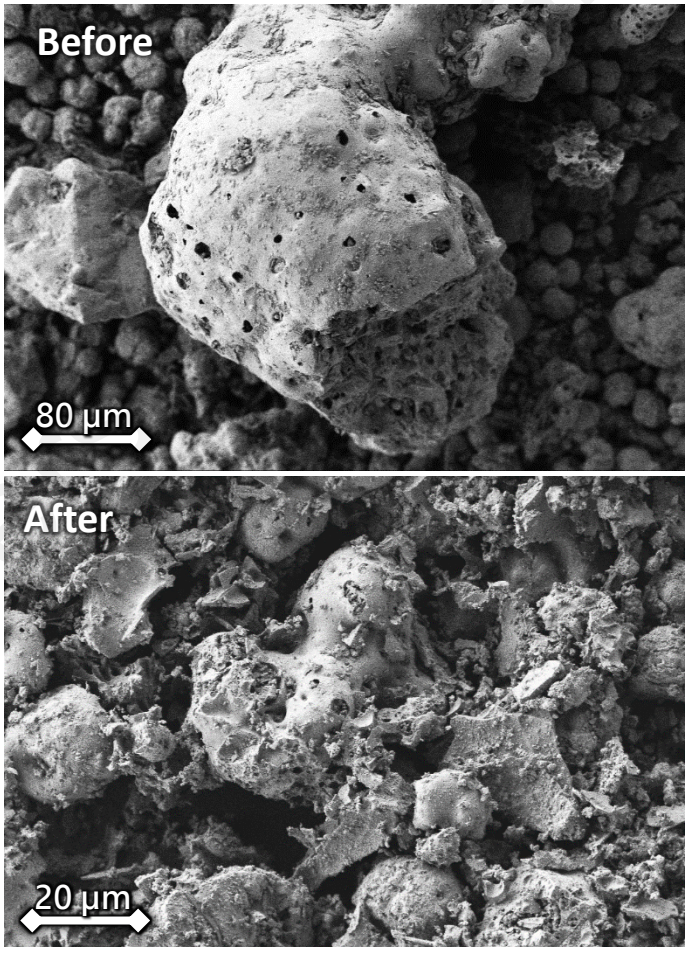

Figure 3.3: Scanning electron microscopy image of POFA before and after grinding

Large chunks of POC was collected from palm oil mill with flaky, porous, and irregular shapes, and then crushed to smaller sizes to segregate coarse and fine POC

aggregates; then the finer portion of POC aggregates that passes through 2.36 mm are ground to obtain POCP; the grinding process adapted for POCP was similar to POFA. Figure 3.4 shows the SEM image of POCP before and after grinding process at the same magnification factor. In addition, Figure 3.5 shows the physical appearance of OPC compared to RHA, POFA and POCP.

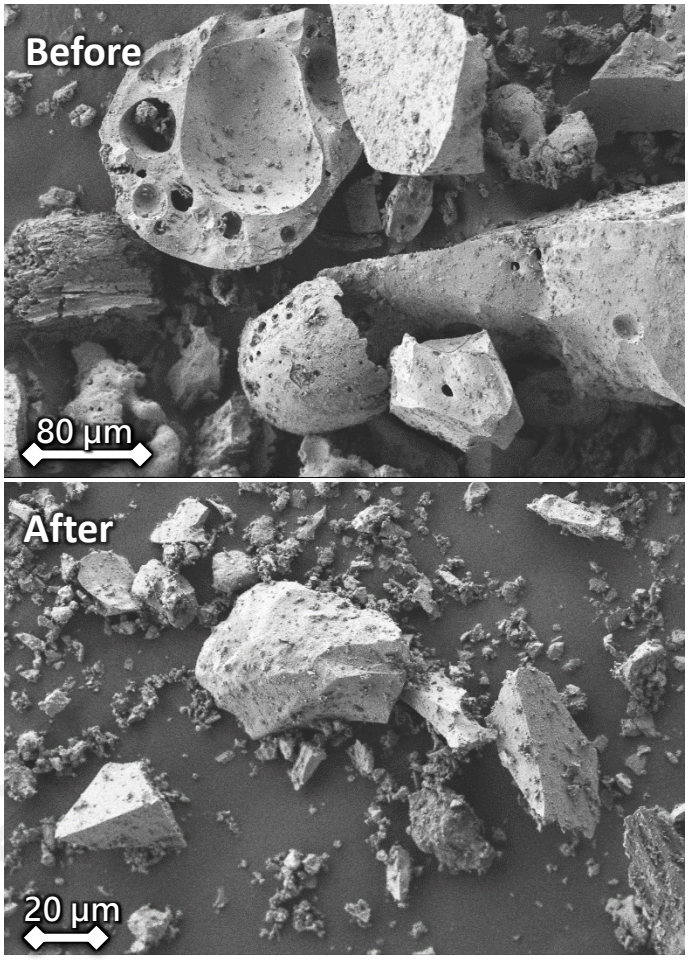

Figure 3.4: Scanning electron microscopy image of POCP before and after grinding

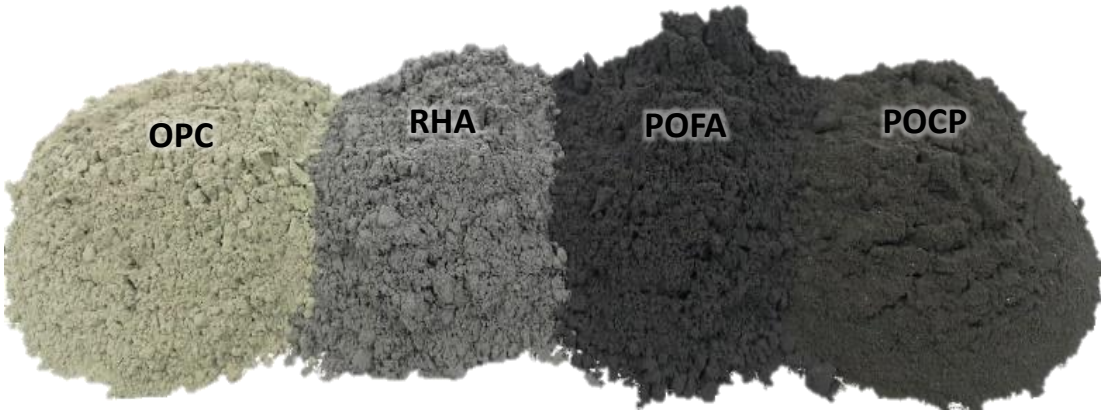

Figure 3.5: Physical appearance of binders

3.2.3 Coarse aggregates

Crushed granite aggregates were used as coarse aggregate in the control mix, while the RA was used in the remaining ten mixes. The physical properties of coarse aggregates are shown in Table 3.1.

Table 3.1. Physical properties of coarse and fine aggregates

Physical properties	Coarse aggregate		Fine aggregate
	Normal	Recycled	
Nominal maximum size (mm)	20	20	4.75
Specific gravity, Oven Dry (OD)	2.60	2.31	2.76
Specific gravity, Saturated Surface Dry (SSD)	2.62	2.42	2.79
Compacted bulk density (kg/m^3)	1481	1370	-
Water absorption (%)	0.77	4.76	1.10
Moisture content (%)	0.15	2.36	0.87

The RA was obtained from old beams, cubes, cylinders and prisms that have been cast, cured and tested by one of the researchers in a controlled environment in concrete technology laboratory in University of Malaya. These old specimens were crushed and sieved to sizes smaller than 20 mm using a jaw crusher similar to a common industry practice, albeit at a smaller scale, as shown in Figure 3.6. The parent concrete of the RA had been produced using OPC, mining sand and crushed granite aggregate. The hardened

properties of parent concrete as obtained from the researcher at the age of 28 days can be found in Table 3.2. The high-strength concrete was chosen for the parent concrete to simulate the recycled concrete that can be obtained from bridges and high-rise buildings. In addition, the RA was extracted from old concrete specimens that has consistent characteristics to minimize the potential effect of impurities on the new concrete. In addition, the quality of demolished structures varies in a wide range due to the different compressive strengths of the structures, and hence, the compressive strength of those old specimens used in this research was known and this would minimize the number of variables. The coarse aggregate gradation used in this study and the limits stated in ASTM C33 is shown in Figure 3.7. In addition, Figure 3.8 shows the NA and RA with a maximum size of 20 mm that were used as coarse aggregates.

Table 3.2: Hardened properties of parent concrete

Hardened properties	Strength (MPa)
Compressive strength	51.7
Splitting tensile strength	4.16
Flexural strength	4.9
Modulus of elasticity	34,120

Figure 3.6: Recycled concrete aggregate from old specimens: (a, b) Preparation of RA from reinforced concrete beams, (c) large chunks of RA, (d) crushing of large chunks of RA using jaw crusher and (e) RA after crushing

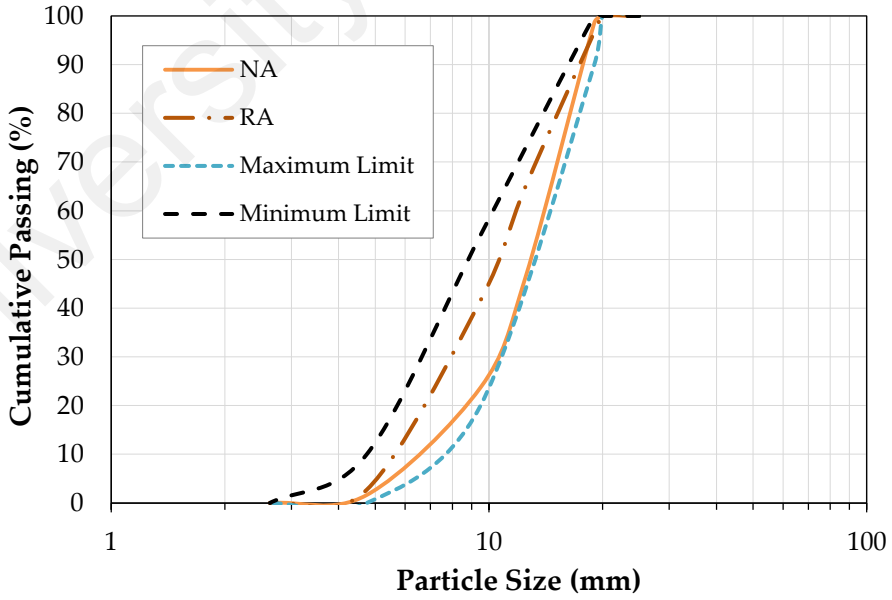

Figure 3.7: Particle size distribution of NA and RA

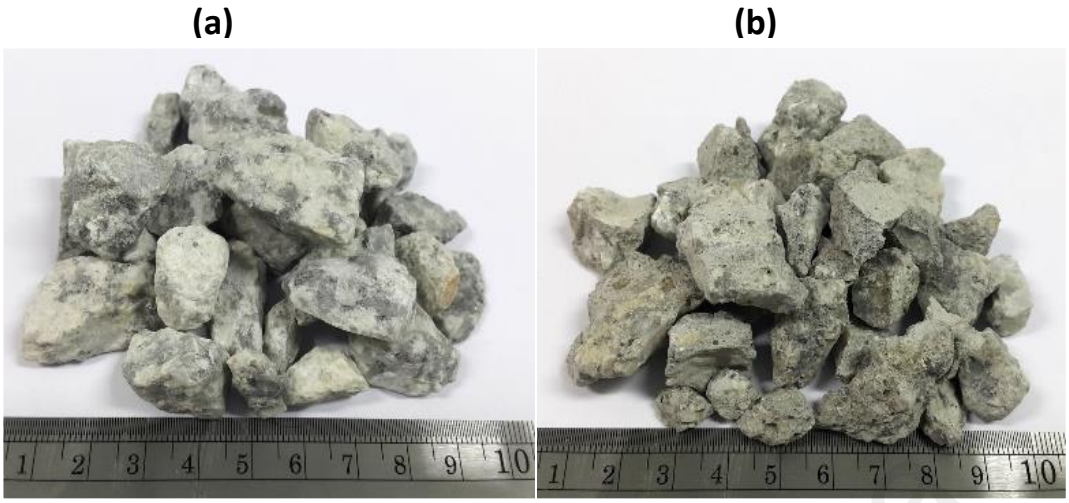

Figure 3.8: The coarse aggregates used in this study (a) crushed granite and (b) recycled concrete

3.2.4 Fine aggregate

Local mining sand with a grain size below 4.75 mm was used as fine aggregate in all eleven mixes. The physical properties of fine aggregate are shown in Table 3.1. The fine aggregate gradation used in this study is shown in Figure 3.9 compared with the limits stated in ASTM C33.

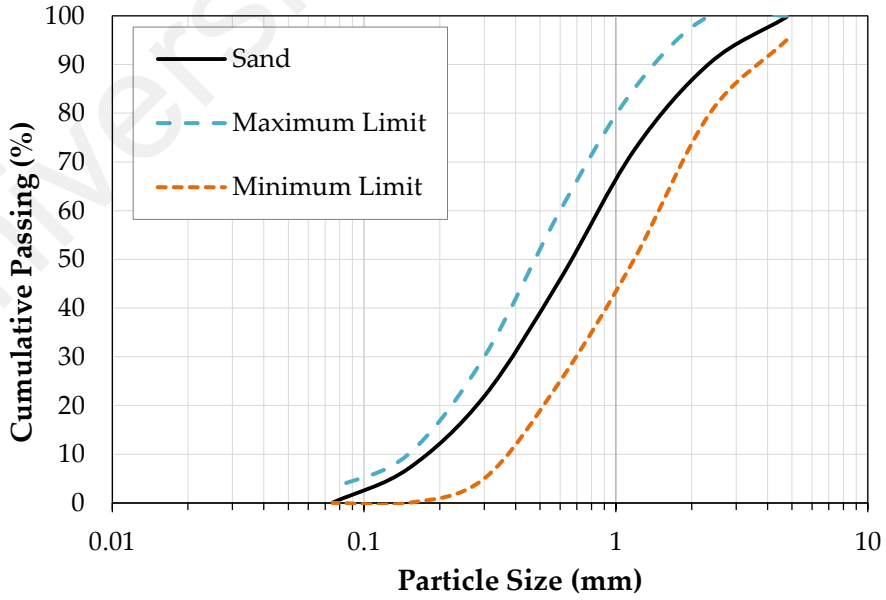

Figure 3.9: Particle size distribution of sand

3.2.5 Superplasticizer

Sika Viscocrete-2199 superplasticizer (SP) was used in this study to achieve the desired workability (slump value) without changing the water/cement ratio of the concrete. The SP conformed to ASTM C494 and the dosage used to maintain the slump values within the targeted range. The SP is assumed to have no effect on the performance of the concrete except for facilitating the workability without affecting the strength.

3.3 Mix proportions

In this study, the Department of Environment (DOE) method was used to design the eleven concrete mixtures with a 28-day characteristic compressive strength of 30 MPa. The normal crushed granite aggregate (NA) was used as the coarse aggregate in the control mix (the mix is defined as NAC in Table 3.3); while for the remaining ten mixes, the NA was wholly replaced by RA using the absolute volume method. The second mix defined as RAC which made of 100% RA and 100% OPC. As this research focused on the effect of cement replacement materials, it was partially replaced by RHA, POFA and POCP at three different levels of 10%, 20% and 30% of cement weight, as shown in Table 3.3 with mix designations based on the type of SCM used and the replacement ratio. The water/binder ratio and cement content were kept constant for all mixes at 0.55 and 380 kg/m^3, respectively. In addition, the effective water content was fixed at 209 kg/m^3 to achieve the designed compressive strength of 30 MPa. Further, before adding cement and fine aggregates in the rotary drum mixer, water equivalent to the respective absorption capacity of all coarse aggregates including crushed granite and RA was added and mixed for five minutes. Sika Viscocrete-2199 superplasticizer (SP) was used in all concrete mixes in order to maintain the slump value between 100 and 150 mm for the S3 concrete workability class in accordance with BS EN 206-1:2000. The mix proportions of all mixes are presented in Table 3.3.

Table 3.3: Mix proportions of concrete mixtures

Mix	w/b ratio	Mix proportions (kg/m^3)									
		Binders				Coarse aggregate		Fine aggregate	Effective water	Mixing water	SP
		OPC	RHA	POFA	POCP	Normal	Recycled				
NAC	0.55	380	-	-	-	1020	-	750	209	215	0.8
RAC	0.55	380	-	-	-	-	943	750	209	232	0.8
RHA10	0.55	342	38	-	-	-	943	750	209	232	0.8
RHA20	0.55	304	76	-	-	-	943	750	209	232	0.8
RHA30	0.55	266	114	-	-	-	943	750	209	232	0.8
POFA10	0.55	342	-	38	-	-	943	750	209	232	0.8
POFA20	0.55	304	-	76	-	-	943	750	209	232	0.8
POFA30	0.55	266	-	114	-	-	943	750	209	232	0.8
POCP10	0.55	342	-	-	38	-	943	750	209	232	0.8
POCP20	0.55	304	-	-	76	-	943	750	209	232	0.8
POCP30	0.55	266	-	-	114	-	943	750	209	232	0.8

3.4 Preparation of specimens

Steel moulds were used for casting of all concrete specimens and compacted using a vibrating table, as shown in Figure 3.10. In order to investigate the air-dried and water-cured compressive strength of the cube specimens, some of these were kept in air curing condition at the specified ages, while the remaining specimens were cured in a water tank at 27 ± 2 °C until the day of testing.

Figure 3.10: Concrete specimens after casting and vibrating

3.5 Test methods

3.5.1 Standard test methods for fresh and hardened properties

3.5.1.1 Slump test

For each concrete mixture, the fresh density and slump of the concrete were measured immediately after mixing in accordance with ASTM C143. A sample of freshly mixed concrete was placed and compacted by rodding in a mold shaped as the frustum of a cone. The mold is raised, and the concrete allowed to subside. The vertical distance between the original and displaced position of the center of the top surface of the concrete is measured and reported as the slump of the concrete, as shown in Figure 3.11.

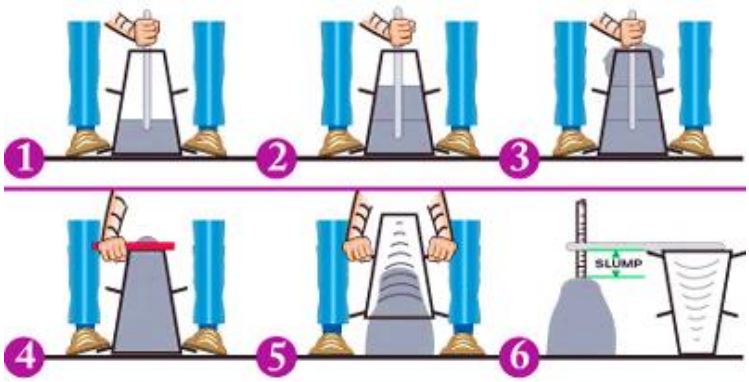

Figure 3.11: Slump test

3.5.1.2 Compressive strength test

The compressive strength was carried out at the ages of 1, 7, 14, 28, 56, and 90 days by using 100-mm cubes in accordance with BS EN 12390-3. This test method consists of applying a compressive axial load to molded cubes at a rate of 2.40 kN/s until failure occurs. The compressive strength of the specimen is calculated by dividing the maximum load attained during the test by the actual cross-sectional area of the specimen.

3.5.1.3 Ultrasonic pulse velocity test

The test procedure for ultrasonic pulse velocity (UPV) is outlined in ASTM C597. This test method is applicable to assess the uniformity and relative quality of concrete, to indicate the presence of voids and cracks, and to evaluate the effectiveness of SCMs. The UPV values were calculated by using Equation 3.1. The schematic of pulse velocity apparatus is shown in Figure 3.12.

$$V = L/T \qquad 3.1$$

where: V is the pulse velocity (km/s), L is the distance between centres of transducer faces (km) and T is the transit time (s).

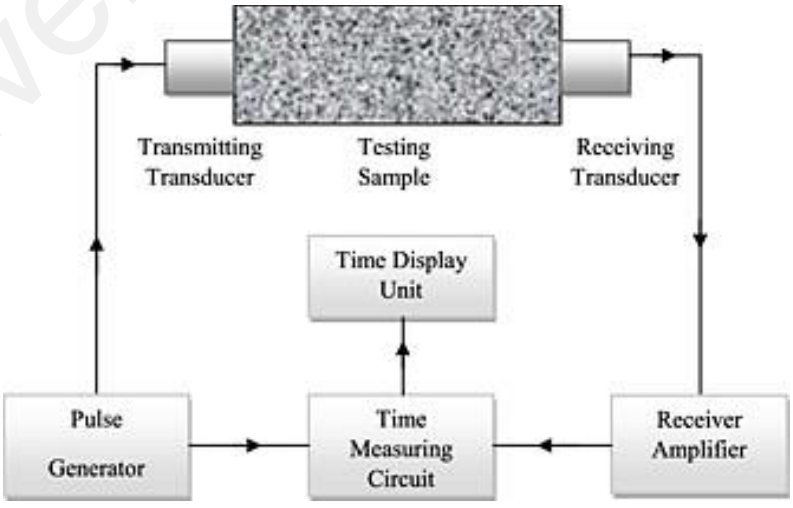

Figure 3.12: Schematic of pulse velocity apparatus

3.5.1.4 Splitting tensile strength test

The splitting tensile strength was conducted based on ASTM C496 at the ages of 28, 56, and 90 days by using 100-mm Ø × 200-mm height cylinders. This test method consists of applying a compressive force along the length of a cylindrical concrete specimen at a rate of 45 kN/min until failure occurs, as shown in Figure 3.13. This loading induces tensile stresses on the plane containing the applied load and relatively high compressive stresses in the area immediately around the applied load. Thin plywood bearing strips were used to distribute the load applied along the length of the cylinder. The splitting tensile strength of the specimen was calculated using Equation 3.2.

$$T = \frac{2P}{\pi l d} \qquad 3.2$$

where:

T = splitting tensile strength (MPa),

P = maximum applied load indicated by the testing machine (kN),

l = length (mm), and

d = diameter (mm).

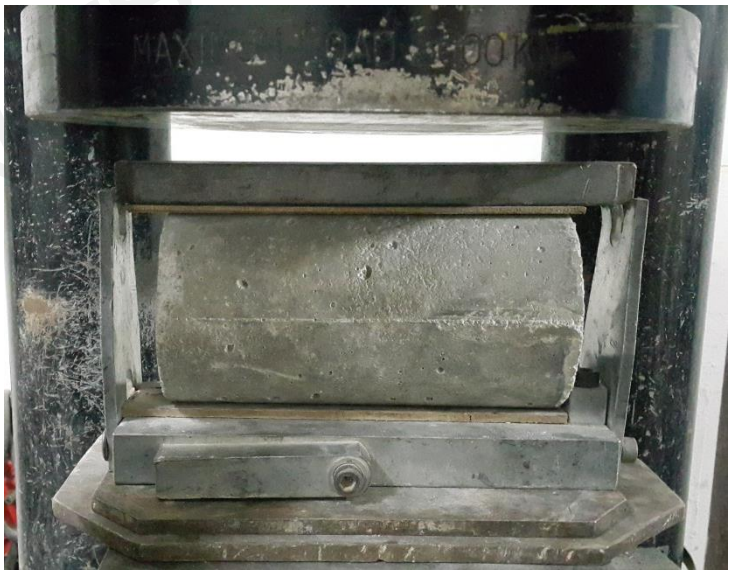

Figure 3.13. Splitting tensile test setup

3.5.1.5 Flexural strength test

The flexural strength determined based on ASTM C78 by using 100 × 100 × 500-mm prisms at the ages of 28, 56, and 90 days. This test method covers the determination of the flexural strength of concrete by the use of a simple beam with third-point loading, as shown in Figure 3.14. The load was applied continuously and without shock at a rate of 4 kN/min that constantly increases the maximum stress by 1.20 MPa/min on the tension face until rupture occurs. The loading rate is calculated using Equation 3.3.

$$r = \frac{Sbd^2}{L} \tag{3.3}$$

where:

r = loading rate (kN/min),

S = rate of increase in maximum stress on the tension face (MPa/min),

b = average width of the specimen as oriented for testing (mm),

d = average depth of the specimen as oriented for testing (mm), and

L = span length (mm).

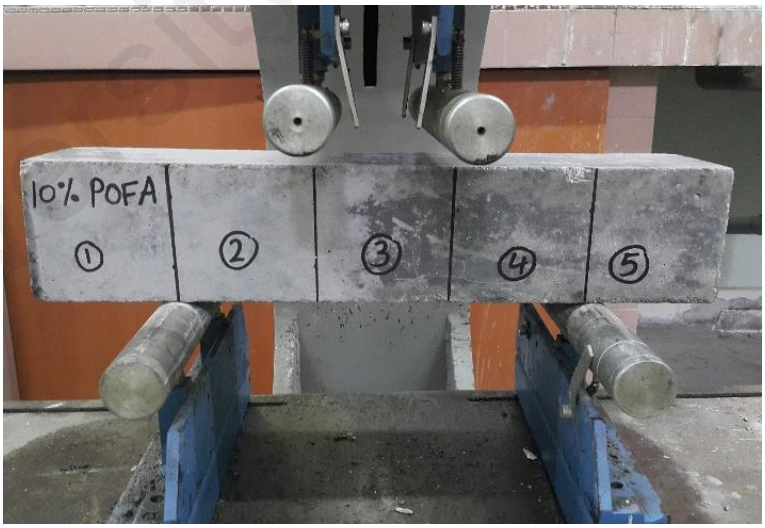

Figure 3.14: Flexural test setup

The flexural strength was calculated using Equation 3.4 for those specimens that failed within the middle third of the span, i.e. in area “3” shown in Figure 3.14.

$$R = \frac{PL}{bd^2} \quad (3.4)$$

where:

R = flexural strength (MPa),

P = maximum applied load indicated by the testing machine (kN),

L = span length (mm),

b = average width of specimen (mm), at the fracture, and

d = average depth of specimen (mm), at the fracture.

3.5.1.6 Static modulus of elasticity test

Cylinders of 150-mm Ø × 300-mm height were used to measure the static modulus of elasticity at the ages of 28, 56, and 90 days, in accordance with ASTM C469. This test method provides a stress to strain ratio value by measuring the deformation caused by customary working stress at a constant rate of 4.4 kN/s until the applied load is 40 % of the average ultimate load of the companion specimens. A compressometer (shown in Figure 3.15) consisting of two yokes, one of which is rigidly attached to the specimen and the other attached at two diametrically opposite points so that it is free to rotate.

Figure 3.15. Compressometer

As shown in Figure 3.16, the deformation (d) of the specimen is equal to one-half the gauge reading (g) since the distances of the pivot rod (c) and the gauge (a) from the vertical plane passing through the support points of the rotating yoke (b) are equal, i.e. $e_g = e_r$. The modulus of elasticity was calculated using Equation 3.5.

$$E = \frac{S_2 - S_1}{\varepsilon_2 - 0.000050} \qquad 3.5$$

where:

E = modulus of elasticity (MPa),

S_2 = stress corresponding to 40 % of ultimate load,

S_1 = stress corresponding to a longitudinal strain, ε_1, of 50 millionths (MPa), and

ε_2 = longitudinal strain produced by stress S_2.

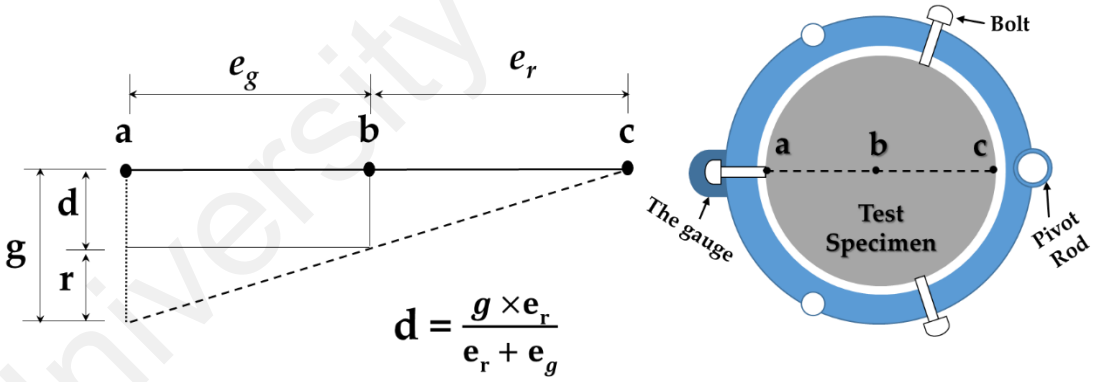

Figure 3.16. Diagram of displacements due to specimen deformation (ASTM C469/C469M−14, 2014)

3.5.2 Standard test methods for durability properties

The following properties were considered to evaluate the effect of SCMs on durability of RA-based concrete.

3.5.2.1 Water absorption test

Concrete cubes of 100-mm were used to obtain the water absorption at the ages of 28 and 90 days, in accordance with ASTM C642. The percentage of water absorbed after immersing concrete specimens in water for 30 minutes and 72 hours to determine the initial and final water absorption, respectively, was calculated using Equation 3.6.

$$\text{Water absorption after immersion (\%)} = \frac{B-A}{A} \times 100 \qquad 3.6$$

where:

A = mass of oven-dried sample in air (g), and

B = mass of surface-dry sample in air after immersion (g)

3.5.2.2 Rate of absorption (sorptivity) of water test

This testing method was intended to determine the susceptibility of concrete to the penetration of water by means of capillary suction (Hall (1989) called the phenomenon "water sorptivity"). The test was conducted on specimens measuring 100-mm Ø × 50-mm height at the ages of 28 and 90 days. The test measures the increase in water depth resulting from the absorption of water when only one surface of 100-mm diameter is exposed to water. The exposed surface of the specimen is immersed in water and water ingress of unsaturated concrete is dominated by capillary suction during contact with water. The measurements were recorded for a period of 8 days, and the correlation between water depth and time was presented, as shown in Figure 3.17. The sorptivity test was performed according to the guidelines stated in ASTM C1585. The test setup is shown in Figure 3.18.

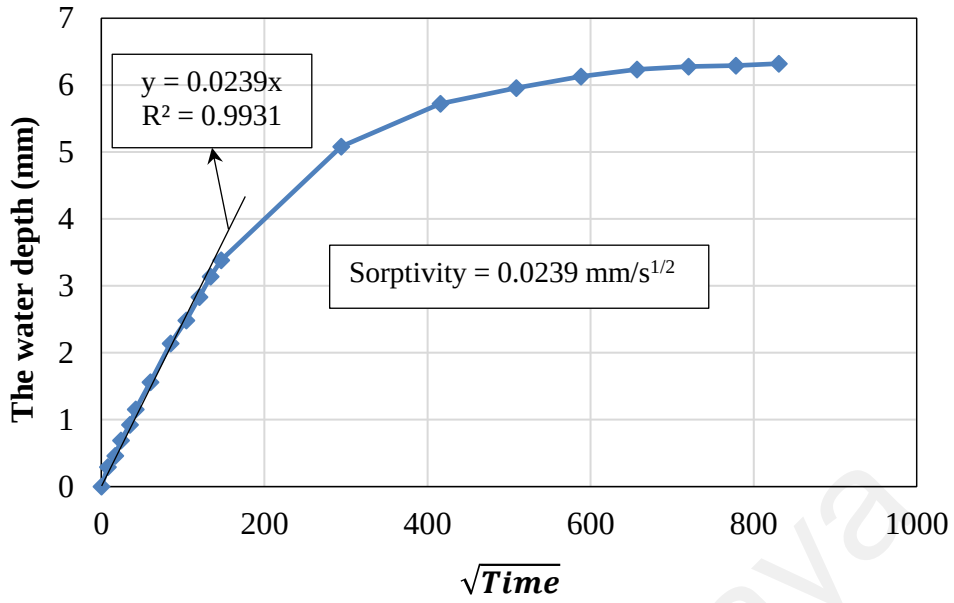

Figure 3.17: Sorptivity calculation example of collected data

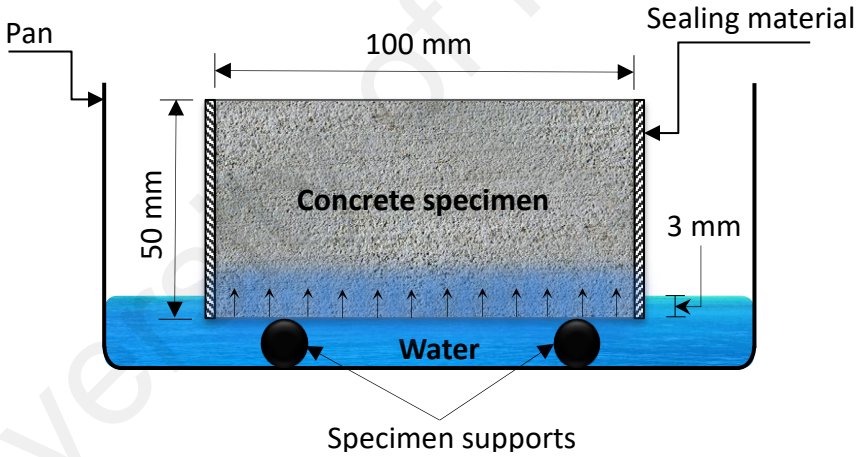

Figure 3.18: Setup of sorptivity test

The absorption (*I*) is the change in mass divided by the product of the cross-sectional area of the test specimen and the density of water, as shown in Equation 3.7. For the purpose of this test, the temperature dependence of the density of water is neglected and a value of 0.001 g/mm^3 is used.

$$I = \frac{m_t}{a \times d} \qquad 3.7$$

where:

I = the absorption (mm),

m_t = the change in specimen mass in grams, at the time t,

a = the exposed area of the specimen, in mm^2, and

d = the density of the water in g/mm^3.

The rate of water absorption ($mm/s^{1/2}$) is defined as the slope of the line that is the best fit to I plotted against the square root of time ($s^{1/2}$). The slope was obtained by using linear regression analysis of the plot of I versus $time^{1/2}$, as shown in Figure 3.17. For the regression analysis, all the points from 1 minute to 6 hours were used.

3.5.2.3 Acid attack test

The resistance of concrete exposed to acid attack was evaluated in accordance with ASTM C267 by immersing cubes of 100-mm in 3% hydrochloric acid (HCl) solution after 28 days of casting. The results obtained by this test method should serve as a guide in, but not as the sole basis for, selection of a chemical-resistant material for a particular application. Figure 3.19 shows the immersed specimens for the test. The volume proportion of acid solution to concrete specimens in a storage container was maintained at 4.0 ± 0.5 times the volume of solution to volume of concrete.

The concrete specimens soaked in HCl solution were used to determine the deterioration depth, mass loss and compressive strength loss after 75 days of immersion (Alsubari et al., 2016). The solution was replaced every two weeks to maintain a constant concentration throughout the test period. Companion specimens cured in water were also tested for comparison. The change in compressive strength and mass was calculated using Equations 3.8 and 3.9, respectively.

$$\text{Compressive strength loss (\%)} = \frac{S_2 - S_1}{S_2} \times 100 \qquad 3.8$$

where:

S_1 = average compressive strength of specimens immersed in HCl solution, and

S_2 = average compressive strength of specimens cured in water.

$$\text{Weight loss (\%)} = \frac{W-C}{W} \times 100 \qquad 3.9$$

where:

C = average mass of specimens immersed in HCl solution, and

W = average mass of specimens cured in water.

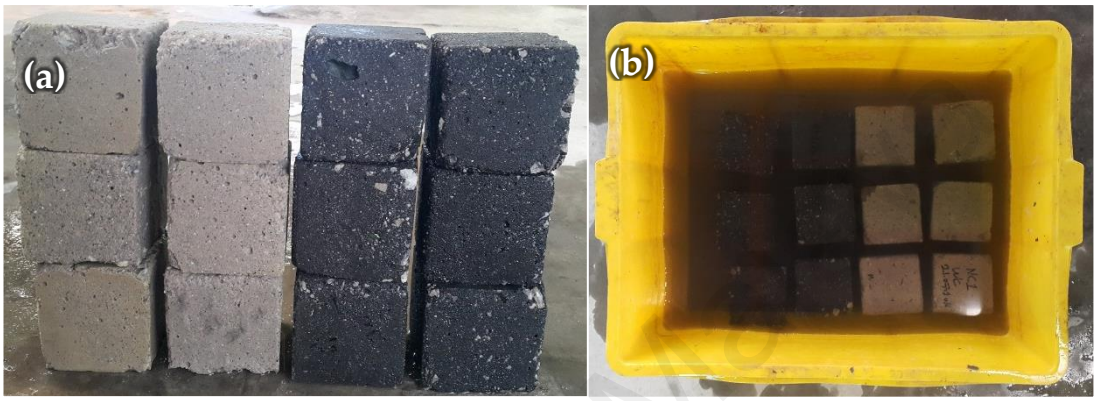

Figure 3.19: Specimens during acid attack test: (a) specimens exposed to acid, and (b) specimens in HCl solution

3.5.2.4 Sulfate attack test

The sulfate resistance of the concrete was evaluated in this study using the method outlined in ASTM C1012. Concrete cubes of 100-mm were exposed to standard solution containing magnesium sulfate ($MgSO_4$) with molarity of 0.352 M or about 5% concentration after 28 days of casting. The change in compressive strength were determined after 28 and 120 days of immersion in the solution and compared with companion specimens cured in water for the same period. Moreover, the solution was replaced at regular intervals of two weeks to maintain the pH value between 6.0 and 8.0 during immersion time. Figure 3.20 shows the immersed specimens for the test. The volume. The volume proportion of sulfate solution to concrete specimens in a storage container was maintained at 4.0 ± 0.5 times the volume of solution to volume of concrete. The change in the compressive strength was calculated using Equation 3.10.

$$\text{Change in compressive strength (\%)} = \frac{S_2 - S_1}{S_2} \times 100 \qquad 3.10$$

where:

S_1 = average compressive strength of specimens immersed in $MgSO_4$ solution, and

S_2 = average compressive strength of specimens cured in water.

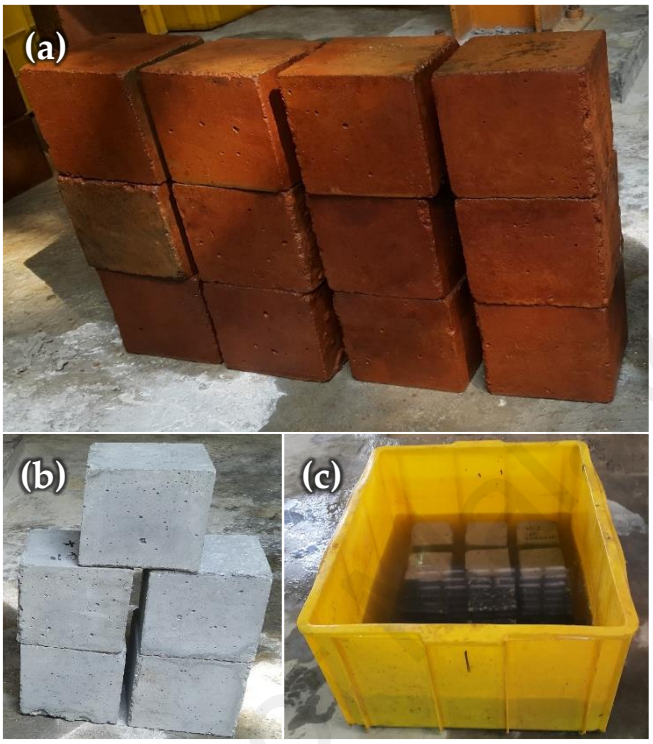

Figure 3.20: Specimens during sulfate attack test: (a) specimens exposed to sulfate, (b) specimens cured in water and (c) specimens in $MgSO_4$ solution

3.5.2.5 Chloride-ion penetration test

The rapid chloride-ion penetration test (RCPT) was performed to provide a rapid indication of concrete's ability to resist the penetration of chloride ions, in accordance with ASTM C1202. This test method consists of monitoring the amount of electrical current passed through 50-mm thick slices of 100-mm nominal diameter cylinders during a 6-h period. A potential difference of 60 V dc is maintained across the ends of the specimen, one of which is immersed in a sodium chloride solution, the other in a sodium hydroxide solution. The total charge passed, in coulombs, has been found to be related to the resistance of the specimen to chloride ion penetration. Qualitative indications of the chloride ion penetrability based on the measured values from this test method are provided in Table 3.4. The setup of the test is shown in Figure 3.21.

Table 3.4: Chloride-ion penetrability based on charge passed

Charge passed (coulombs)	Chloride-ion penetrability
>4,000	High
2,000–4,000	Moderate
1,000–2,000	Low
100–1,000	Very Low
<100	Negligible

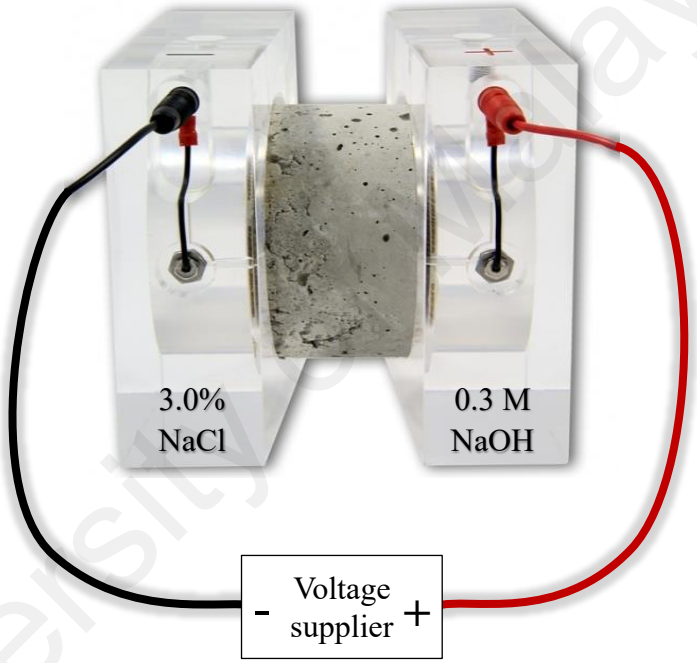

Figure 3.21: RCPT configuration

3.5.2.6 Electrical resistivity test

Electrical resistivity meter was used to provide a rapid indication of the concrete's resistance to corrosion. The test was performed on prisms of 100 × 100 × 300-mm at saturated condition after 28 and 90 days of water curing. The method of testing that used in this study evaluated the surface electrical resistivity of concrete and it is very close to the standardized testing method provided by ASTM C1760, which measures the bulk electrical resistivity. Figure 3.22 illustrates the test configuration. The electrical resistivity is a function of the voltage drop between the two inner probes when a current is applied

to the two outer probes. Qualitative indications of the electrical resistivity compared to the corrosion rate limits suggested by ACI Committee 222 are provided in Table 3.5.

Table 3.5: Electrical resistivity compared to the corrosion rate limits suggested by ACI Committee 222

Electrical resistivity (kΩ.cm)	Corrosion rate
0 - 5	Very High
5 - 10	High
10 - 20	Low to Moderate
> 20	Low

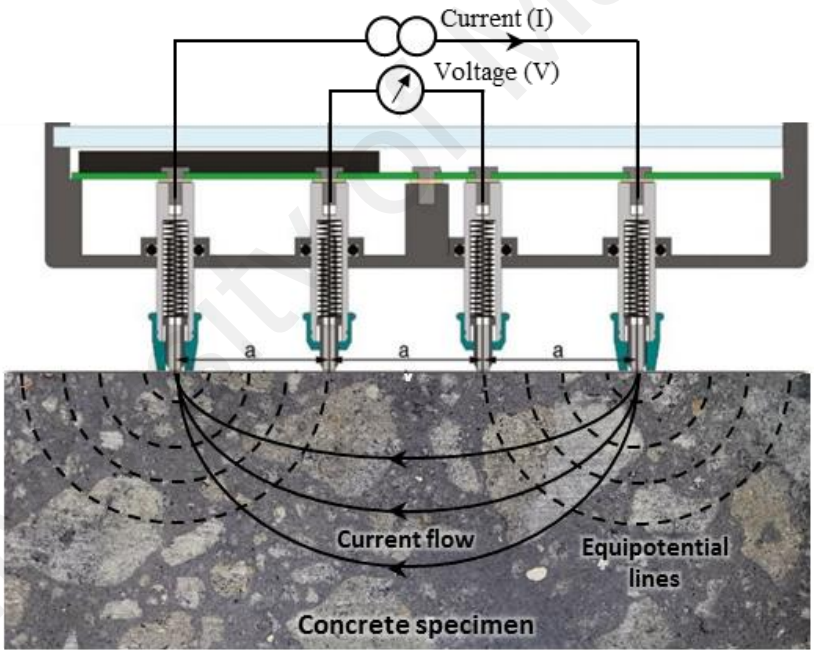

Figure 3.22: Electrical resistivity test configuration

3.5.3 Standard test method for elevated temperatures

A high temperature laboratory furnace (shown in Figure 3.23) designed for a maximum temperature of 1800 °C was used. The specimens were exposed to a maximum temperatures of 200 °C, 400 °C, 600 °C and 800 °C with heating rate of 10 °C per minute based on RILEM (1995) recommendation. Concrete cubes of 100 mm were used to determine the residual compressive strength and mass loss. The temperature was

maintained for 2 hours followed by cooling at the same rate to room temperature in the furnace, as shown in Figure 3.24.

Figure 3.23: A high temperature laboratory furnace used in the test

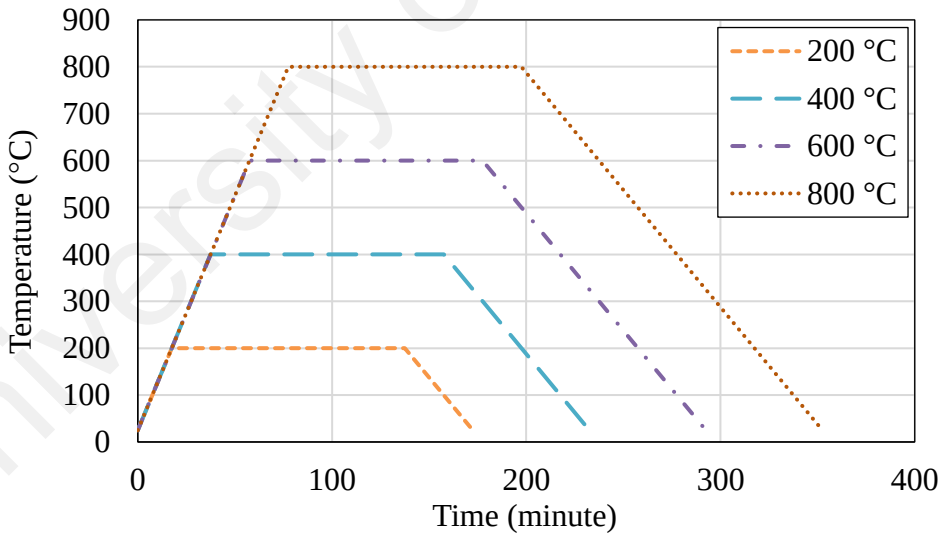

Figure 3.24: Heating patterns of the specimens starting from room temperature

3.5.4 Testing method for scanning electron microscopy

The scanning electron microscopy (SEM) is one of the most versatile instruments available for the examination and analysis of the microstructural characteristics of concrete. The primary reason for the SEM's usefulness is the high resolution that can be obtained when bulk objects are examined. The SEM provides images that can range in

scale from a low magnification (for example, 15×) to a high magnification (for example, 50 000× or greater) of concrete specimens. These images can provide information indicating compositional or topographical variations in the observed specimen. To get an understanding of the particle shape and surface texture, SEM imaging was conducted on selected SCMs. SEM machine employs an electron beam to penetrate about 1 μm deep into a sample. This beam focuses on a point and detectors read signals and convert them into intensities on the attached computer to create an image. Before the test, the samples were mounted on a holder using carbon tape to prevent charging of the samples.

3.5.5 Testing method for X-ray diffraction

Mineralogical analysis of the composites were carried out with an X-ray powder diffractometer, CuKa, Ni-filtered radiation (the wavelength was 1.54184 Å). The radiation was generated at 40 mA and 40 kV. The analysis was performed on fine grains of ground samples. Specimens were step-scanned as random powder from 5 to 90 °C, 2 Θ steps were integrated at the rate of 2 s per step.

CHAPTER 4: RESULTS AND DISCUSSION

4.1 Introduction

The results are presented and discussed on various parts such as fresh, hardened and durability properties. As recycled aggregate is being introduced for use in the construction industry, the aforementioned studies are required to understand its real characteristics and behavior in concrete containing SCMs. Waste materials from rice and palm oil industry in Malaysia were characterized through a detailed feasibility study whereby the physical and chemical were scrutinized. Investigation on RA concrete containing SCMs was carried out to assess the enhancement and positive contribution of these materials. Fresh properties of RA concrete were discussed pertaining to the different SCM replacement ratio. Tests on fresh concrete carried out in this research work comprise of slump test and fresh density. Moreover, tests on mechanical properties were carried out on RA concrete incorporating SCM to establish a relationship between the addition of SCM and mechanical properties. These relationships were then correlated with available standard models provided by ACI 318 and previous studies. Durability properties of RA concrete were evaluated to understand further the effect of using SCM. The durability properties tests include water absorption, sorptivity, penetration of chloride ions, electrical resistivity, sulfate attack and acid attack. Besides durability performance, microanalysis was also conducted on selected mixes to check the enhancement of the concrete exposed to aggressive environments. These analyses comprise of scanning electron microscopy analysis and X-ray diffraction analysis.

4.2 Physical and chemical analyses of OPC, RHA, POFA and POCP

Three types of agricultural wastes were evaluated for the use as SCMs, namely RHA, POFA and POCP. Their chemical and physical properties can be found in Table 4.1 and 4.2, respectively. The specific gravity and the total particles passing through 45-µm sieve for RHA were 2.03 g/cm^3 and 98.3%, respectively. The total contents of silicon dioxide

(SiO_2), aluminum oxide (Al_2O_3) and iron oxide (Fe_2O_3) were about 92% by mass. The physical properties and X-ray fluorescence analysis revealed that RHA conforms to the requirements of pozzolanic material in accordance with ASTM C618. The amount retained, when wet-sieved on 45 μm (No. 325) sieve, was about 12% and 29% for POFA and POCP, respectively. It can be well noted that the loss on ignition of POFA is higher due to the higher amount of un-burnt carbon compared to RHA and POCP. As per ASTM C618, the loss of ignition should be less than 12. Based on these results, both POFA and POCP confirmed the fineness requirement to be used as pozzolanic materials as per ASTM C618.

Table 4.1: Chemical properties of OPC, RHA, POFA and POCP

Chemical compositions (%)	OPC	RHA	POFA	POCP	ASTM C618 class F
SiO_2	21.0	91	64.17	60.29	
Al_2O_3	5.9	0.35	3.73	5.83	
Fe_2O_3	3.4	0.41	6.33	4.71	
$SiO_2 + Al_2O_3 + Fe_2O_3$	30.3	91.76	74.24	70.83	70 (minimum)
CaO	64.7	0.49	5.80	3.28	
MgO	2.5	0.81	3.46	4.20	
SO_3	2.4	1.21	0.74	0.31	5 (maximum)
TiO_2	0.002	-	0.06	0.10	
P_2O_5	0.07	-	3.30	3.78	
Loss on ignition	0.9	4.81	11.56	5.23	12 (maximum)

Table 4.2: Physical properties of OPC, RHA, POFA and POCP

Physical properties	Specific gravity	Retained on 45-μm sieve (%)	Median particle size (μm)
OPC	3.14	13.6	22.47
RHA	2.03	1.7	19.41
POFA	2.14	11.6	17.62
POCP	2.53	29.0	37.97
ASTM C618 class F		34% (maximum)	

Figures 4.1-4.4 illustrate the scanning electron microscopy (SEM) image of the particle shape and surface texture of OPC, RHA, POFA and POCP. It can be seen that the particles of OPC are solid and generally spherical in shape. On the other hand, RHA, POFA and POCP have angular and irregularly-shaped particles. In addition, the microscopic image shows that the outer surface of POFA has a porous texture, which could lead to water absorption, while RHA and POCP particles have sharp edges that could have negative impact on the workability of fresh concrete. The porous texture of POFA results in a reduction of workability due to higher specific surface area of the POFA particles which led to more water demand. On the other hand, the sharp edges of RHA and POCP leads to increase the friction between cement and aggregates, and preventing the movement and rolling of particles over each other, and thus reducing the workability. However, the increased specific surface area of porous POFA can facilitate the pozzolanic reaction between the particles in the concrete and improve the compressive strength at the later age. In case of RHA and POCP, the angular sharp edges of particles can improve the cohesion of the concrete matrix.

The particle size distribution of the binding materials is presented in Figure 4.5. It can be clearly seen from the curves that RHA and POFA have similar fineness of OPC. The particle size of POCP is relatively coarser than OPC, however, most of the particles sizes are less than 100 μm and around 50% POCP particles are smaller than 20 μm.

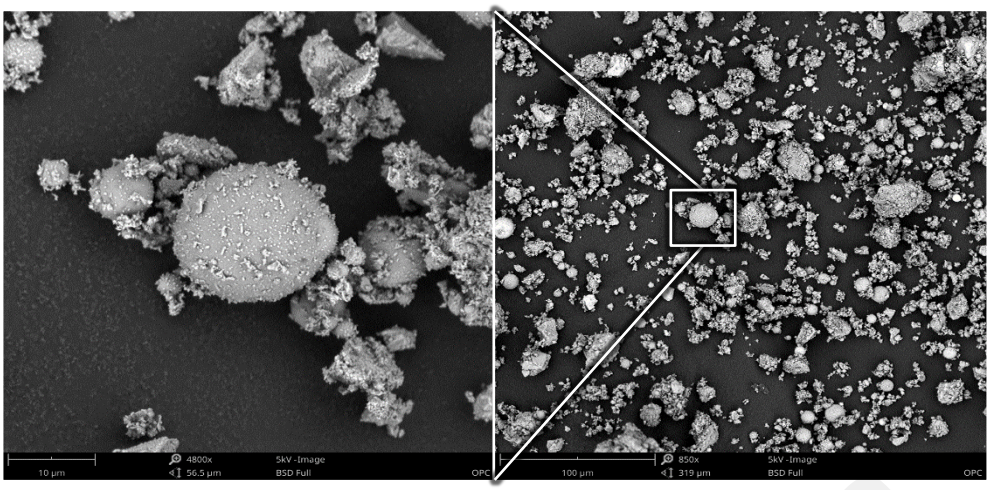

Figure 4.1: Scanning electron microscopy image of cement

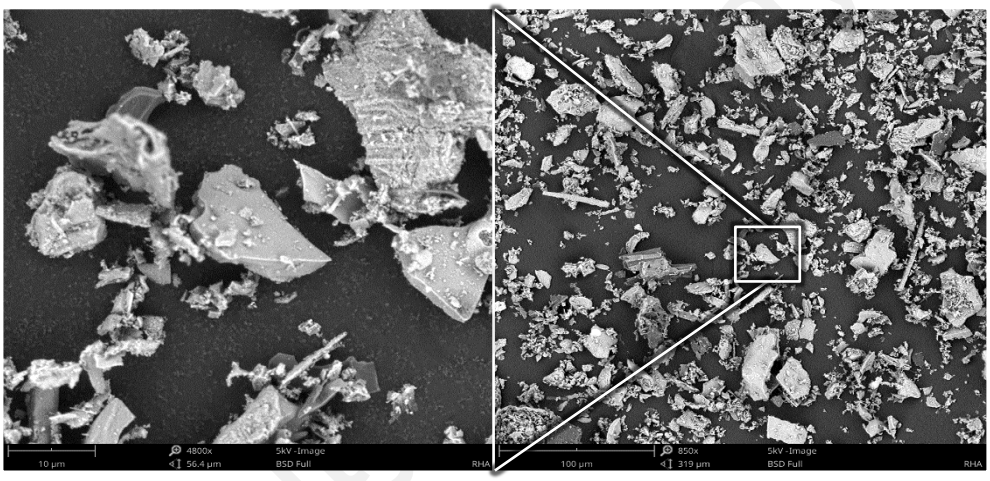

Figure 4.2: Scanning electron microscopy image of RHA

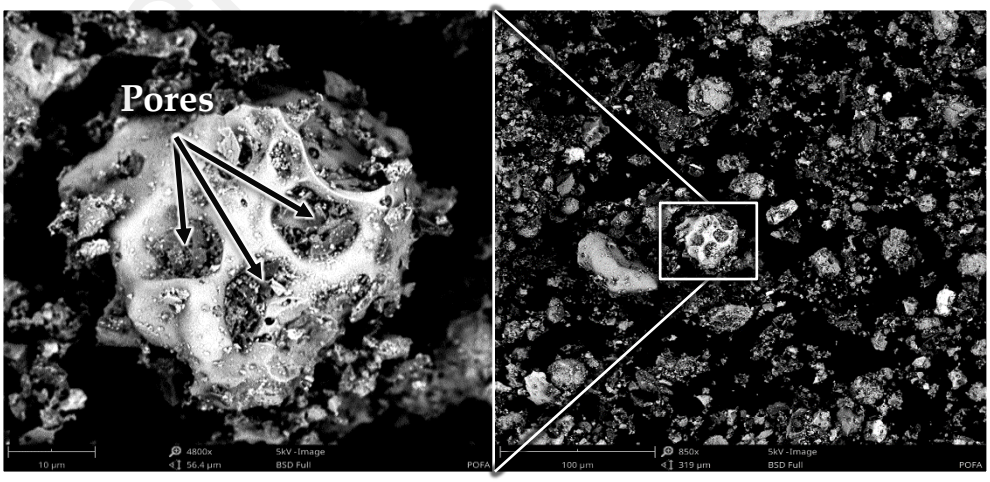

Figure 4.3: Scanning electron microscopy image of POFA

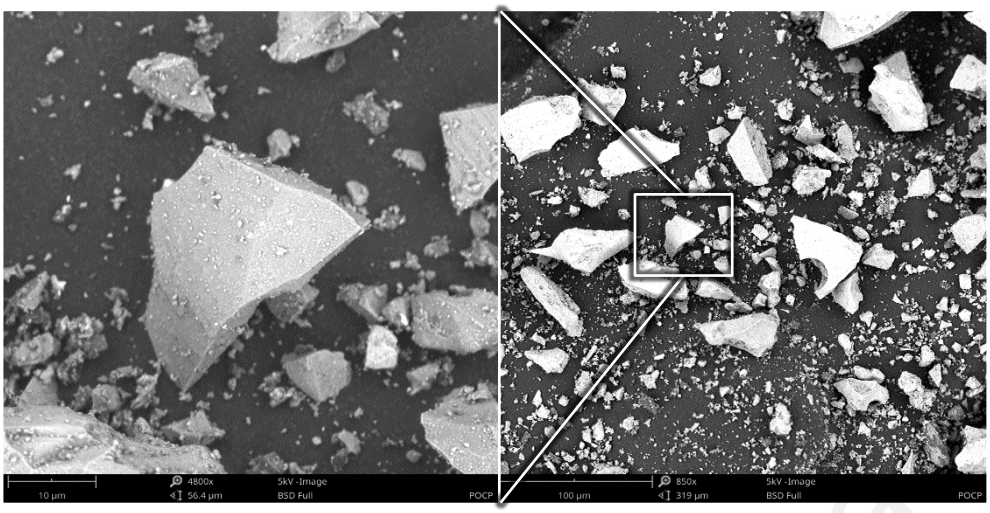

Figure 4.4: Scanning electron microscopy image of POCP

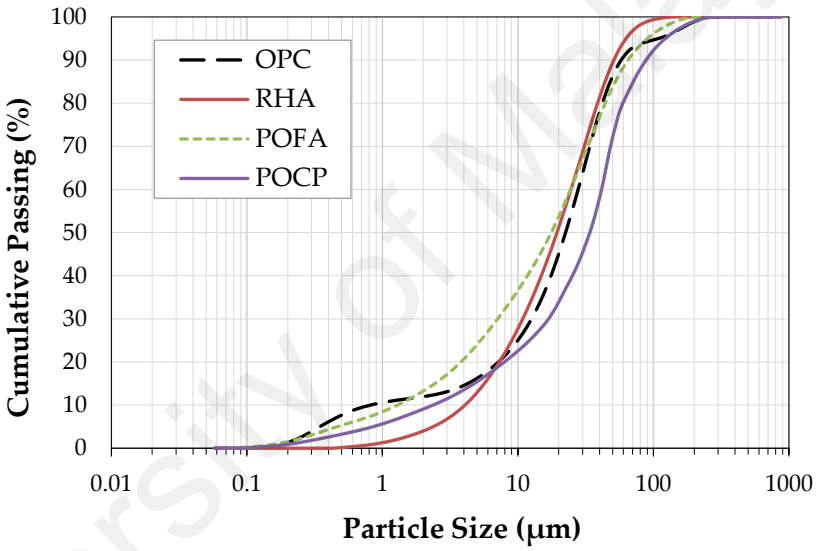

Figure 4.5: Particle size distribution of binders

4.3 Fresh and hardened properties

4.3.1 Workability

The slump test measures homogeneity of fresh concrete starting from the mixing stage until the stage of casting and finishing. The workability and amount of superplasticizer of the mixes were designed for slump ranging from 100 –150 mm. It can be seen from Table 4.3 and Figure 4.6 that the slump value of the RAC mix with 100% RA was slightly lower than the corresponding normal concrete mix-NAC. This could be attributed to the surface roughness and greater angularity of RA because of the adhered old mortar on its

surface, which decreases the workability of concrete and makes it more difficult to finish properly. The trend of decreasing the slump of RAC observed in this study also confirmed the reported findings in previous research by Safiuddin et al. (2011), which was due to the porous adhered cement paste on the RA, and thus, increased the overall water absorption and decreased its workability. Figure 4.7 shows the slump of all the mixes and the variation due to increase in the SCMs content.

Table 4.3: Slump results of concretes

Mix	NAC	RAC	RHA			POFA			POCP		
			10%	20%	30%	10%	20%	30%	10%	20%	30%
Slump	140	125	110	90	80	120	115	80	140	115	95

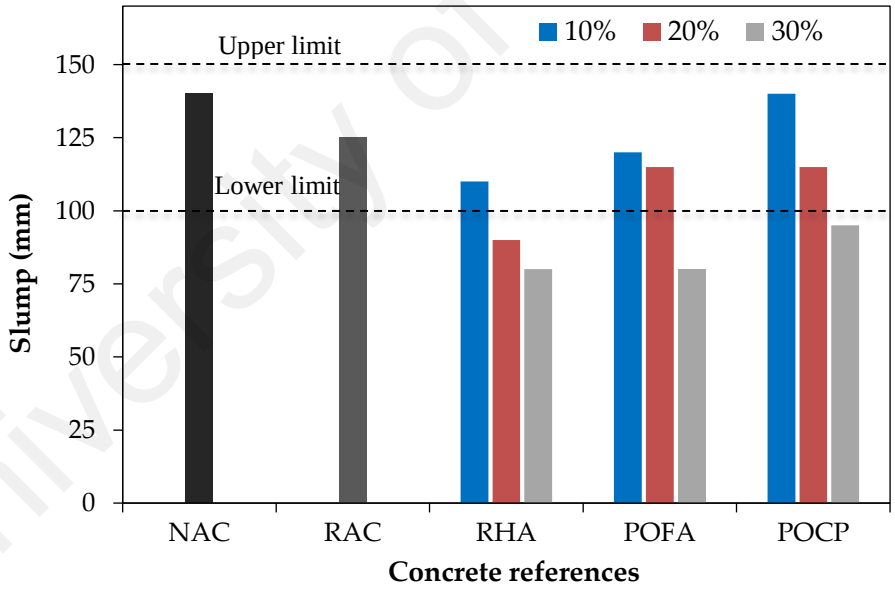

Figure 4.6: Slump results of concretes compared with target slump

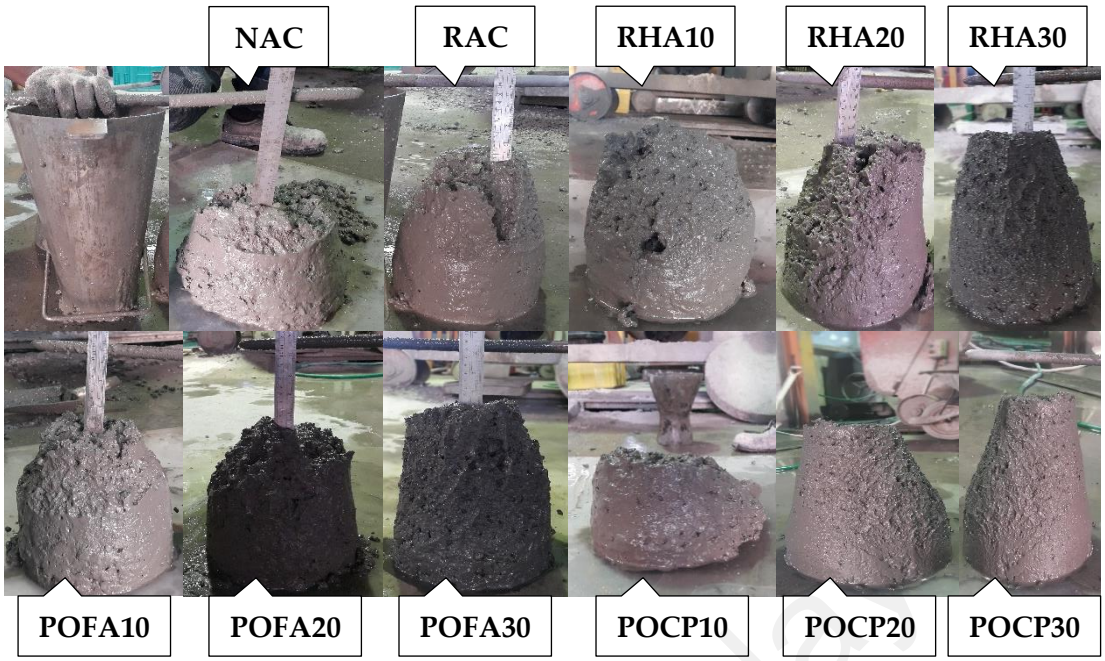

Figure 4.7: Appearance of slump test for all concrete mixes

The slump values of concrete containing RHA decreased compared to the control RAC as the replacement ratio was increased. It can be observed that RHA needs more water to ensure good workability due to its higher fineness compared with OPC. The slump values of POFA- and POCP-based concretes with replacement ratio up to 20% were within the targeted range of 125 ± 25 mm. However, the slump values were lower than the target slump range with greater replacement ratios. The lower slump values could be attributed to the high LOI values in POFA and POCP, which in turn absorb more water to be workable. In addition, as noticed from the SEM morphology in Figure 4.3, the porous texture of POFA particles led to higher water absorption and lower slump values, while the sharp edges of POCP made the particles difficult to roll on each other, which in turn reduces the workability of fresh concrete. The replacement of OPC by SCMs was in terms of weight instead of volume for comparison purposes as the total binder content was kept constant for all mixes. Hence, there was an increase in the binder volume when the replacement levels were varied from 0–30% as a result of the lower specific gravity of RHA, POFA and POCP compared to that of OPC. This extra volume of binder can absorb more water, which in turn affected the workability of concrete. Comparable results were

also reported by Alsubari et al. (2015) specifically that an increase in the replacement level of POFA with low specific gravity affects the workability of concrete. Further, Sata et al. (2007) attributed the reduction in slump to the high absorbency of POFA that resulted in lower slump values.

4.3.2 Fresh and hardened density

The fresh and hardened densities of RAC were expected to be lower than the control mix made from normal aggregate, as RA is about 7.5% lighter than normal aggregate. The fresh densities of all mixtures are shown in Table 4.4, and it can be seen that the fresh density of RAC was found to be 6.0% lower compared with NAC. Similarly, the 28 days hardened density of RAC was 9.4% lower compared with NAC, as old mortar that adhered to the RA reduces the density of aggregate, as shown in Table 4.4. López-Gayarre et al. (2009) stated that the density of concrete is clearly affected by the type of aggregate. It has been found that incorporation of RHA, POFA and POCP in RAC did not affect the density. The fresh and hardened concrete densities were found in the range of 2161–2253 kg/m^3 and 2140 kg/m^3–2191 kg/m^3, respectively.

Table 4.4: Fresh and hardened density of concretes

Mix	Fresh density (kg/m^3)	Hardened density (kg/m^3)
NAC	2408	2340
RAC	2264	2194
RHA10	2216	2186
RHA20	2201	2164
RHA30	2161	2158
POFA10	2229	2180
POFA20	2212	2157
POFA30	2196	2140
POCP10	2253	2191
POCP20	2251	2180
POCP30	2246	2162

4.3.3 Compressive strength development

The compressive strength development for all concrete mixes under water curing (WC) and air curing (AC) conditions at the ages of 1, 7, 14, 28, 56 and 90 days is shown in Table 4.5.

Table 4.5: Compressive strength under air curing (AC) and water curing (WC) conditions

Mix	Compressive strength (MPa)										
	1 Day	7 Days		14 Days		28 Days		56 Days		90 Days	
	AC	AC	WC	AC	WC	AC	WC	AC	WC	AC	WC
NAC	16.1 (0.64)	27.4 (0.85)	32.3 (1.45)	29.2 (0.06)	38.0 (1.50)	37.0 (0.75)	45.4 (0.76)	38.0 (2.90)	47.6 (2.00)	39.8 (1.85)	48.3 (1.13)
RAC	13.0 (0.71)	22.0 (0.85)	26.2 (0.42)	24.5 (1.31)	31.0 (1.06)	28.8 (0.06)	35.8 (1.15)	30.3 (0.26)	37.1 (0.15)	31.4 (1.33)	38.4 (0.81)
RHA10	14.0 (0.31)	26.0 (0.25)	29.0 (0.51)	30.8 (0.75)	34.2 (0.12)	34.3 (1.70)	38.9 (1.47)	34.5 (0.32)	45.2 (0.85)	34.7 (1.90)	46.2 (1.81)
RHA20	12.7 (0.85)	24.4 (0.93)	27.0 (0.26)	30.8 (0.23)	32.2 (0.31)	33.3 (0.55)	37.0 (1.25)	34.5 (0.40)	41.4 (0.90)	33.6 (0.40)	43.3 (1.57)
RHA30	11.3 (0.36)	19.5 (1.40)	22.9 (0.80)	21.0 (0.79)	27.2 (0.76)	29.8 (0.82)	33.3 (0.61)	28.9 (0.75)	35.6 (0.25)	31.4 (1.40)	38.0 (1.31)
POFA10	12.7 (0.15)	20.2 (1.22)	22.8 (1.87)	24.7 (1.80)	26.0 (0.46)	27.4 (0.74)	31.0 (1.21)	28.7 (1.97)	37.3 (1.66)	29.5 (1.61)	39.3 (1.05)
POFA20	11.0 (0.67)	19.3 (1.05)	21.4 (2.81)	22.7 (0.81)	24.2 (1.01)	25.3 (1.27)	28.5 (1.23)	24.8 (1.43)	32.7 (0.10)	27.0 (0.83)	36.5 (0.71)
POFA30	10.5 (0.36)	17.5 (0.95)	19.3 (0.20)	19.7 (0.31)	22.1 (0.10)	23.2 (0.29)	26.1 (0.06)	25.3 (0.62)	30.0 (1.35)	26.1 (0.75)	32.5 (0.64)
POCP10	12.6 (0.31)	21.1 (1.10)	23.3 (1.46)	21.8 (0.55)	25.7 (0.46)	26.2 (1.04)	29.7 (2.46)	27.1 (0.71)	35.3 (1.25)	27.4 (0.46)	37.4 (0.91)
POCP20	12.2 (0.26)	20.5 (0.38)	23.1 (0.17)	24.2 (0.93)	27.0 (1.25)	26.9 (0.10)	30.4 (2.12)	27.0 (0.50)	34.2 (0.89)	28.3 (0.17)	36.7 (0.60)
POCP30	9.7 (0.15)	16.0 (0.44)	18.9 (0.57)	21.0 (0.55)	23.0 (0.25)	24.5 (0.50)	26.5 (0.87)	25.1 (0.85)	29.7 (1.16)	26.0 (0.89)	32.1 (0.90)

Notes: 1) The compressive strength value shown in the table is the average of three specimens. 2) The standard deviation of the compressive strength is shown in the brackets ().

4.3.3.1 Effect of water curing condition

Based on the test results in Table 4.5 and Figure 4.8, it was found that at all ages, the compressive strength decreased as normal aggregates were wholly replaced by RA. After 28 days of water curing, the reference concrete prepared with normal aggregate (NAC) had a compressive strength of about 45 MPa, compared to 36 MPa for RAC with a reduction of about 20%. This reduction could be attributed to the presence of weak and

loose adhered mortar on the surface of the RA, which makes it porous. Accordingly, the compressive strength will be controlled by the strength of the aggregate itself, where it is the weakest point. However, Etxeberria et al. (2007) observed that the concrete with the target compressive strength of 45–60 MPa can be determined by the strength of the aggregate itself when they reported that the compressive strength of RA concrete was 20%–25% lower than concrete made from normal aggregate at the age of 28 days. Besides, Andreu and Miren (2014)stated that the 100% replacement of natural coarse aggregate by RA would be possible if RA concrete produced from old (parent) concrete with a minimum compressive strength of 60 MPa. Moreover, a similar behavior was observed by Kou and Poon (2015) when they indicated that the reduction in the strength was notable for RA concretes derived from parent concrete with lower strength, while the strength was similar for RA concretes derived from parent concrete with higher strength.

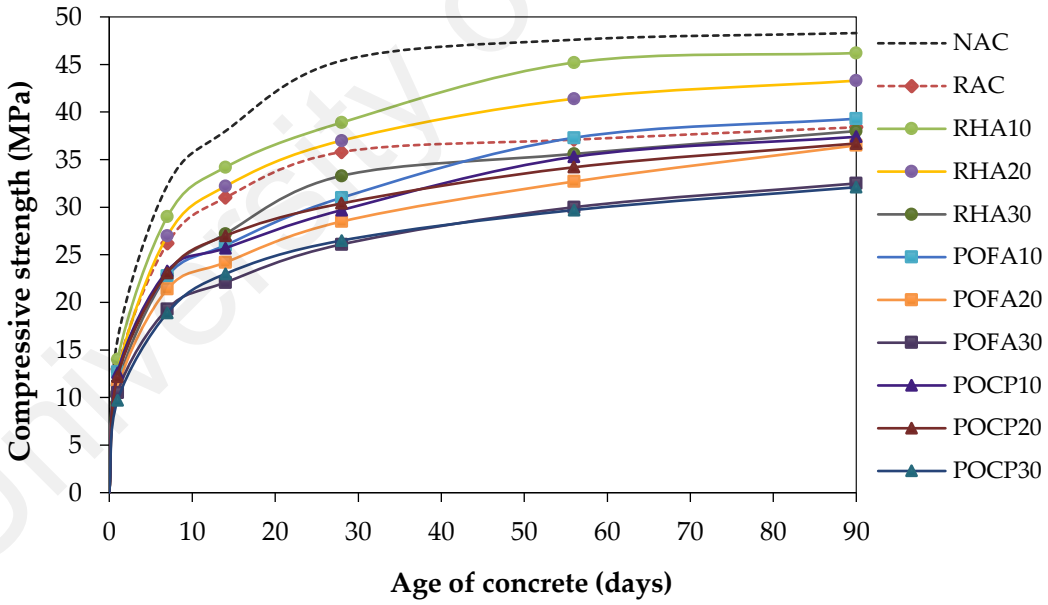

Figure 4.8: Compressive strength development of SCMs concretes cured in water

Figure 4.9 shows the development of the compressive strength of RHA concretes at different replacement ratios up to 90 days. It can be seen that the compressive strengths of concrete that contains RHA up to 20% were higher than RAC at all ages under the water curing condition. The compressive strengths of RHA10 and RHA20 concretes at

the age of 28 days were about 39 MPa and 37 MPa, respectively, which were higher than that of RAC concrete (36 MPa), while RHA30 gave lower compressive strength of about 33 MPa. This can be explained partially to the high silica content of RHA and partially to the extra calcium silicate hydrate (C-S-H) that was generated as a result of pozzolanic reaction between RHA particles and $Ca(OH)_2$. Consequently, as shown in Figure 4.10, the compressive strength was enhanced at the later ages for RHA10, RHA20 and RHA30 with about 46, 43 and 38 MPa or 120%, 113% and 99% of RAC at the age of 90 days, respectively.

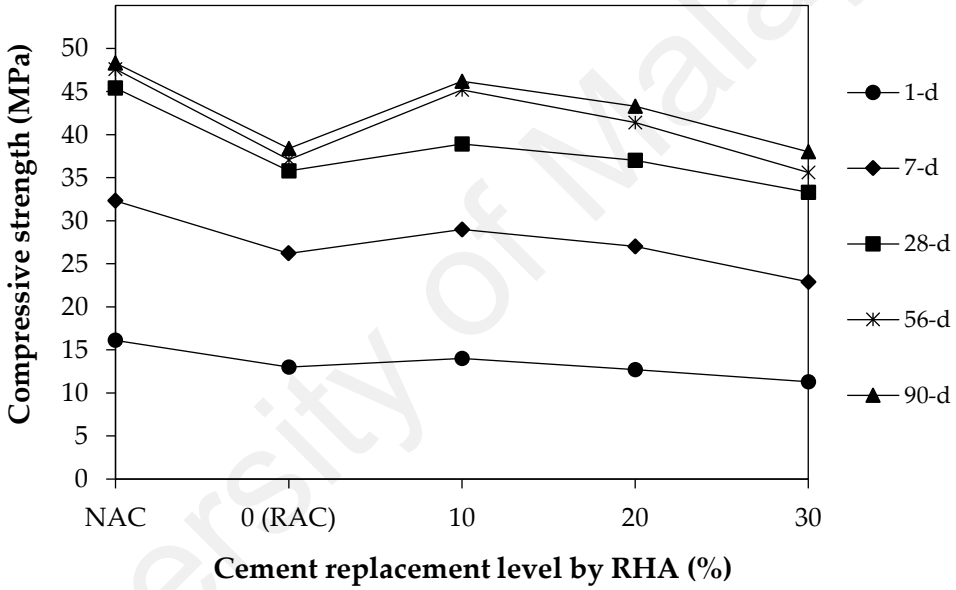

Figure 4.9: Relationship between the compressive strength of RHA concretes and replacement level

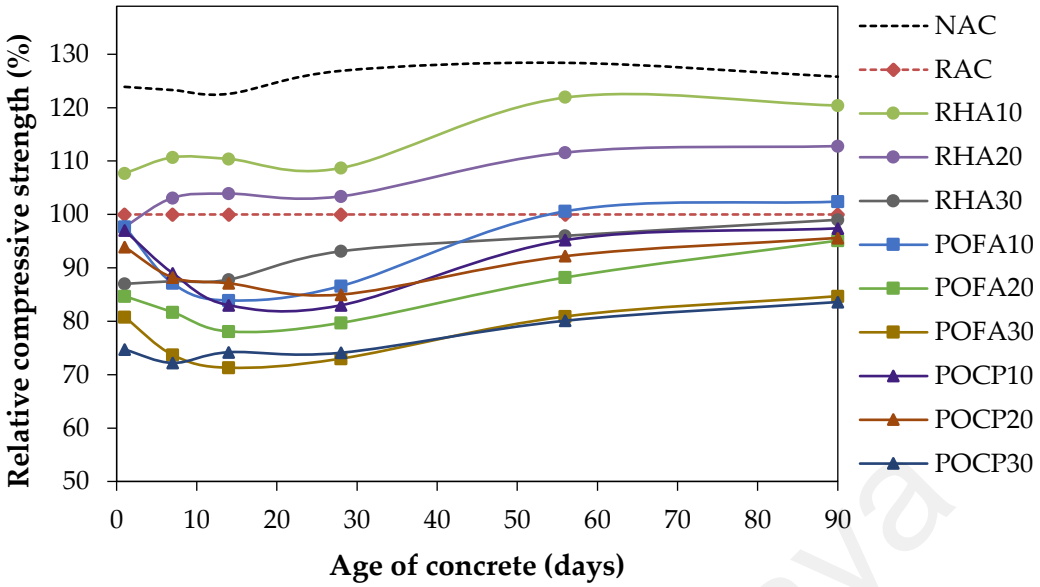

Figure 4.10: Relative compressive strength of RA concrete with SCMs

The compressive strengths of concretes made with POFA at different replacement ratios are shown in Figure 4.11. The RA concretes with POFA yielded lower compressive strength than RAC mix without POFA at the early age (< 28 days). For instance, the compressive strength at 28 days for RAC concrete was 36 MPa, and it was higher than POFA10, POFA20 and POFA30 concretes with 31, 29 and 26 MPa or 86%, 81% and 72% of RAC mix, respectively. After 90 days, at a cement replacement of 10% by POFA, the compressive strength tended to increase with 39 MPa or 103% of RAC mix, while it was about 37 and 33 MPa or 97% and 87% for POFA20 and POFA30, respectively, compared with RAC. It can be observed that the replacement of POFA in concrete mixes as binder will cause a reduction in the compressive strength at an early age, as shown in Figure 4.10. On the other hand, the compressive strength development showed an increasing trend at the later ages (>28 days) as a result of the formation of extra C-S-H gel upon reaction between the high content of SiO_2 from POFA with the $Ca(OH)_2$ produced during the cement hydration process (Sata et al., 2004). Moreover, as mentioned by Alsubari et al. (2016) and Mujah (2016), the increase in compressive strength was due to the densification effect and the improvement of the micro-structure of concrete containing POFA.

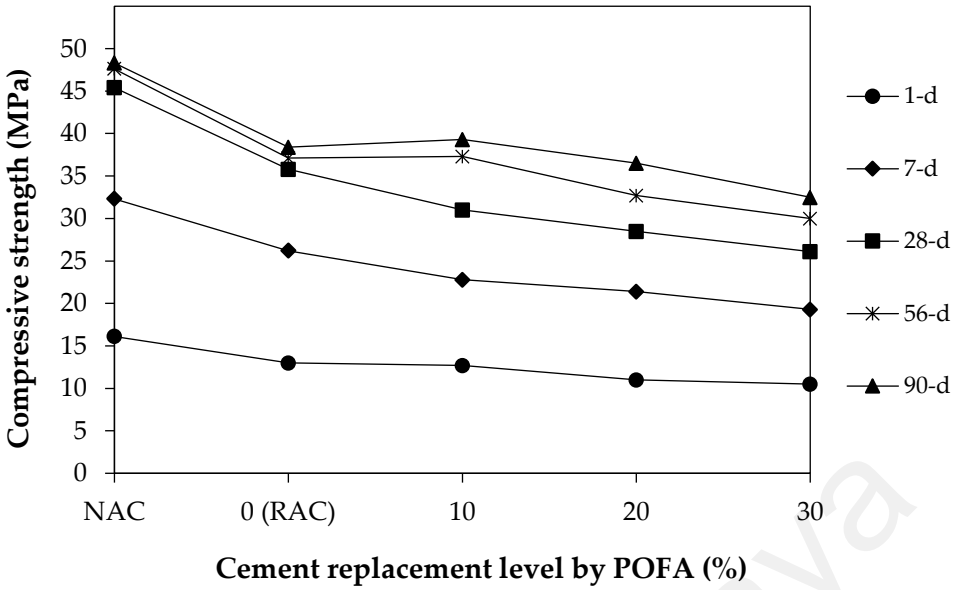

Figure 4.11: Relationship between the compressive strength of POFA concretes and replacement level

The relationship between compressive strength and cement replacement level of POCP concretes is shown in Figure 4.12. At the first day, the incorporation of POCP with RA concrete recorded a compressive strength of about 13, 12 and 10 MPa; and the strength increased to 23, 23 and 19 MPa at the age of 7 days for POCP10, POCP20 and POCP30, respectively. Subsequently, after 28 days of water curing, the POCP concretes exhibited lower compressive strength than RAC concrete with strength values of about 30, 31 and 27 MPa or 83%, 86% and 75% of RAC concrete for POCP10, POCP20 and POCP30, respectively. Figure 4.10 indicates that the early strength attainment was relatively slow for POCP concretes due to the lower reaction between OPC and POCP compared to high pozzolanic materials, such as RHA. In addition, the higher compressive strength of POCP concretes at replacement level of 10% and 20% than that of 30% is attributable to the high content of cement (90% and 80%) in POCP10 and POCP20 concretes, which generates a higher hydration reaction than that of POCP30 concrete at the early age as reported by Kanadasan and Abdul Razak (2015). At the age of 90 days, the compressive strengths for POCP10, POCP20 and POCP30 were 37.4 MPa, 36.7 MPa and 32 MPa or

97.4%, 95.6% and 83.6% of RAC, respectively. It is apparent that the compressive strength of POCP concretes did not exceed the strength of that without POCP (RAC).

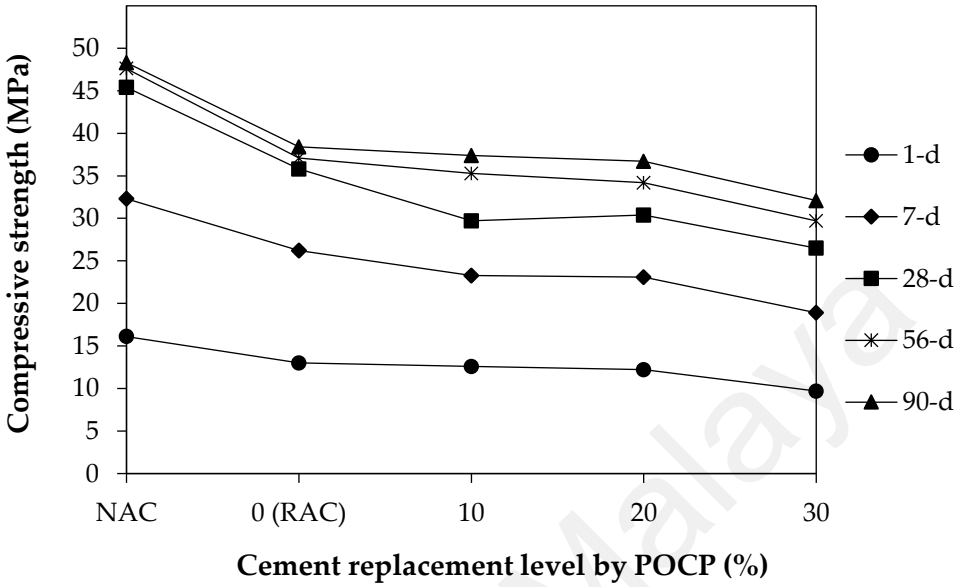

Figure 4.12. Relationship between the compressive strength of POCP concretes and replacement level

Figure 4.13 shows the evolution of compressive strength from 28–90 days for concretes containing SCMs as compared with recycled and normal concrete. Although the compressive strength of RAC was lower than NAC, the increment in the strength was similar between 28 and 90 days at 6.0%. Similar trends of strength evolution were observed by Kou and Poon (2013) when they investigated the properties of 10-year-old concrete made from 100% RA. On the other hand, the compressive strength increased by about 16%, 15% and 12% for RHA10, RHA20 and RHA30, respectively, between 28 and 90 days. Moreover, POFA10, POFA20 and POFA30 showed an increment of 21%, 22% and 20%, respectively. Furthermore, the increment for POCP10, POCP20 and POCP30 was 21%, 17% and 18%, respectively. It is clear that the strength increment of concrete mixes with SCMs was higher than that of corresponding concrete mix without SCMs (NAC and RAC) between 28 and 90 days.

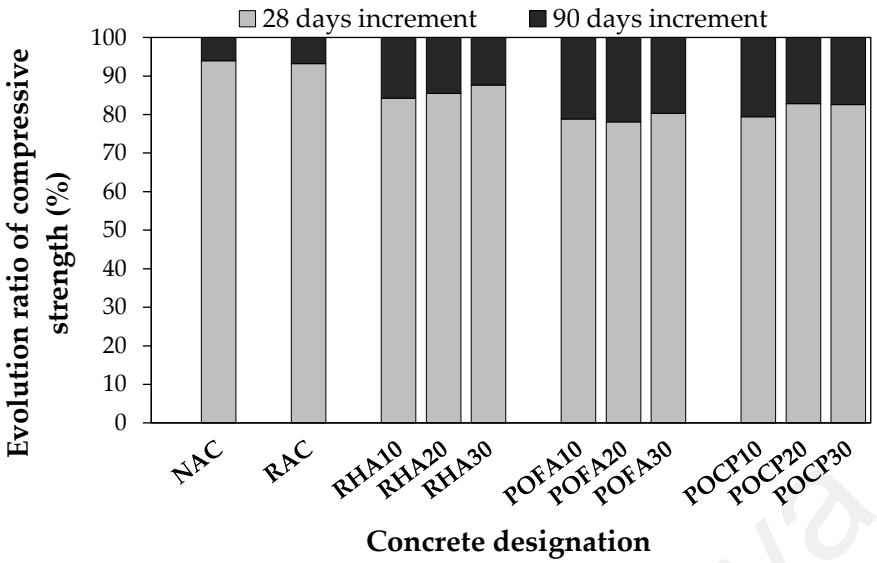

Figure 4.13: Evolution of compressive strength from 28-days to 90-days of concrete series

Generally, the results revealed that the optimum cement replacement using RHA, POFA and POCP was 10% for concrete made from 100% RA. However, if the amount of pozzolanic materials increased beyond 10% and with the subsequent reduction in cement content, these would lead to a dilution effect, where the reaction between SiO_2 and $Ca(OH)_2$ will also be reduced. In addition, the results show that the targeted strength of 30 MPa for RA concrete can be achieved at the age of 90 days by replacing up to 30% of RHA, POFA and POCP for cement. This finding is similar to the findings of the study by Sata et al. (2007) on the utilization of RHA and POFA in making high-strength concrete. Furthermore, the replacement of cement by using sustainable SCMs through RHA, POFA and POCP in the development of concrete would result in environmentally-friendly construction compared to the conventional concrete.

4.3.3.2 Effect of air curing condition

As expected, it is clearly seen from Figure 4.14 that generally, the water-cured concretes exhibited higher compressive strength than the air-cured concretes. Nevertheless, the main observation is that at the early age (< 28 days), the concretes containing SCMs gained higher compressive strengths of about 7%–12% as a result of

water curing, while the respective increment for NAC and RAC was about 19%. However, the strength developed exponentially between the 28- and 90-day period for concretes with SCMs, which increased at the range of 22% – 27% as a result of water curing; as the mixes NAC and RAC had no SCM, the increment was about 18% in the water curing condition. This indicates that the acceleration of the rate of the hydration in the water curing condition at later stage for concrete mixes containing SCMs. Similarly, Islam et al. (2016b) and Shafigh et al. (2016) reported that the water-cured concrete containing pozzolanic materials exhibited a higher rate of increment at the later age compared to those without pozzolanic materials.

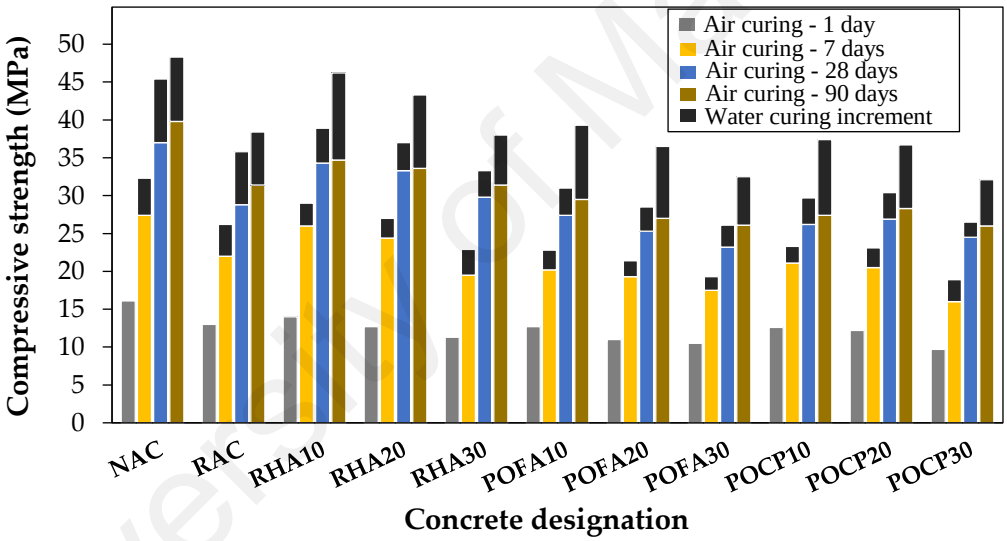

Figure 4.14: Effect of curing conditions on the compressive strength of concrete

4.3.3.3 Strength efficiency

The strength efficiency of concrete indicates the yielded compressive strength per kilogram cubic meter of cement and denoted as MPa/kg.m^{-3}. The effect of RHA, POFA and POCP on the compressive strength efficiency of RA-based concrete is shown in Figure 4.15. At the age of 28 days, the strength efficiency of concretes containing RHA, POFA and POCP was in the ranges of 0.114-0.125, 0.091-0.098 and 0.087-0.100 MPa/kg.m^{-3}, respectively, compared to 0.094 MPa/kg.m^{-3} for RAC. Moreover, the 90 days strength efficiency increased to the ranges of 0.135-0.143, 0.115-0.122 and 0.109-

0.121 MPa/kg.m^{-3} corresponding to the concrete containing RHA, POFA and POCP, respectively. It can be observed that the 90 days strength efficiency values are 1.1-1.4 times higher than that of RAC (0.101 MPa/kg.m^{-3}), depending on the type and the level of SCM incorporated. In addition, the results show that the higher amount of SCM content, the higher the strength efficiency. Similar results obtained by Chao-Lung et al. (2011) for the effect of RHA on the strength efficiency of concrete. They pointed out that the 90-d efficiency value of concrete containing RHA up to 30% was 1.2–1.5 times higher than that of the control concrete.

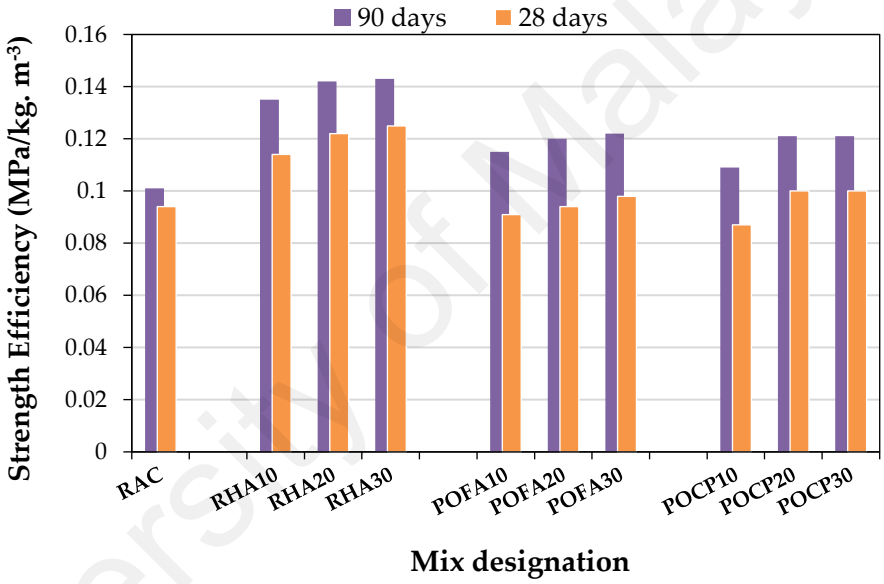

Figure 4.15: The effect of SCMs on the compressive strength efficiency of RA-based concrete

4.3.4 Ultrasonic pulse velocity

The ultrasonic pulse velocity (UPV) is a non-destructive test to check the strength and quality of concrete element by measuring the velocity of an ultrasonic pulse passing through the concrete element. Figure 4.16 shows the UPV values for all mixes at the ages of 1, 7, 28 and 90 days under air and water curing conditions. It can be seen that the UPV values for concrete mixtures prepared from 100% RA were found to be lower than those made from normal aggregate. After 28 days of water curing, the UPV value of NAC was 4.60 km/s, and this shows that the concrete is of "excellent" quality, while the UPV value

of 4.31 km/s obtained for RAC exhibits "good" quality concrete (Saint-Pierre et al., 2016). This could be related to the porous structure of the RA, which led to a reduction in the pulse velocity because of the impeding effect of air. A similar concept was reported by Trtnik et al. (2009) when they mentioned that the UPV is influenced by the type of aggregate. In the case of concrete mixes containing SCMs, at 28 days, the UPV values ranged between 4.05 km/s and 4.49 km/s, and this could be categorized as "good" quality concrete. After 90 days of water curing, the UPV values of RHA10, RHA20, POFA10 and POCP10 exceeded 4.5 km/s, and hence, it can be inferred that the pozzolanic reaction resulted in concrete of "excellent" quality. This enhancement could be attributed to the densification effect of the additional C-S-H gels, which were produced during the pozzolanic reaction after 90 days of curing.

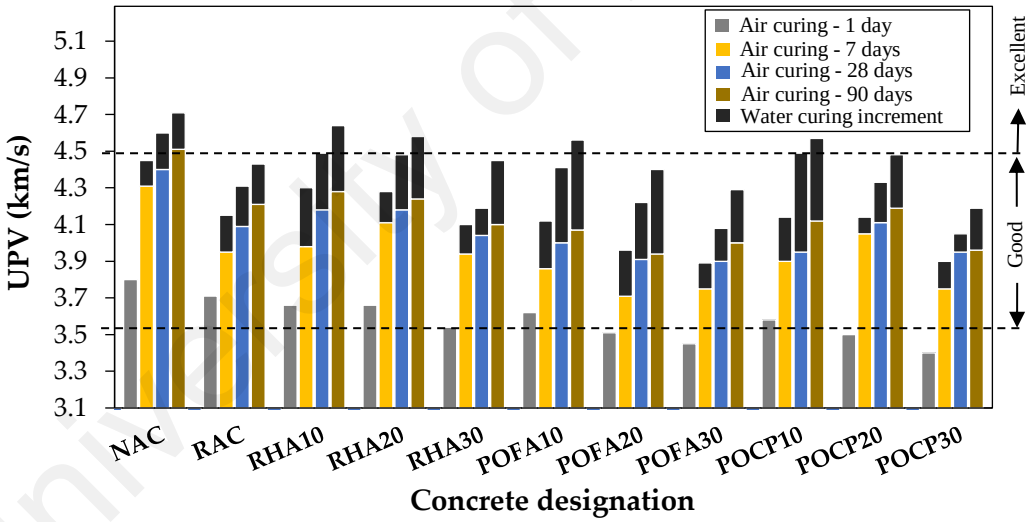

Figure 4.16: Ultrasonic pulse velocity (UPV) values under air and water curing conditions for SCM concretes

Figure 4.17 illustrates the correlation for prediction of the compressive strength based on the UPV values for concretes containing SCMs. Generally, for all concrete mixes, the UPV improved when the curing age was increased as a result of the hydration process in concrete. These values are comparable with the results obtained by Kou et al. (2011) for concrete containing fly ash and silica fume as SCMs in RA concrete.

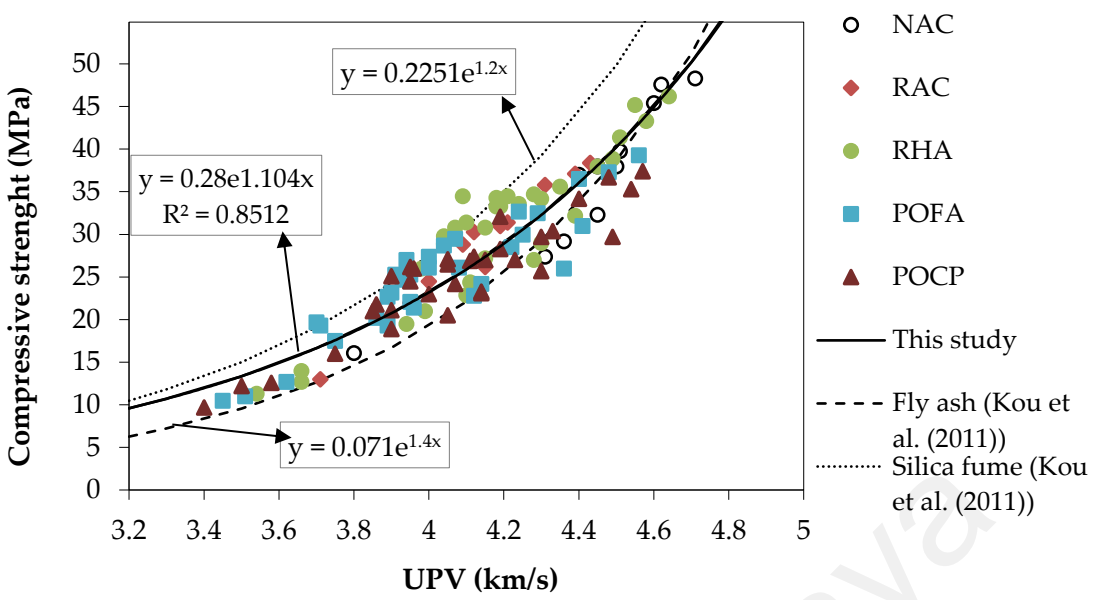

Figure 4.17: Relationship between compressive strength and UPV of RA concrete containing SCMs

4.3.5 Splitting tensile strength

The results of splitting tensile strength for all mixtures at the ages of 28, 56 and 90 days can be found in Table 4.6. The 28 days and 90 days splitting tensile strengths of RAC were found as 3.28 and 3.56 MPa; however, for NAC, as expected, the respective results were slightly higher than RAC, and the values of 3.50 and 3.87 were obtained at the ages of 28 days and 90 days, respectively. One of the salient points is that the utilization of 100% RA in concrete did not substantially affect the splitting tensile strength due to the high quality of parent concrete with compressive strength of about 52 MPa. Tabsh and Abdelfatah (2009) summarized that RA concrete made from parent concrete with compressive strength of 50 MPa is as strong as the normal concrete in tensile strength. Another study by Sagoe-Crentsil et al. (2001) shows that the tensile strength depends mainly on the binder rather than the aggregate type. In addition, the angular shape of RA minimized the adverse effect on splitting tensile strength due to the better interlocking of aggregates that can be obtained because of angularity of the RA. Furthermore, the failure in NAC mix occurred in the ITZ between the aggregate and cement matrix (the weakest point), while the weakest point in the RA concrete is the old

cement paste; Hence, the failure occurred along the RA itself rather than the ITZ. On the other hand, the splitting tensile results of concretes with SCMs showed a comparable trend with the results of compressive strength at 28 days. As explained in the compressive strength, the effect of SCMs were felt at a later age, as the 90 days splitting tensile strengths of the mixes RHA10, RHA20 and POFA10 exhibited enhancement in the tensile strength by about 108%, 102% and 101%, respectively compared to the RAC. Further, the mix POCP30 produced the lowest 90 days splitting tensile strength of 3.05 MPa, and it was about 86% of RAC mix, as shown in Figure 4.18. The enhancement in the splitting tensile strength of RHA and POFA concretes could be due to the enhanced microstructure of the bond between the new cement paste and the RA. Since the RA is more porous than normal aggregates, part of the SCM particles penetrate into the pores of RA, which subsequently improve the ITZ bonding between the paste and aggregate as reported by Kou et al. (2011), while the trend of reduced tensile strength of POCP concretes gave an indication that it was not effective in improving the ITZ between aggregate and cement matrix.

Table 4.6: Splitting tensile strength of concrete

Mix	Splitting tensile strength (MPa)		
	28 Days	56 Days	90 Days
NAC	3.50	3.60	3.87
RAC	3.28	3.36	3.56
RHA10	3.47	3.56	3.85
RHA20	3.39	3.52	3.62
RHA30	2.99	3.22	3.37
POFA10	3.06	3.27	3.61
POFA20	3.08	3.15	3.28
POFA30	2.82	2.94	3.16
POCP10	2.89	2.98	3.20
POCP20	2.95	3.13	3.17
POCP30	2.80	2.97	3.05

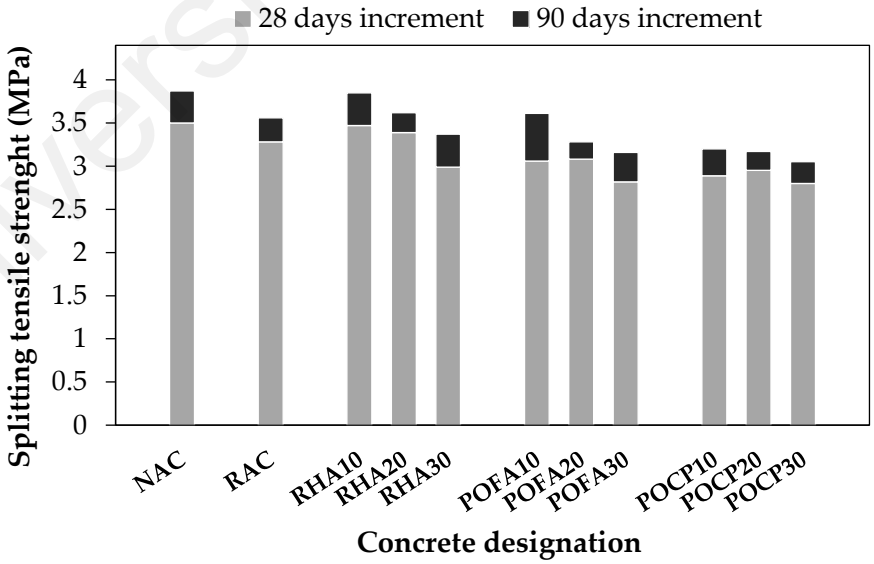

Figure 4.18: Evolution of splitting tensile strength between 28 and 90 days.

Generally, the results at the age of 28 days showed that the ratio between splitting tensile strength and compressive strength for NAC is about 8%, while for concretes containing RA and SCMs, it was in the range between 9% and 11%. After 90 days, the splitting tensile values ranged between 8% and 10% for concretes containing SCMs, which is almost similar to NAC mix with 8%. These results are comparable with the results published by Çakır (2014) with values ranged from 7.7% – 11.4% for RA concrete with mineral additives, such as silica fume and GGBS. In addition, the results indicated that the ratio between splitting tensile strength and compressive strength decreases when the compressive strength increases.

Figure 4.19 shows the splitting tensile strength of RA concretes as a function of the compressive strength and compared to the reference equation suggested by ACI 318-14 for normal concrete and the equation suggested by Çakır (2014) on the utilization of RA concrete with mineral additives, i.e., silica fume and GGBS as SCMs. It can be seen that the splitting tensile strength obtained from this study for RA concrete blended with RHA, POFA and POCP is lower than that of the values proposed by ACI 318-14, which could be due to the low correlation between the results of RA concrete with SCMs, as represented by the trend line, and the correlation proposed by ACI 318-14. This might be due to the fact that the incorporation of RA affected the compressive strength which reflected on the equation proposed by ACI 318-14, though the splitting tensile strength was not affected much. However, closer values were obtained from the equation proposed by Çakır (2014), which is more suitable since it was generated for RA-based concrete with SCMs.

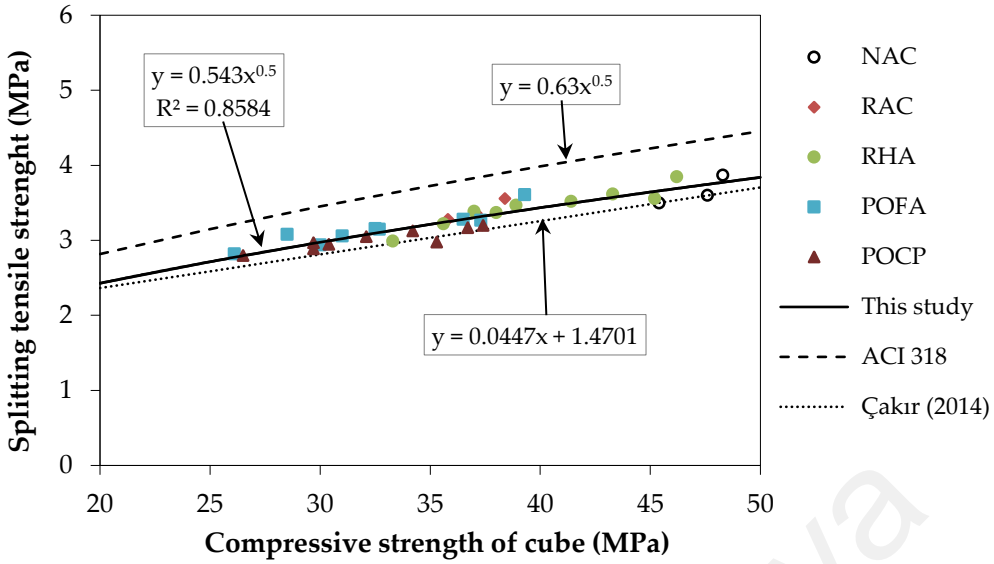

Figure 4.19: Splitting tensile strength of RA concrete containing SCMs as a function of the compressive strength

4.3.6 Flexural strength

The effect of SCMs with various replacement levels on flexural strength at the ages of 28, 56 and 90 days is shown in Table 4.7. After 28 days of water curing, the NAC mix using normal aggregate showed flexural strength of 4.50 MPa, while the RAC mix with 100% RA showed flexural strength of 3.81 MPa. According to these results, it can be observed that RAC has a flexural strength reduction of about 15% and follows a trend similar to those results of compressive strength compared to NAC. A similar trend can be seen, as Sheen et al. (2013) reported about a 10%–23% reduction in the flexural strength for the specimens prepared with RA when compared with control specimens with normal coarse aggregate. The lower flexural values could be attributed to the weak nature of the RA, which allows the aggregate to fail faster compared to the cement paste. At the age of 28 days, the results of RA concrete containing SCMs did not show any improvement in the flexural strength except for the mix RHA10, which was 4.06 MPa or about 7% higher than the corresponding result for RAC. However, as in the case of compressive and splitting tensile strengths, after 90 days, the flexural strengths of RHA10, RHA20 and POFA10 were found to improve, as the flexural strengths of 4.90 MPa, 4.74 MPa and 4.72 MPa or 110%, 106% and 105%, respectively, of the control RAC were obtained.

These results showed that the utilization of RHA up to 20% and POFA at a replacement level of 10% will improve the flexural strength of RA concrete. Nevertheless, the incorporation of POCP at any replacement levels lowered the flexural strength compared to the control specimens, and this could be attributed to the lower pozzolanic activity of POCP compared to other pozzolanic materials (Karim et al., 2016). The substantial increase in the later-age flexural strength of mixes with incorporation of RHA and POFA as shown in Figure 4.20 could be attributed chemically to the pozzolanic reaction, which improves the interfacial bonding between the aggregates and pastes and physically due to the filler effect and enhanced microstructure of the matrix (Jaturapitakkul et al., 2011; Rukzon et al., 2009).

Table 4.7: Flexural strength of concrete

Mix	Flexural strength (MPa)		
	28 Days	56 Days	90 Days
NAC	4.50	4.71	4.93
RAC	3.81	4.18	4.36
RHA10	4.06	4.54	4.90
RHA20	3.66	4.46	4.74
RHA30	3.53	4.05	4.39
POFA10	3.79	4.42	4.72
POFA20	3.53	4.08	4.44
POFA30	3.36	3.72	4.17
POCP10	3.75	4.12	4.46
POCP20	3.64	3.89	4.40
POCP30	3.30	3.86	3.99

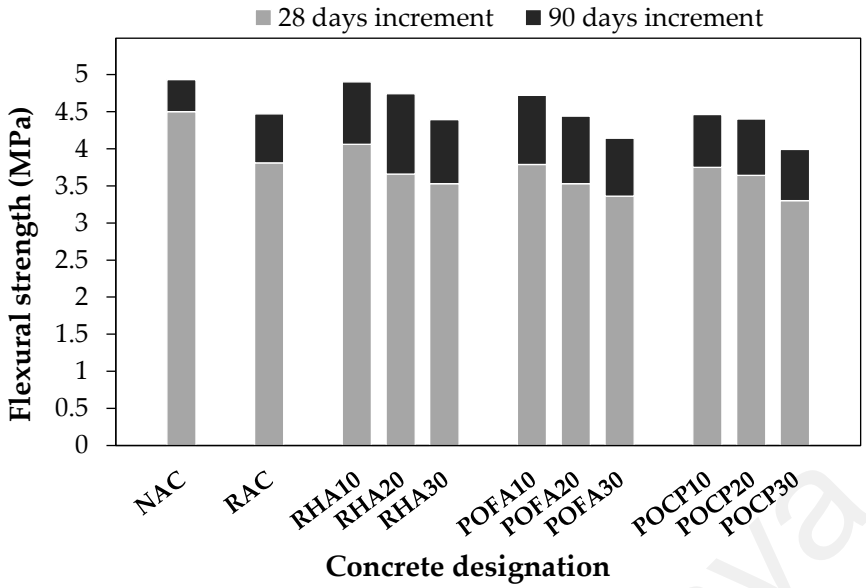

Figure 4.20: Evolution of flexural strength between 28 and 90 days

Figure 4.21 demonstrates the relationship between the flexural strength of RA concrete and its compressive strength compared to the relation suggested by ACI 318-14 in addition to the relation established by Xiao et al. (2006), who reviewed the flexural strength of the RA concrete obtained by various researchers. It was found that the flexural strength of RA concrete blended with RHA, POFA and POCP is lower than that provided by Xiao et al. (2006). In addition, the equation suggested by ACI 318-14 is slightly lower than that of this study. This is due to that the ACI 318 equation is very conservative for natural aggregate concrete without any SCMs, where the quality of original concrete seems to restrict the qualities achievable in recycled aggregate concrete. However, the complex effects and interactions of various variables make it difficult to come up with specific predictions regarding the behavior of RA in concrete without conducting tests under applicable circumstances.

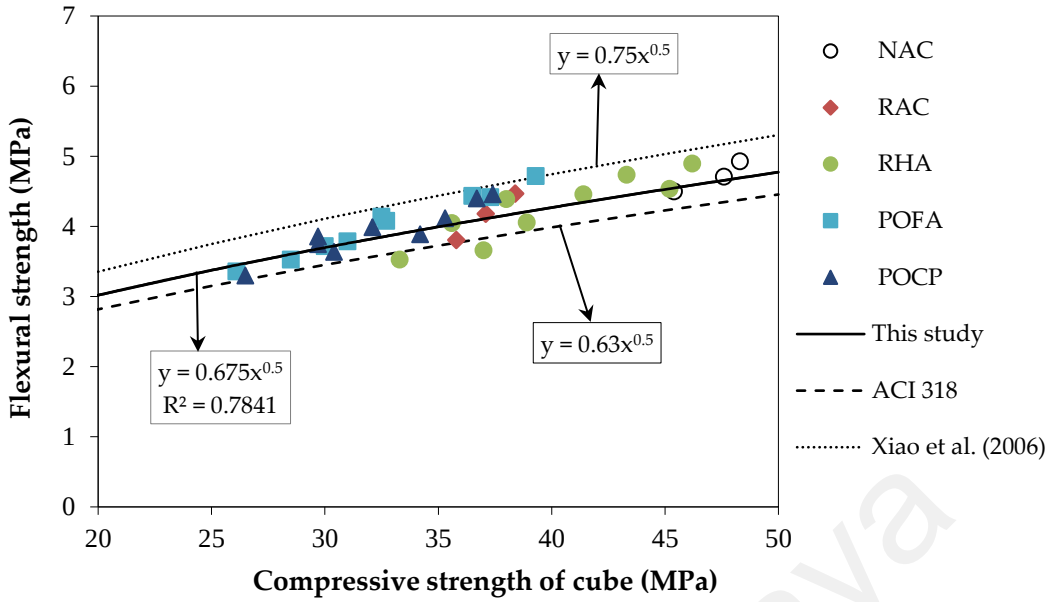

Figure 4.21: Flexural strength of RA concrete containing SCMs as a function of the compressive strength

4.3.7 Modulus of elasticity

Table 4.8 shows the development of static modulus of elasticity at the ages of 28, 56 and 90 days for all mixes. It was found that the 28, 56 and 90 days moduli of elasticity of RAC and NAC mixes were about 23, 25 and 26 GPa and 30, 31 and 32 GPa, respectively. These values show that concrete made from RA produced about a 19% – 23% lower modulus of elasticity compared with the normal concrete. The main reason for the reduction in the modulus of elasticity could be the presence of old mortar with a relatively low modulus of elasticity; the RA, due to its porosity, affects the modulus of elasticity of concrete, as its inability to resist the deformation directly influences the modulus of elasticity of concrete. A similar result was obtained by Etxeberria et al. (2007), who attributed the reduction in the modulus of elasticity of RA concrete from 32 GPa down to 28.6 GPa (11%) to the lower modulus of RA than the corresponding modulus of normal aggregate. Nevertheless, Adams et al. (2016) revealed that RA-based concrete with a low modulus of elasticity is less susceptible to cracking due to its ability to sustain more deformation. They opined that the residual mortar content in RA particles has a beneficial effect in reducing the differential strains caused by the differences in the moduli of

elasticity between the cement paste and natural aggregates, which in turn decreases crack propagation in the ITZ. Thus, there may be a beneficial effect in minimizing the cracks when RA is incorporated in concrete.

Table 4.8: Modulus of elasticity of concrete

Mix	Modulus of elasticity (GPa)		
	28 Days	56 Days	90 Days
NAC	29.5	30.8	31.3
RAC	23.0	24.6	25.6
RHA10	23.6	25.3	26.7
RHA20	22.8	24.4	25.4
RHA30	20.5	22.2	22.8
POFA10	21.2	23.9	24.3
POFA20	21.1	21.6	22.6
POFA30	19.8	20.7	21.3
POCP10	22.1	22.5	25
POCP20	21.7	22.4	24.4
POCP30	19.0	20.4	21.0

In the case of RA concretes containing RHA, POFA and POCP, the moduli of elasticity values at the age of 28 days were in the range from 19 GPa–24 GPa for all mixes, regardless of the type and level of material used to replace the cement. It can be observed that only RHA10 exhibited a higher 28 days modulus of elasticity value of about 23.6 GPa (about 103%) than that of RAC. After 90 days, the results did not show any significant increase in modulus of elasticity values, as shown in Figure 4.22. For example, the results show that RHA10, RHA20 and RHA30 increased 12%, 11% and 10% between 28 and 90 days, respectively. Moreover, POFA10, POFA20 and POFA30 increased 13%, 6% and 7%, respectively. Furthermore, POCP10, POCP20 and POCP30 increased 12%,

11% and 10%, respectively. On the other hand, the increments in the compressive strength between 28 days and 90 days, as mentioned in Section 4.2.3.1, were higher than these values. For instance, POFA10 had the highest increment of 21% in the case of compressive strength, while it was 13% in the case of the modulus of elasticity for the same mixture.

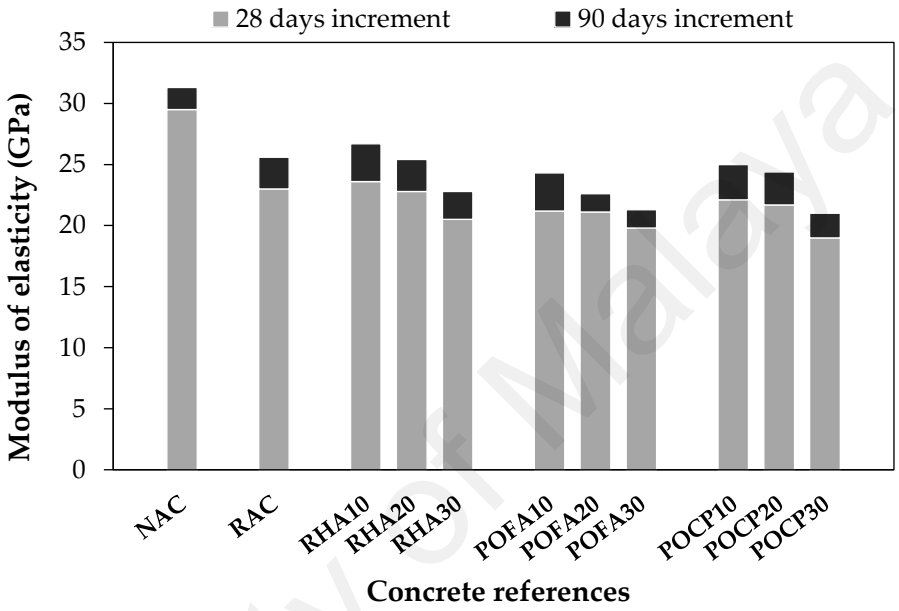

Figure 4.22: Evolution of modulus of elasticity between 28 and 90 days

According to these results, it can be observed that the concrete prepared from 100% RA and containing SCMs contributed more to the compressive strength than the modulus of elasticity. The reason attributed to that is the elastic property of the aggregate has a more significant effect than the strength of the cement matrix. Therefore, the overall stiffness was largely influenced when the normal aggregate was fully replaced by RA, and consequently, the modulus of elasticity was significantly affected. The same concept was observed by Fonseca et al. (2011) as they attributed the lower modulus of elasticity values of RA concrete to the lower stiffness and higher porosity of RA compared with normal aggregate. On the other hand, despite partial replacement of cement with SCMs at different levels, the overall stiffness was not substantially influenced. However, the RA concrete with and without SCMs still related to the compressive strength, where the

concretes with higher compressive strength values have higher modulus of elasticity values.

Figure 4.23 shows the relationship between modulus of elasticity determined based on cylinder samples of Ø150 mm and 300 mm in length, as well as the cylinder compressive strength. It can be seen that, generally, the modulus of elasticity values of RA concretes with and without SCMs are less than the values predicted by ACI 318-14. Besides, it can be seen that the equation proposed by Tangchirapat et al. (2008) for concrete made from 100% RA and RHA predicts modulus of elasticity values closer to the values of this study. According to Silva et al. (2016), RA concretes were expected to present a parallel development of the modulus of elasticity regardless of SCM contents.

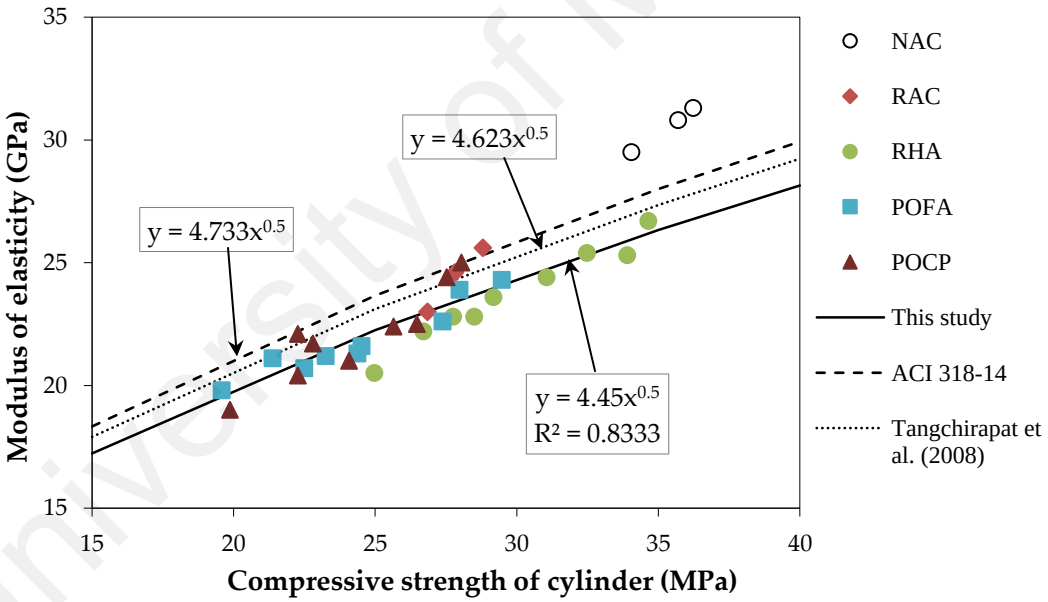

Figure 4.23. Modulus of elasticity of recycled aggregate concrete containing SCMs as a function of the compressive strength

4.4 Durability properties

4.4.1 Water absorption

The water absorption of concrete plays a significant role in controlling its durability. Thus, the relationship between the water absorption and the characteristics of pore structure was conducted to develop criterion for concrete durability. It is well-known that

more pores in concrete means higher susceptibility towards the penetration of fluids. Table 4.9 shows the percentage of water absorbed after fully immersing the specimens in water for 30 minutes and 72 hours to determine the initial and final water absorption, respectively, at the ages of 28 and 90 days. According to the results of 28 days, the initial water absorptions of NAC and RAC were 2.5% and 3.2%, while the final water absorptions were 5.2% and 6.7%, respectively. It can be observed that the water absorption of RAC was about 28% higher than that of NAC, which could be attributed to the high absorbency of the old cement mortar found in RA particles; the same concept has been reported by other researchers as well (Dilbas et al., 2014; Kou & Poon, 2012). For concretes containing RA and SCMs, the initial and final water absorptions at the age of 28 days varied in narrow range of 3.0-3.7% and 6.5-7.5%, respectively. On the other hand, after 90 days of water curing, concrete specimens containing SCMs showed a significant enhancement against water absorption, where they decreased to the ranges of 2.3-3.3% and 4.8-6.7% corresponding to the initial and final water absorption, respectively. The results showed that the resistance of RA-based concrete against water absorption was enhanced after long curing period of 90 days using RHA, POFA and POCP at replacement levels of up to 30%. The improved performance of concrete containing the aforementioned SCMs in terms of resisting water absorption was due to the fact that they have high SiO_2 content, thus producing additional C–S–H gel, which the latter has the potential to fill the existing voids and enhance the pore structure. Givi et al. (2010) reported that the water absorption of concrete decreases significantly with the increase in RHA content up to 10%, and even at 20% RHA, the values were lower compared to control concrete due to the reduction in permeable voids. Moreover, Ranjbar et al. (2016) observed an enhancement against water absorption of concrete incorporating POFA up to 20% due to the closed pore structure, which led to improve the microstructure of the cement matrix. Furthermore, Ahmmad et al. (2017) recommended the addition of

POCP up to 15% as pozzolanic material to enhance the performance of concrete against water absorption.

Table 4.9: The percentage of water absorption of concrete

Mix	Initial water absorption (%)		Final water absorption (%)	
	28 days	90 days	28 days	90 days
NAC	2.5	2.2	5.2	5.1
RAC	3.2	3.1	6.7	6.8
RHA10	3.0	2.5	6.5	4.9
RHA20	3.3	2.3	6.6	4.8
RHA30	3.5	2.9	6.9	5.2
POFA10	3.4	2.7	7.0	6.7
POFA20	3.5	2.8	7.1	6.4
POFA30	3.7	3.1	7.5	6.5
POCP10	3.2	2.9	6.9	6.5
POCP20	3.3	2.6	7.0	6.3
POCP30	3.6	3.3	7.2	6.6

4.4.2 Sorptivity

The rate of ingress of water or other liquids due to capillary rise is linked, to a large extent, with the penetrability of the pore system, which largely affects the performance of concrete subjected to aggressive environments. The effect of curing age on the rate of water absorption of RA-based concrete specimens prepared with different replacement levels of RHA, POFA, and POCP is illustrated in Figure 4.24. In addition, Figure 4.25 presents sorptivity values determined from Figure 4.24 by calculating the slope of the line that is the best fit to the points between 0 - 147 $s^{0.5}$ (i.e. 0 - 6 h). The 28-day sorptivity values of NAC and RAC were 0.016 and 0.022 $mm/s^{0.5}$, respectively. It can be observed that RAC has sorptivity value higher by about 38% than that of NAC, which could be attributed to the porous nature of RA compared with NA, leading to higher rate of water

absorption; this has also been reported by Debieb et al. (2010) for concrete made from 100% of RA.

The 28-day sorptivity values of concretes containing RHA, POFA and POCP were in ranges of 0.019-0.022, 0.024-0.028 and 0.023-0.030 mm/s$^{0.5}$, respectively. These results indicate that only the pore structure of RHA-based concrete was improved, since the values were lower than that of RAC. Moreover, it can be seen that the sorptivity of specimens containing POFA and POCP was higher than that of RAC, and it increases with increasing replacement level. According to Mo et al. (2016), the early hydration of OPC that is near to completion at the age of 28 days could be the reason for the better sorptivity values of RAC with 100% OPC compared to those incorporating POFA and POCP. However, the sorptivity of concrete specimens containing SCMs showed a significant enhancement after a curing age of 90 days. At this age, the ranges of sorptivity improved to 0.014-0.017, 0.018-0.023 and 0.020-0.023 mm/s$^{0.5}$ for concretes containing RHA, POFA and POCP, respectively, compared with 0.021 mm/s$^{0.5}$ for RAC. The results showed that the resistance of RA-based concrete against water absorption was enhanced after long curing period (>28 days) using RHA, POFA and POCP at replacement levels of up to 30%, 20% and 10%, respectively. The improved performance of concrete containing the aforementioned SCMs in terms of resisting water absorption was due to the fact that they have high SiO_2 content, thus producing additional C–S–H gel, which the latter has the potential to fill the existing voids and enhance the resulting pore structure. Mohammadhosseini et al. (2016) and Islam et al. (2016a) reported that the enhancement against capillary water absorption of POFA-based concrete is due to the pozzolanic reaction during prolonged curing age, which produced a denser microstructure, subsequently resulting in a reduction of sorptivity compared to OPC concrete.

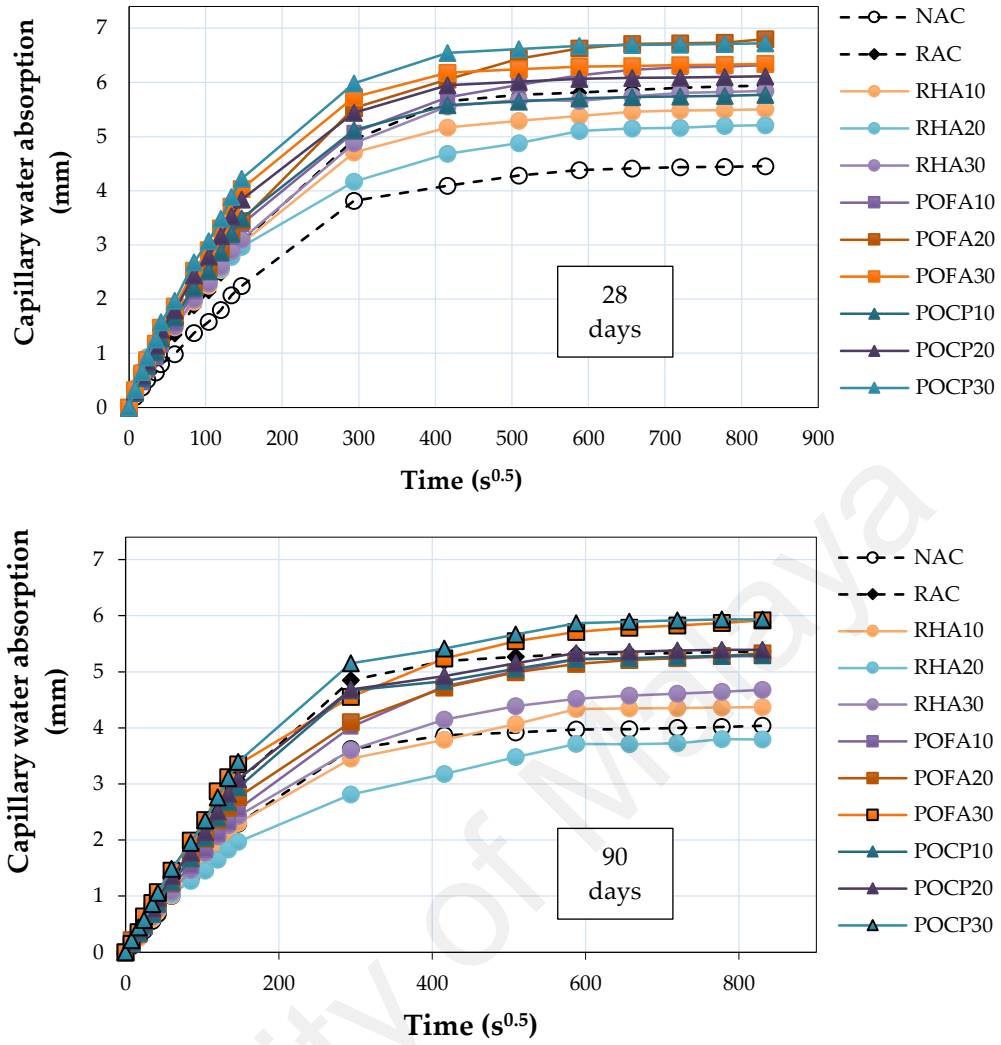

Figure 4.24: The rate of water absorption at the ages of 28 and 90 days

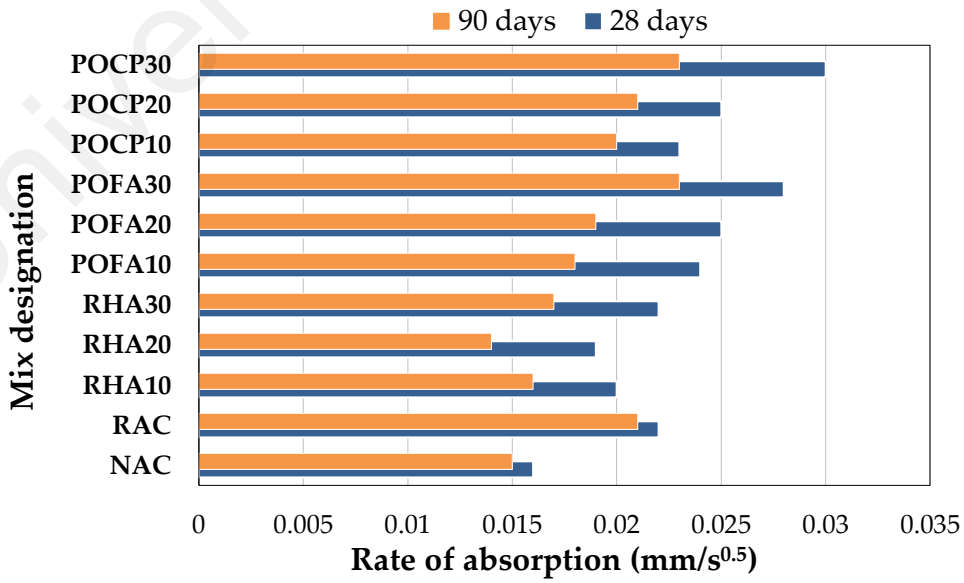

Figure 4.25: Sorptivity values of concrete specimens at the ages of 28 and 90 days

4.4.3 Effect of hydrochloric (HCl) acid

4.4.3.1 Decomposition of cement paste

Figure 4.26 illustrates the decomposition process of concrete due to HCl acid attack. The decomposition process yields a tenuous layer, which progressively increases during the attack (Beddoe, 2016). The salient observation is the role of the old cement mortar found in the RA particles in facilitating the penetration of HCl ions, leading to further deterioration in the sound concrete. Hence, the decomposition of cement matrix leads to increase porosity and permeability of the concrete, which in turn causes a reduction in strength and mass.

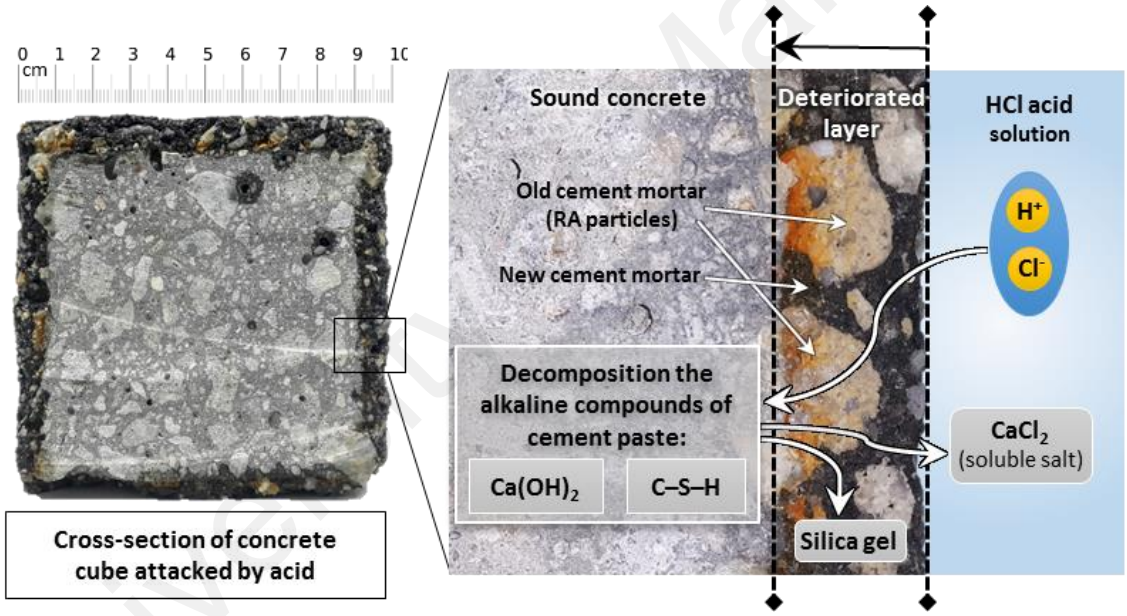

Figure 4.26: Decomposition process summary of concrete due to attack by HCl acid

Figure 4.27 shows the deteriorated depth of hardened cement paste after exposure to 3% HCl solution for a period of 75 days. It can be seen that the deteriorated depth of RAC is slightly higher than that of NAC, which could be attributed chemically to the presence of additional $Ca(OH)_2$ in the old mortar, and physically to the permeable voids found in the mortar attached on the RA particles, promoting a further ingress of acid ions and leading to more increase in porosity. In addition, the results showing that the RA-based concretes containing RHA, POFA and POCP have an improvement in the deteriorated

layer; it was about 2-4 times less than that of RAC, depending on the cement replacement level. Moreover, concretes with 30% replacement level of RHA, POFA and POCP show lower deterioration. Besides, it is well-known that the presence of $Ca(OH)_2$ is low in the cement paste of concrete containing SCMs, due to its consumption during the pozzolanic reaction (Lothenbach et al., 2011). As a result of this, the concretes containing SCMs are less susceptible to deterioration. However, although the incorporation of SCMs has reduced the amount of $Ca(OH)_2$, HCl ions still have the ability to react with other calcium compounds in cement paste (Chatveera & Lertwattanaruk, 2011).

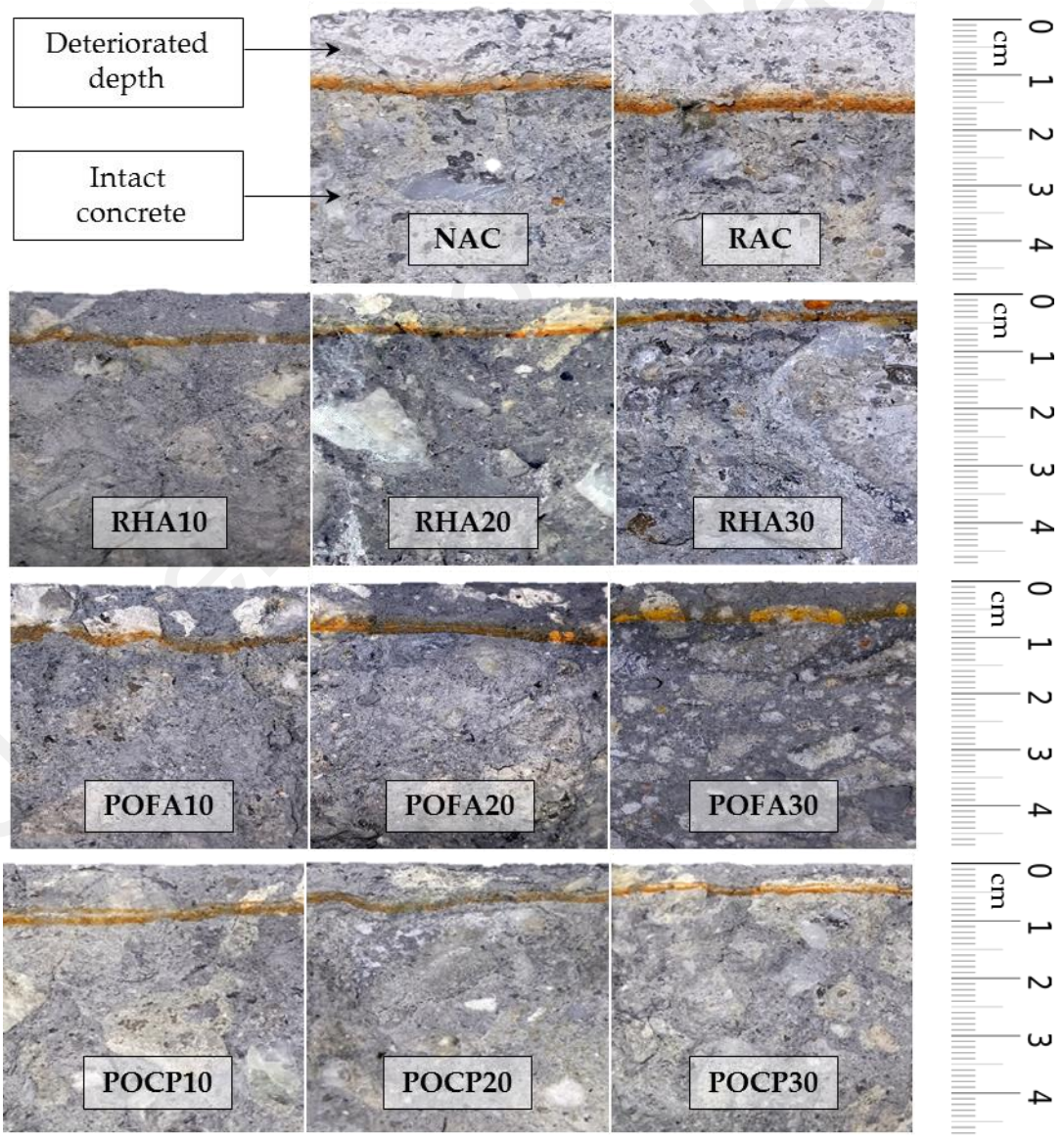

Figure 4.27: Deteriorated depth of concrete specimens exposed to HCl acid

4.4.3.2 Mass loss

The percentage of mass loss due to HCl acid attack on specimens made of RA and incorporating RHA, POFA and POCP can be found in Figure 4.28. Based on the results, it can be inferred that replacing NA with RA further increases the mass loss from 8.4% for NAC to 10.3% for RAC. This was due to the high water absorption and volume of permeable voids of RAC compared to NAC. Moreover, Nuaklong et al. (2016) pointed out that the presence of $Ca(OH)_2$ in the old mortar found in RA particles reacts with HCl ions, leading to further loss in mass. The ranges of mass loss for the specimens incorporating RHA, POFA and POCP were 2.1-3.7%, 4.7-6.9% and 3.5-5.7%, respectively. It can be seen that the SCM-based concretes yielded lower mass loss than that of RAC without SCM. Further, RHA-based concrete showed lower mass loss than POFA- and POCP-based concretes, which could be primarily due to the high pozzolanic activity of RHA with 91% SiO_2 content compared with 64% and 60% for POFA and POCP, respectively. Furthermore, mass loss decreases when the replacement level of the cement by RHA, POFA and POCP increases up to 30%. This is mainly attributed to the lower adverse effect of $Ca(OH)_2$, since it will be consumed at a greater range at higher replacement levels. Consequently, the specimens containing SCMs suffers from minor surface erosion and less corner loss, as shown in Figures 4.29-4.33. Ranjbar et al. (2016) observed a low mass loss and corner deterioration for concrete containing high amounts of POFA due to the progressive depletion of $Ca(OH)_2$ when POFA content increased. Kannan and Ganesan (2014) reported that the specimens prepared with up to 30% RHA experienced lower mass loss than those without RHA after 12 weeks of immersion in 5% HCl solution due to the reduction of capillary pores by the formation of extra C–S–H gel during the pozzolanic reaction.

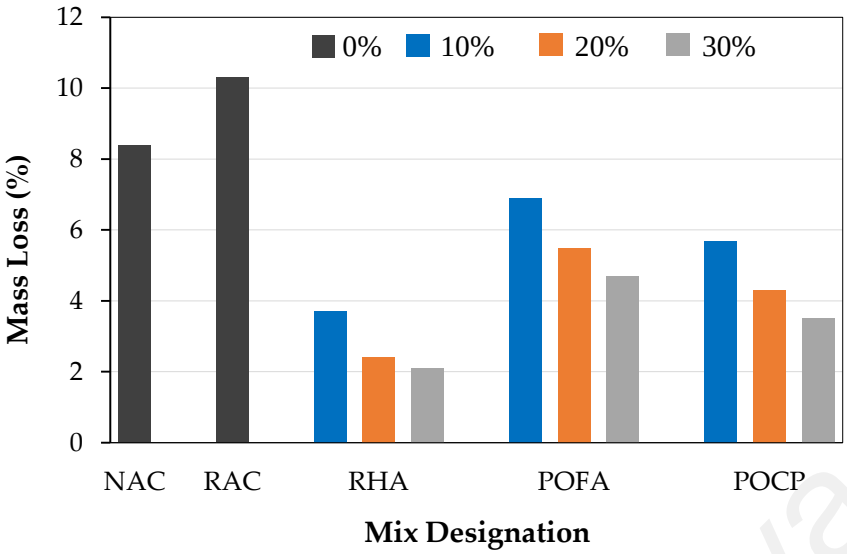

Figure 4.28: Mass loss of the specimens after exposure to HCl solution

Figure 4.29: NAC mix attacked by HCl acid before and after compression test

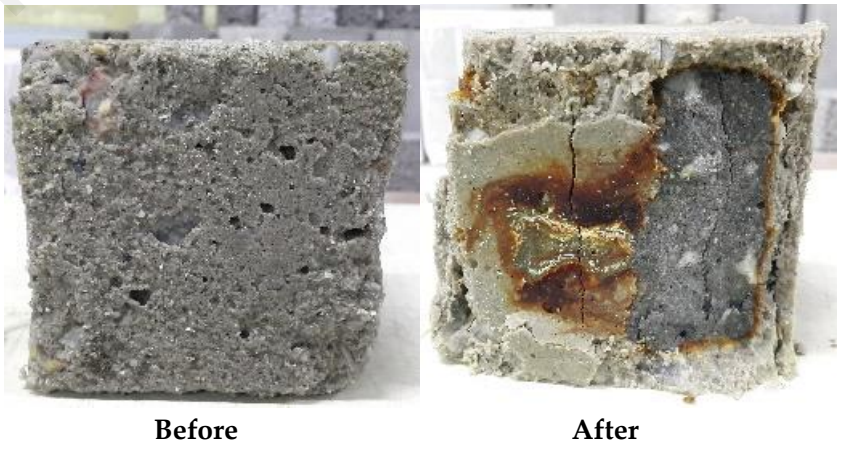

Figure 4.30: RAC mix attacked by HCl acid before and after compression test

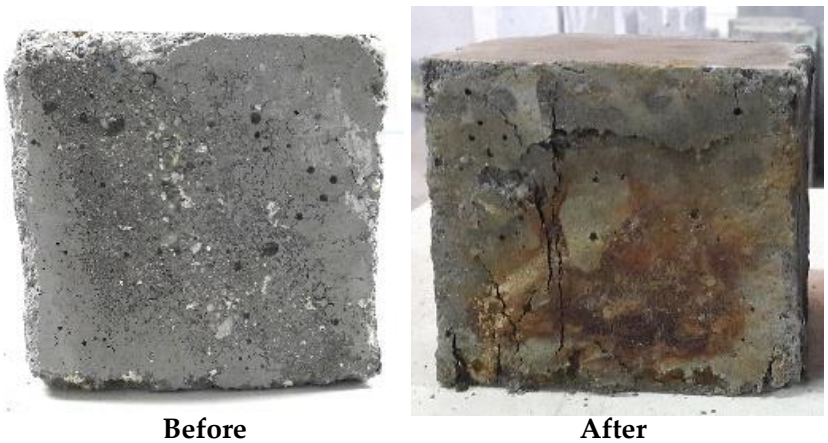

Before After

Figure 4.31: RHA30 mix attacked by HCl acid before and after compression test

Before After

Figure 4.32: POFA30 mix attacked by HCl acid before and after compression test

Before After

Figure 4.33: POCP30 mix attacked by HCl acid before and after compression test

4.4.3.3 Compressive strength loss

The compressive strength of concrete specimens exposed to 3% HCl acid solution and those cured in water for a period of 75 days can be found in Table 4.10. In addition, Figure

4.34 illustrates the percentage of loss in compressive strength after exposure to HCl acid. It can be seen that RAC suffered from 67% loss in the compressive strength compared to 63% for NAC. The high water absorption and porosity of RA particles allowed the HCl ions to penetrate through the concrete, thus resulting in increased dissolution of $Ca(OH)_2$ and decalcification of C–S–H. In the case of RA-based concrete containing RHA, POFA and POCP, the loss in compressive strength was in the range of 34-59%, depending on the cement replacement level, which is lower than that of RAC. Moreover, the loss percentage in the compressive strength was lower, when the replacement level of cement by SCM increased. For instance, the lowest compressive strength loss of 34% was recorded for the mix containing 30% RHA compared to 38% and 48% for the mixes containing 10% and 20% RHA, respectively. Moreover, the compressive strength loss was 51%, 52% and 59% for mixes prepared with 10%, 20% and 30% POFA, respectively. Furthermore, the incorporation of 10%, 20% and 30% POCP led to a compressive strength loss of 50%, 50% and 53%, respectively. Part of the reason that led to lower compressive strength loss of RA-based concrete incorporating SCMs is the denser and less porous structure (as discussed in the section 4.5 on Microstructural investigation) of the cement matrix as a result of the pozzolanic reaction, which prevents the penetration of the HCl ions into the inner part of concrete. Furthermore, the reduced effect of HCl acid on concretes incorporating RHA, POFA and POCP is attributed to the limited portlandite content available for reaction compared to that of RAC. Chatveera and Lertwattanaruk (2014) reported a similar concept, where the use of RHA to replace OPC positively influenced acid resistance due to the improvement in density and impermeability of the concrete. Alsubari et al. (2016) concluded that when POFA was used as a cement replacement, a denser concrete with lower susceptibility to HCl attack was produced, thus the deterioration process was reduced.

Table 4.10: Compressive strength of concrete specimens cured in water and HCl solution

Mix	Compressive strength (MPa)	
	Cured in water (103 days)	Cured in HCl solution (28 days in water + 75 days in acid)
NAC	50.7	18.8
RAC	39.0	12.9
RHA10	49.1	25.5
RHA20	45.1	27.9
RHA30	39.3	26.0
POFA10	39.7	16.4
POFA20	37.7	18.0
POFA30	33.6	16.5
POCP10	38.4	18.0
POCP20	37.6	18.6
POCP30	32.9	16.2

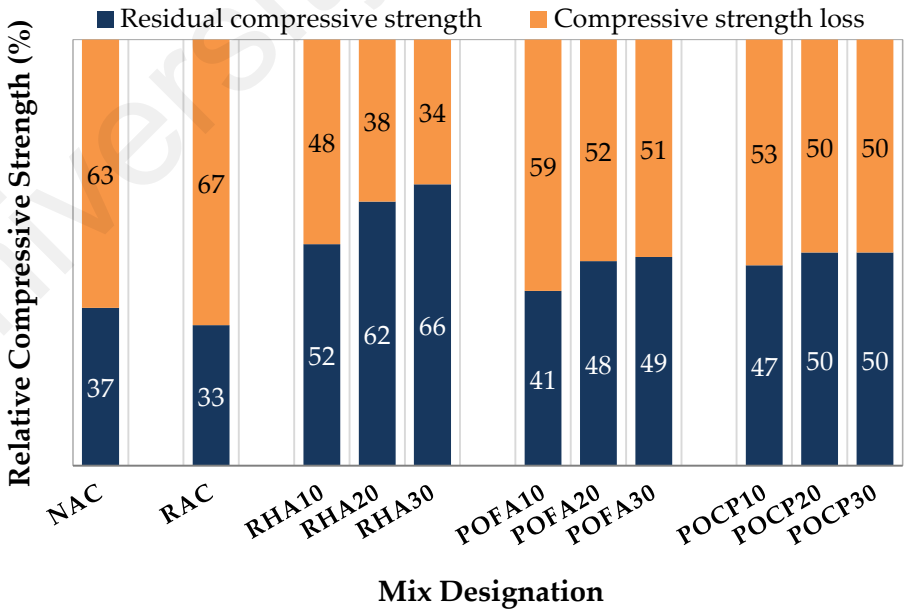

Figure 4.34: Percentage of loss in compressive strength after exposure to HCl acid

4.4.4 Effect of magnesium sulfate ($MgSO_4$)

4.4.4.1 Effect of sulfate attack on compressive strength

Sulfate attack in concrete causes chemical reactions that typically lead to the formation of ettringite within the concrete matrix. This later formation of ettringite causes expansion in the concrete which can ultimately lead to cracking, spalling, loss of integrity, and deterioration (Bizzozero et al., 2014; Müllauer et al., 2013). Figure 4.35 shows the complex and overlapping reactions between concrete and $MgSO_4$ solution that disintegrate the sound concrete (Alexander et al., 2013).

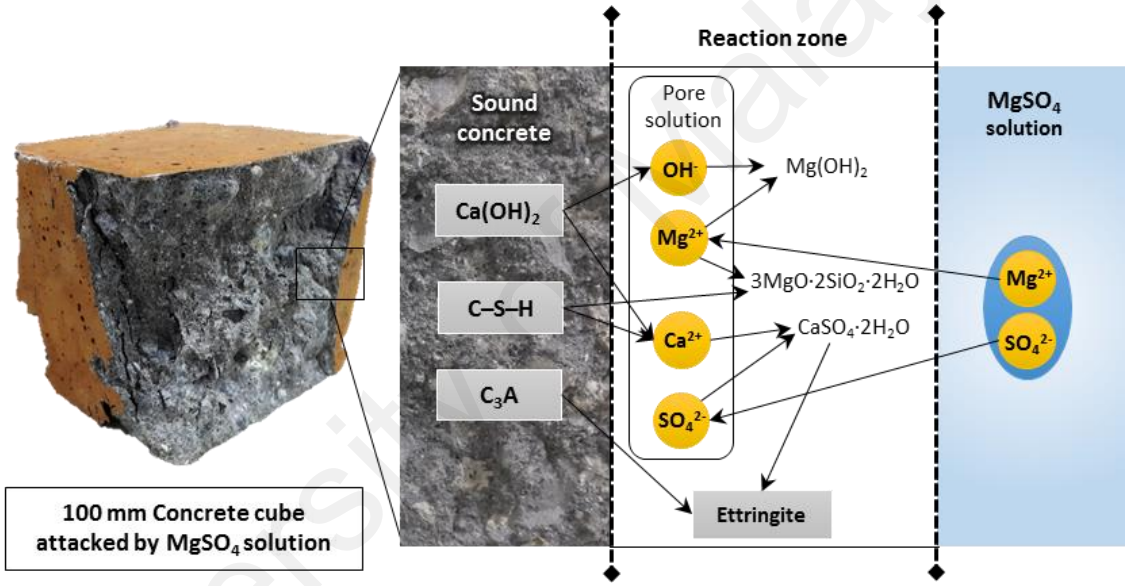

Figure 4.35: Possible reactions between concrete and $MgSO_4$ solution

The compressive strengths of concrete specimens initially cured in water for 28 days (zero time) and then immersed in 5% $MgSO_4$ solution for a period of 28 and 120 days are shown in Table 4.11. It can be seen in Figure 4.36 that the compressive strength slightly increased after 28 days of immersion, then decreased after 120 days of immersion in $MgSO_4$ solution compared to the specimens cured in water. After 28 days of immersion, the relative compressive strength of NAC and RAC was about 105% and 107%, respectively, while it was in the range of 101-103% for the specimens incorporating SCMs. On the other hand, after 120 days of immersion, the relative compressive strength decreased to about 91% and 88% for NAC and RAC, respectively, while for concretes

containing RHA, POFA, and POCP, it decreased to the ranges of 95-97%, 92-93% and 94-95%, respectively. It is apparent that the incorporation of RHA, POFA and POCP decreases the negative impact of $MgSO_4$ solution on concrete. Furthermore, the superficial increase of compressive strength of the specimens exposed to $MgSO_4$ solution for a period of 28 days could be attributed to the formation of ettringite, which leads to a more closed pore structure and slight increase in compressive strength. The same concept was also reported by Jo et al. (2017), who stated that the presence of more voids in the pore structure of cement matrix are able to accommodate the expansive ettringite during the early stages of immersion. Consequently, the continuous formation of ettringite, that has a relatively large volume, caused internal cracks due to continuous expansion and resulted in a decrease in the compressive strength after 120 days of immersion. A similar phenomenon was observed by Heikal et al. (2015), when they revealed that the compressive strength of specimens subjected to aggressive sulfate solution increased with curing time up to 90 days, then showed a reduction after 120 days of immersion. However, the decalcification of hydration products can be reduced using SCMs due to the pozzolanic reaction, which prevents the diffusion of sulfate ions throughout the cement matrix. Limbachiya et al. (2012) pointed out that the inclusion of fly ash in RA-based concrete would decrease the reactive aluminates (C_3A) content, hence reducing the formation of ettringite. Chindaprasirt et al. (2007) reported a similar observation when using pozzolanic materials to produce blended cement. They revealed that the use of fly ash and RHA at replacement level of up to 40% improve resistance against sulfate attack. Tangchirapat et al. (2009) concluded that the concrete specimens incorporating 10% and 20% POFA had higher compressive strengths than those without POFA, even after soaking in sulfate solution for period up to 180 days, due to the pore refinement process that occurred as a result of pozzolanic reaction.

Table 4.11: Compressive strength of the specimens cured in water and $MgSO_4$ solution

Mix	Compressive strength (MPa)			
	28 days		120 days	
	Cured in water	Cured in $MgSO_4$	Cured in water	Cured in $MgSO_4$
NAC	47.6	49.8	53.0	48.1
RAC	37.1	39.5	40.2	35.5
RHA10	45.2	45.9	52.0	49.5
RHA20	41.4	42.0	50.8	49.2
RHA30	35.6	35.8	46.5	45.1
POFA10	37.3	38.2	42.9	39.4
POFA20	32.7	33.4	40.3	37.3
POFA30	30.0	30.2	36.5	34.0
POCP10	35.3	35.8	41.7	39.0
POCP20	34.2	34.4	42.2	39.7
POCP30	29.7	30.0	38.3	36.5

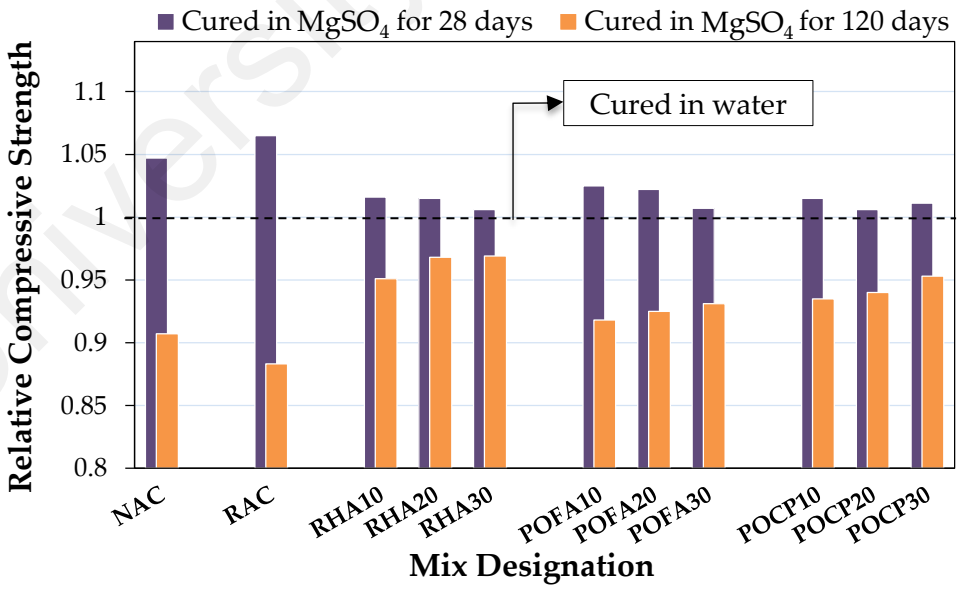

Figure 4.36: Relative compressive strength of the specimens cured in 5% $MgSO_4$ solution for 28 and 120 days compared with those cured in water

4.4.5 Penetration of chloride ions

The RCPT method was used to check the effect of RHA, POFA and POCP on the RA-based concretes by measuring the total charge in coulombs passing through the concrete specimen over a period of 6 hours. It should be noted that lower charge values signify a higher resistance to chloride intrusion. The total charge passed through concrete specimens at the ages of 28 and 90 days can be found in Figure 4.37. The results of 28 days show that the total charge passed through RAC specimens made of 100% RA was 4400 coulombs compared to 3407 coulombs for NAC specimens made of conventional aggregate. The increase in charge passed through RAC specimens could be attributed to the increase in volume of the paste (old mortar found in RA particles + new paste), which considered as the weakest point for penetration of chloride ions (Kou & Poon, 2012). The risk of corrosion of RAC mix could be classified as "high" based on corrosion ranges of ASTM C1202. At the age of 28 days, the charge passed through concrete specimens containing RHA, POFA and POCP indicates that only the pore structure of RHA- and POFA based concrete was improved, since the values were lower than that of RAC. However, the resistance to the penetration of chloride ions of RA-based concrete significantly enhanced with the use of SCMs after 90 days of water curing. It can be seen from Figure 3.37 that best performance of resisting the penetration of chloride ions was recorded for concretes containing 10% and 20% RHA, where the charge passed was about 1000 coulombs, indicating a "low" risk of corrosion. In addition, the risk of corrosion of the specimens containing POFA and POCP decreased to "moderate" after 90 days of water curing. The superior performance of concretes incorporated with SCMs can be explained by the enhancement in impermeability of the pore structure, where a reduction in the average pore size of the paste and an improvement of the interfacial transition zone occurred. Mujah (2016) and Islam et al. (2016a) revealed that blended cement with POFA was very effective to prevent the ingress of chloride ions in concrete due to the increase

of C–S–H gel content that is formed in the pozzolanic reaction. Kou and Poon (2012) suggested that the use of fly ash was found to be effective as the chloride resistance of RA-based concrete was increased due to the formation of extra C–S–H gel, which blocked the ingress path of chloride ions.

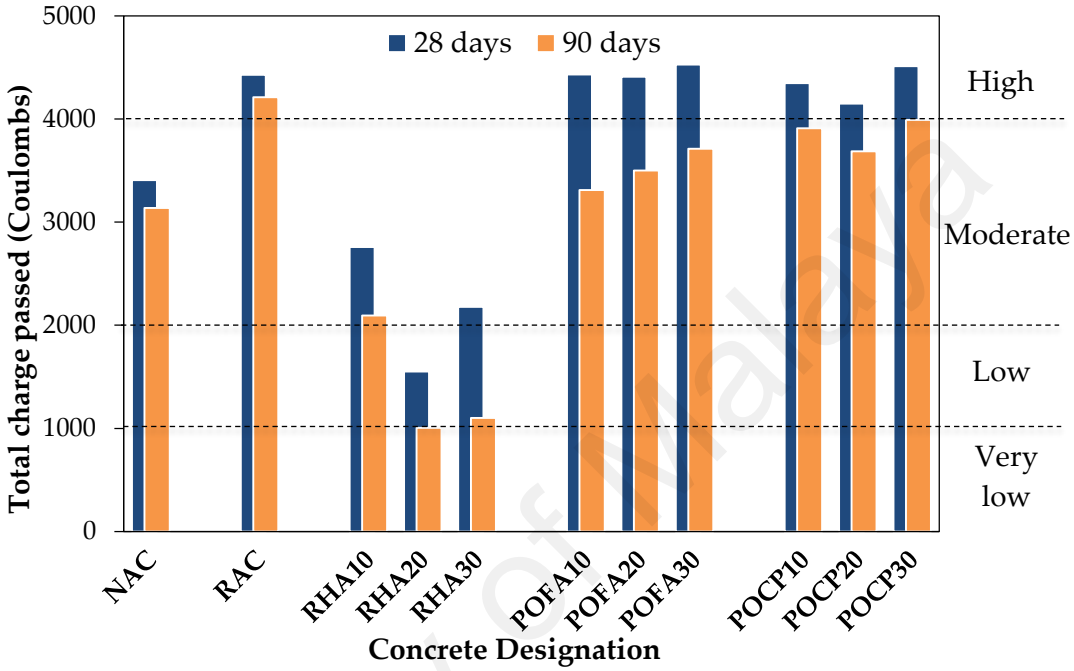

Figure 4.37: Total charge passed through concrete specimens

4.4.6 Electrical resistivity

The electrical resistivity of concrete gives an indication of its ability to resist the corrosion of steel reinforcement. The relationship between corrosion rate of reinforcing steel and the electrical resistivity of concrete has been conducted in previous studies (Baroghel-Bouny et al., 2011; Hornbostel et al., 2013; Sabet et al., 2013). Figure 4.38 shows the electrical resistivity of all mixtures at the ages of 28 and 90 days compared to the limits suggested by ACI Committee 222. It is obvious that the higher values (>10) indicate a greater endurance of concrete against corrosion. At the age of 28 days, the resistivity values of NAC and RAC were less than 10 kΩ.cm, indicating a “high” possibility of corrosion. Nevertheless, the main observation is the improvement of resistivity for RA-based concretes containing SCMs especially for those incorporated with RHA at the age of 90 days. For instance, the resistivity values of RHA10, RHA20

and RHA30 were 24.0, 25.5 and 28.4 kΩ.cm, respectively, indicating a "very low" possibility of corrosion compared to 8.3 kΩ.cm for RAC with a "high" possibility of corrosion. Further, the resistivity values of concrete containing POFA up to 30% were in the range of 13.8-15.7 kΩ.cm, indicating a "low to medium" possibility of corrosion. Furthermore, the resistivity values of concrete containing POCP up to 30% were in the range of 10.1-13.2 kΩ.cm, indicating a "low to medium" possibility of corrosion. The improved performance of concrete containing SCMs in terms of resisting corrosion could be attributed to the fact that they have high SiO_2 content, and thus forming an additional C–S–H gel, which has the potential to block the existing voids and to enhance the pore structure. Similar concept was observed by Chao-Lung et al. (2011), who revealed that the solidification brought by pozzolanic reaction can indeed increase the electrical resistance of concrete containing RHA. The previous studies showed that the resistivity value of 8.5 kΩ.cm is considered to be effective to prevent the corrosion of reinforcing steel in concrete (Chao-Lung et al., 2011; Kanadasan & Razak, 2015).

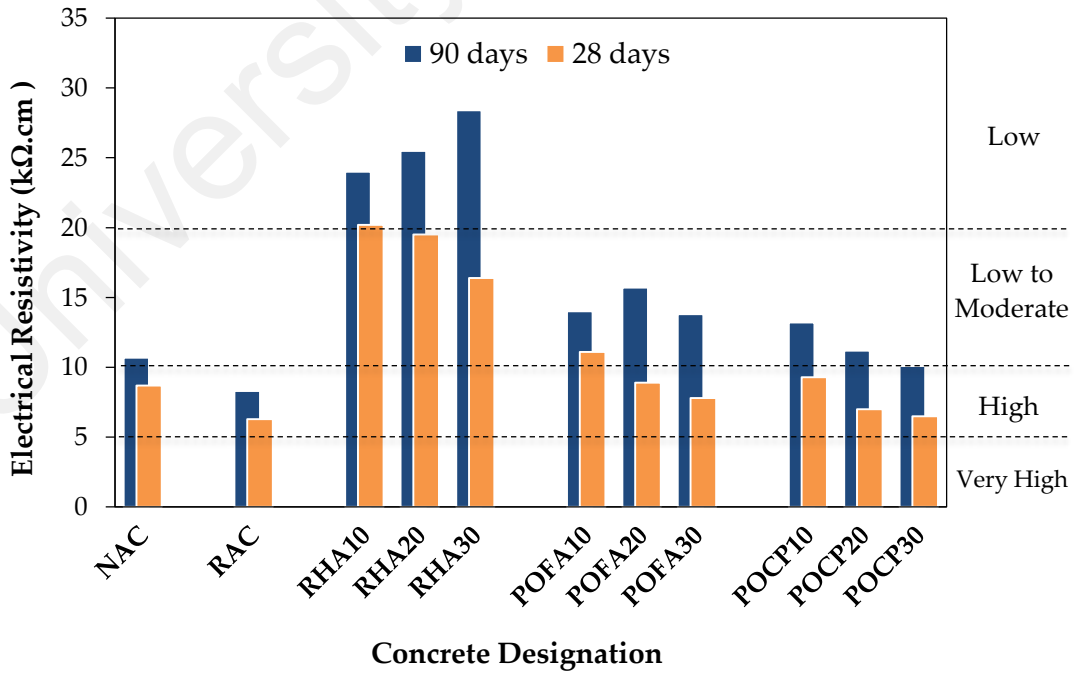

Figure 4.38: Electrical resistivity of concrete and the corrosion rate limits

4.5 Effect of elevated temperatures

Evaluation of the concrete's resistance to fire is significantly important in structural stability and life safety. The performance behavior of RA concrete containing SCMs was investigated after exposure to elevated temperatures to check its resistance against fire. It is well-known that the decomposition of cement matrix occurs at temperatures higher than 400 °C due to the decomposition of $Ca(OH)_2$ and the dissipation of crystal water. Hence, the incorporation of SCMs may reduce the amount of $Ca(OH)_2$ during pozzolanic reaction so that decreasing the degradation of cement matrix. However, the degradation still can happen due to the decomposition of C–S–H but at higher temperatures than $Ca(OH)_2$. Thus, it is vital to study the behavior of RA-based concrete against elevated temperatures using waste products as SCMs to check their suitability in concrete.

4.5.1 Residual compressive strength

The residual compressive strengths of concrete specimens at the ages of 28 and 90 days after exposure to different elevated temperatures are shown in Table 4.12. It can be seen, generally, that the relative compressive strength increased when the specimens were subjected to an elevated temperature of up to 200 °C compared with corresponding non-heated specimens, which were placed in ambient conditions at 25 °C. The increments for specimens containing SCMs were in the range of 102-121% which were higher than RAC with 104% at the age of 28 days. This increment could be an indication on the hydration of non-hydrated cement particles, and the higher increments for SCM specimens could be attributed to the effect of 200 °C temperature on stimulating the pozzolanic reaction between SiO_2 particles from SCM and $Ca(OH)_2$ produced during cement hydration process as stated by (Delhomme et al., 2012). Moreover, when the specimens made with SCM at the age of 28 days were exposed to temperatures of 400 °C, 600 °C and 800 °C, the ranges of relative compressive strength decreased to 88-99%, 46-64% and 17-30%, which were higher than that of RAC with 73%, 46% and 23%, respectively. The reduction

in compressive strength after exposure to temperature higher than 400 °C could be due to the decomposition of hydrated products that leads to the propagation of micro-cracks in cement matrix, as shown in Figures 4.40 and 4.41; this leads to the reduction in the strength, as shown in Figure 4.39. Further, the incorporation of SCMs reduced the amount of $Ca(OH)_2$ during pozzolanic reaction so that decreasing the degradation of $Ca(OH)_2$ and decreasing the prevalence of micro-cracks at high temperatures in which the values of compressive strength retained at a higher levels (Ma et al., 2015).

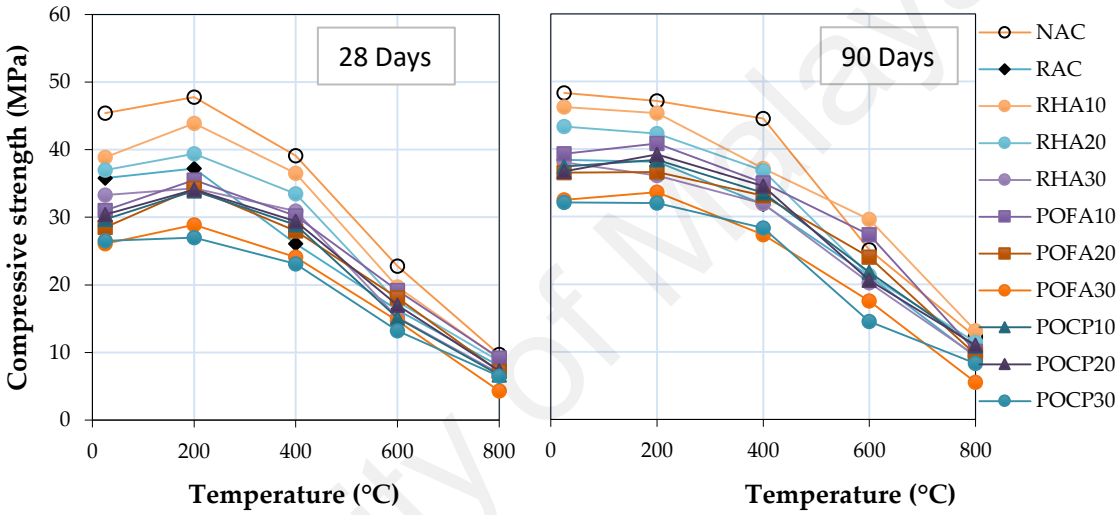

Figure 4.39: Residual compressive strength after exposure to elevated temperatures at the ages of 28 and 90 days

Table 4.12: Residual compressive strength after exposure to elevated temperatures

Mix		28 days					90 days				
		25°C	200°C	400°C	600°C	800°C	25°C	200°C	400°C	600°C	800°C
NAC	*fc'*	45.4	47.8	39.1	22.8	9.7	48.3	47.1	44.5	25.1	12.2
	fc'/fc'(25°C)	100	106	87	51	22	100	98	93	52	26
	σ	0.76	2.61	1.19	1.35	0.69	1.13	1.22	1.36	1.41	0.54
RAC	*fc'*	35.8	37.2	26.1	16.3	8.0	38.4	38.1	31.8	21.2	9.3
	fc'/fc'(25°C)	100	104	73	46	23	100	100	83	56	25
	σ	1.15	1.37	1.72	0.66	2.38	0.81	0.75	1.32	1.13	0.33
RHA10	*fc'*	38.9	43.9	36.5	19.7	9.1	46.2	45.3	37.1	29.6	13.1
	fc'/fc'(25°C)	100	113	94	51	24	100	99	81	65	29
	σ	1.47	1.67	1.70	0.42	0.50	1.81	1.77	1.41	0.85	0.14
RHA20	*fc'*	37.0	39.4	33.5	17.5	8.7	43.3	42.3	36.8	21.3	11.4
	fc'/fc'(25°C)	100	107	91	48	24	100	98	85	50	27
	σ	1.25	1.56	2.12	0.71	0.44	1.57	0.28	1.34	0.35	0.21
RHA30	*fc'*	33.3	34.3	30.9	15.2	6.9	38	36.1	31.9	20.2	9.4
	fc'/fc'(25°C)	100	104	93	46	21	100	95	84	54	25
	σ	0.61	1.16	1.52	0.92	0.19	1.31	1.58	1.44	0.21	0.31
POFA10	*fc'*	31.0	35.5	30.2	19.2	9.2	39.3	40.8	35.0	27.3	10.1
	fc'/fc'(25°C)	100	115	98	62	30	100	104	90	70	26
	σ	1.21	1.07	1.61	0.78	0.70	1.05	1.78	2.12	0.35	0.75
POFA20	*fc'*	28.5	34.3	28.0	18.1	7.2	36.5	36.6	33.1	24.0	9.6
	fc'/fc'(25°C)	100	121	99	64	26	100	101	91	66	27
	σ	1.23	1.15	1.41	0.57	0.18	0.71	0.72	0.67	0.85	0.14
POFA30	*fc'*	26.1	28.9	24.1	14.7	4.3	32.5	33.6	27.3	17.5	5.5
	fc'/fc'(25°C)	100	111	93	57	17	100	104	84	54	17
	σ	0.06	1.14	1.71	0.27	0.13	0.64	1.42	0.77	0.25	0.17
POCP10	*fc'*	29.7	33.9	28.9	15.1	6.7	37.4	38.4	33.5	21.8	10.8
	fc'/fc'(25°C)	100	115	98	51	23	100	103	90	59	29
	σ	2.46	1.78	1.90	1.29	0.28	0.91	1.84	0.71	1.06	0.85
POCP20	*fc'*	30.4	34.1	29.4	17.0	7.3	36.7	39.2	34.5	20.6	11.0
	fc'/fc'(25°C)	100	113	97	56	25	100	107	95	57	30
	σ	2.12	1.44	1.22	0.09	0.28	0.60	1.41	0.99	1.27	0.71
POCP30	*fc'*	26.5	27	23.1	13.2	6.5	32.1	32.0	28.3	14.5	8.3
	fc'/fc'(25°C)	100	102	88	50	25	100	100	88	46	26
	σ	0.87	1.14	1.27	0.79	0.18	0.90	1.11	1.79	0.07	0.21

Notes: 1) fc'= Cube compressive strength (MPa), fc'/fc'(25°C)= Relative compressive strength (%) and σ= Standard deviation of the compressive strength.
2) The compressive strength value shown in the table is the average of three specimens.

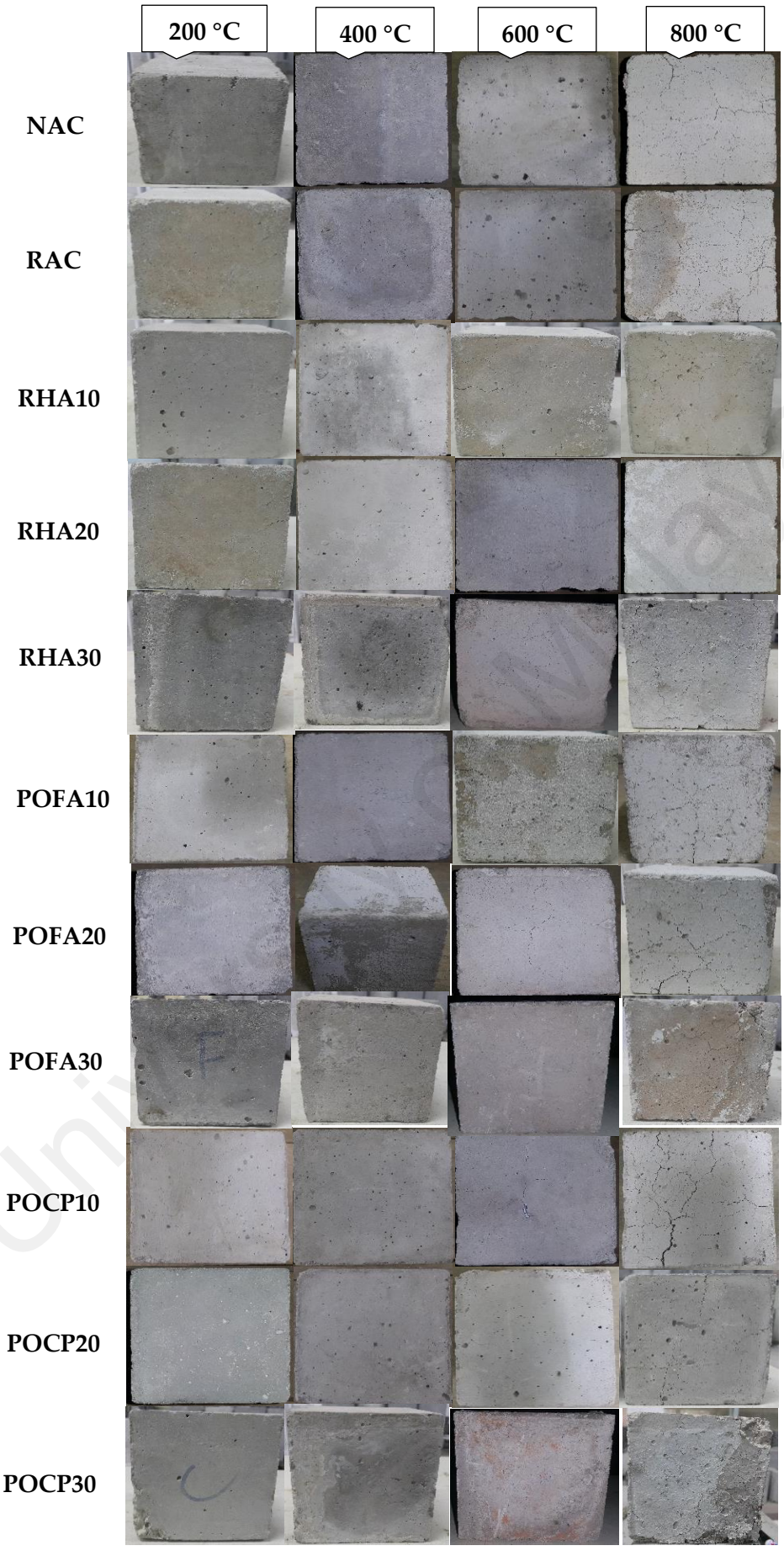

Figure 4.40: Concrete specimens exposed to elevated temperatures

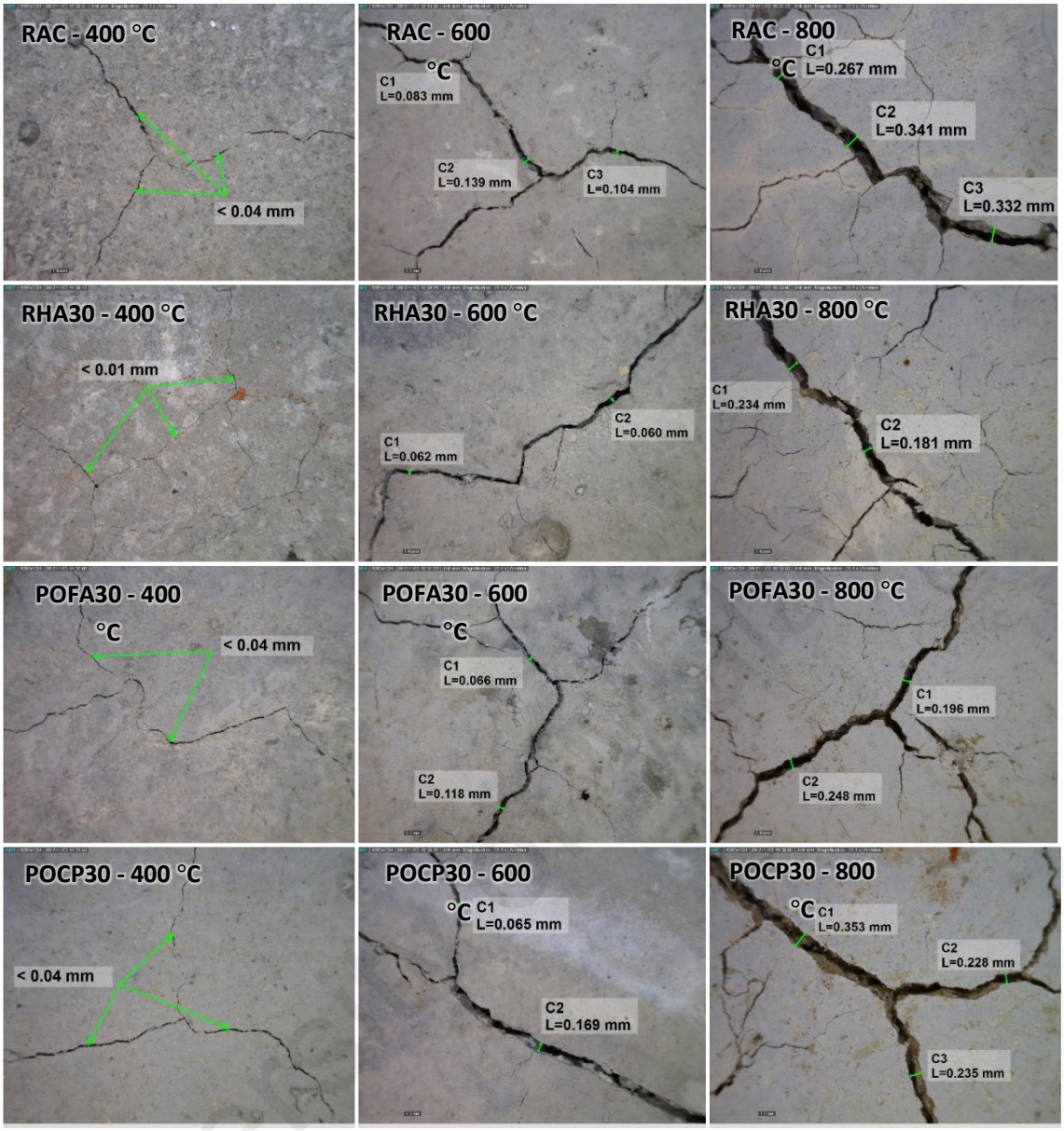

Figure 4.41: The development of micro-cracks after exposure to elevated temperatures.

4.5.2 Mass loss

There were four temperature ranges considered in order to investigate the mass loss, namely 25–200 °C, 200–400 °C, 400–600 °C and 600–800 °C. Figure 4.42 shows the mass lost during these temperature ranges. It should be noted that the mass loss of RAC mix is considerably higher than that of NAC mix because concrete with RA contains more evaporable water than the normal concrete due to the higher water absorption of the RA than the normal aggregate. For all concrete mixes, it is obvious that the mass loss is increasing gradually with the increase of target temperature due to the release of water,

which is considered as the main reason for the mass loss in the specimens during the exposure to high temperatures (Guo et al., 2014). For instance, the RA concretes containing SCM lost most of the mass when the temperature was elevated from 25°C to 200°C, which was in the range of 3.3-4.3%, regardless of the type and the replacement level of cement by SCM; this reduction in the mass could be attributed to the evaporation of water in the capillary pores as stated by (Chen et al., 2014). The mass was continuously decreasing in the range of 200–400°C due to the evaporation of gel water, and the mass loss was in the range of 2.0-4.1%. After that, between 400 and 600°C, the water particles (known as crystal water) were non-evaporable because they are chemically bound with $Ca(OH)_2$ compound, which cannot be driven out from the cement paste until the chemical decomposition of $Ca(OH)_2$ occurs at temperature between 400°C and 600°C; and therefore, the range of mass loss for RA concretes containing SCM (0.9-1.5%) was lower than that of RAC mix without SCM (2.5%) due to the lower amount of $Ca(OH)_2$ that consumed during pozzolanic reaction. Likewise, in the range of 600–800°C, the mass loss takes place due to the dissipation of crystal water leads to the decomposition of C–S–H; and thus the mass loss rate was in the range of 1.9-2.5% for RA concretes incorporated with SCM, which was higher than the value of RAC with 0.7% mass as a result of the additional C–S–H produced during pozzolanic reaction. The same concept was observed by Rashad (2015) after the specimens with fly ash were exposed to 800°C, the C–S–H phase disappeared when XRD technique was used, and it could be a part of the reason why the mass loss was obtained at 800°C

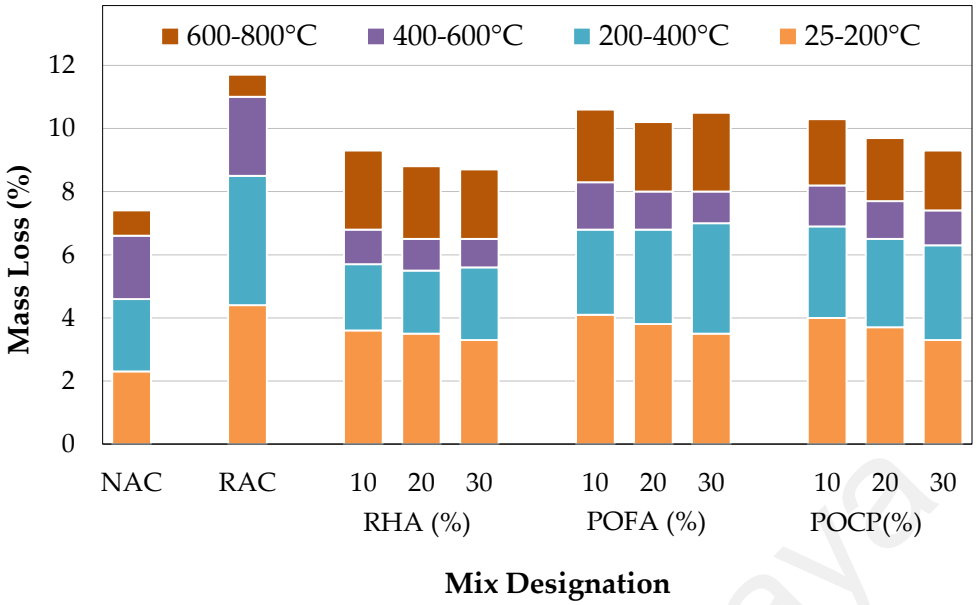

Figure 4.42: Effect of elevated temperatures on mass loss

4.6 Microstructural analysis

4.6.1 Effect of RA on interfacial transition zone of concrete

In order to detect the effect of RA on the microstructure of RA-based concrete, some specimens have been analyzed by scanning electron microscopy (SEM). Figure 4.43a illustrates the interconnection between old cement paste (represented by RA particles) and new cement paste in the interfacial transition zone (ITZ) of RA-based concrete. In addition, Figure 4.43b shows how cement paste is bonding with stone particle in the ITZ of NA-based concrete. It can be observed that the ITZ in RA-based concrete is more entangled than the one observed in NA-based concrete, which could be due to the rougher surface of RA particles than that of NA (Safiuddin et al., 2013). The observed ITZ structure is consistent with the obtained results. When old cement pastes are more porous than stone particles, some of cement particles will be able to penetrate into the pores of RA leading to enhance the bonding in ITZ between RA and cement matrix. Moreover, it is well-known that the cement paste has inferior quality than the stone particles; hence, when the concrete approaches the ultimate load in case of compressive, splitting tensile and flexural strengths, the failure is observed to be passed through zones of weakness

represented by failure in ITZ in case of NA-based concrete and failure in RA itself in case of RA-based concrete. This phenomenon is illustrated in Figures 4.44-4.47.

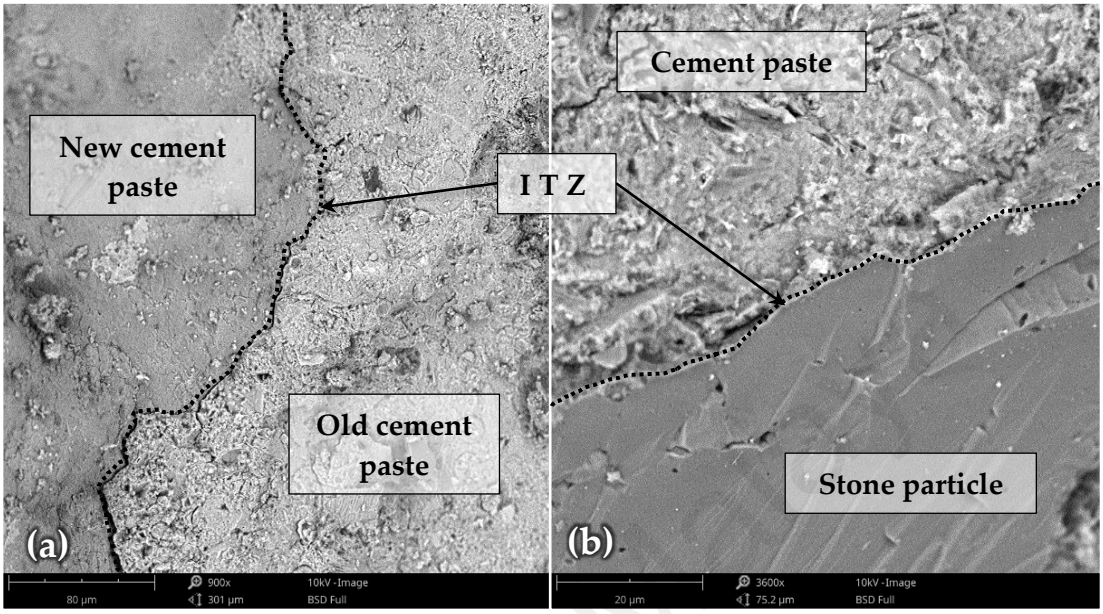

Figure 4.43: ITZ of (a) RA-based concrete and (b) NA-based concrete

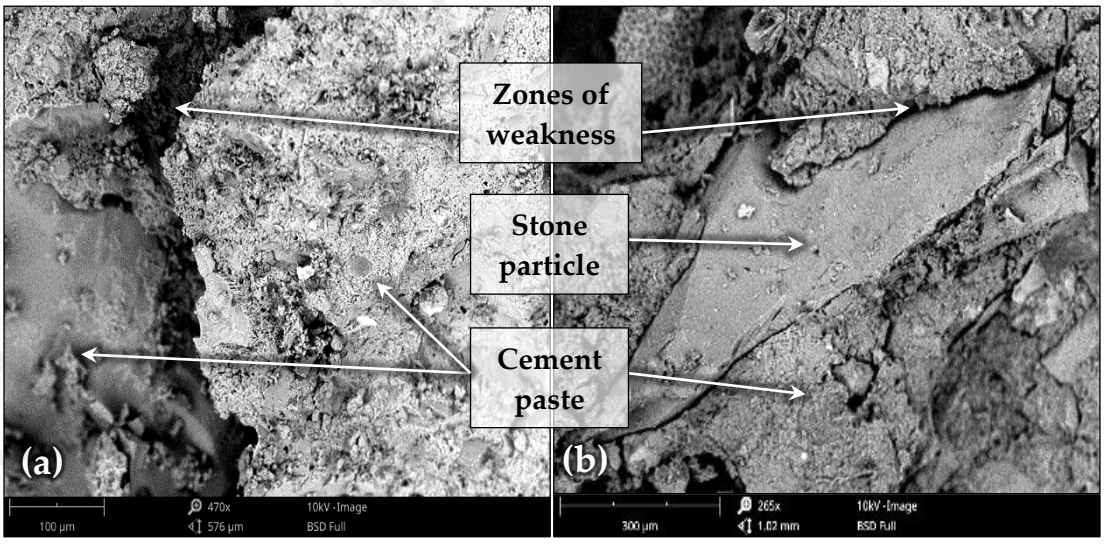

Figure 4.44: Zones of weakness in (a) RA-based concrete and (b) NA-based concrete

Figure 4.45: Zones of weakness in RAC and NAC mixes due to compression

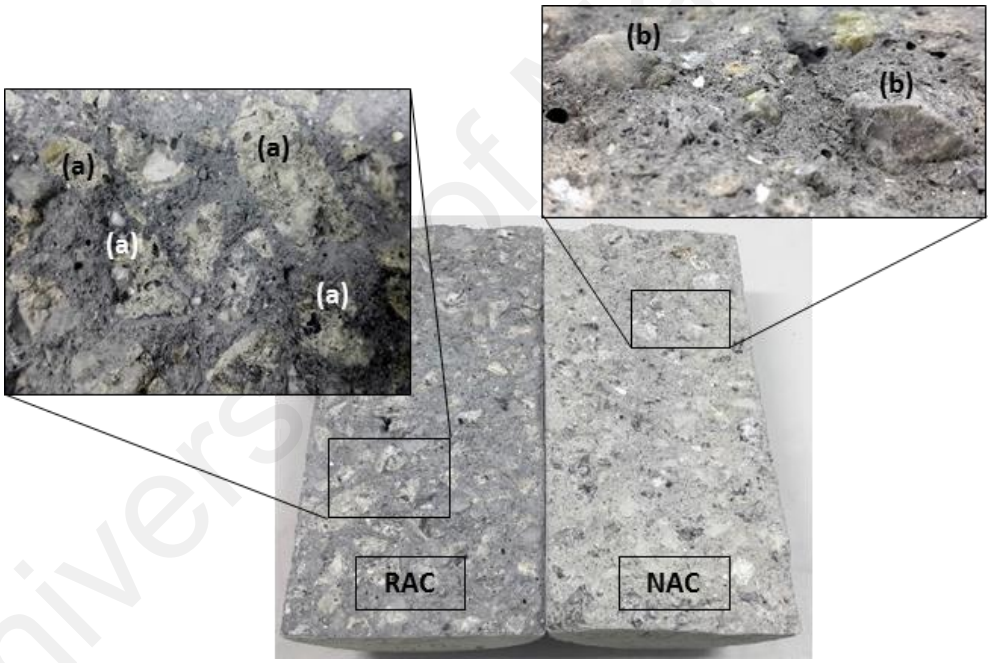

Figure 4.46: Failure mode of RAC and NAC mixes due to splitting tensile: (a) failure in the RA itself; (b) failure in the ITZ

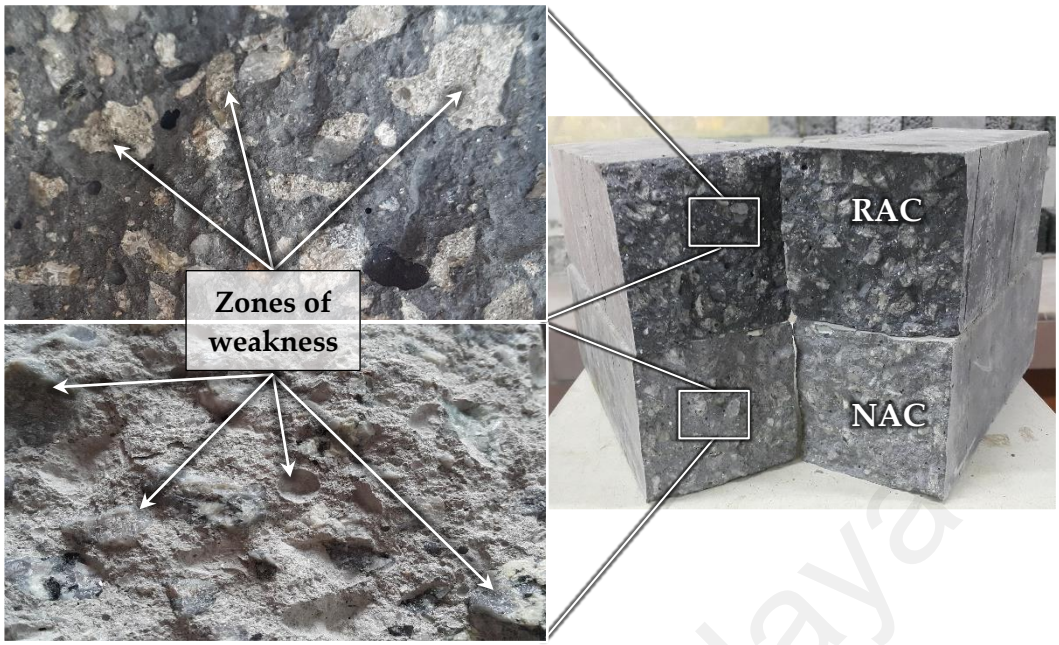

Figure 4.47: Zones of weakness in RAC and NAC mixes due to flexural

4.6.2 Effect of SCMs on microstructure of concrete

SEM imaging was performed on concrete samples containing RHA, POFA and POCP at replacement level of 30% for comparison with RAC samples. This replacement level was selected, since the concrete with 30% SCMs showed superior resistance against acid and sulfate attacks than the other mixes. The samples were extracted from concrete exposed to HCl solution for 75 days and $MgSO_4$ solution for 120 days, and was compared to those cured in water.

4.6.2.1 Water curing condition

It can be seen from the SEM images in Figure 4.48 that the cement matrix of concretes blended with RHA, POFA and POCP at level of 30% has a uniform and more closed microstructure than that of RAC under water curing condition, which could be the result of extra C–S–H produced during the pozzolanic reaction; this might be the main reason for the superior performance of blended concretes against the aggressive chemicals compared with unblended concrete, i.e. RAC.

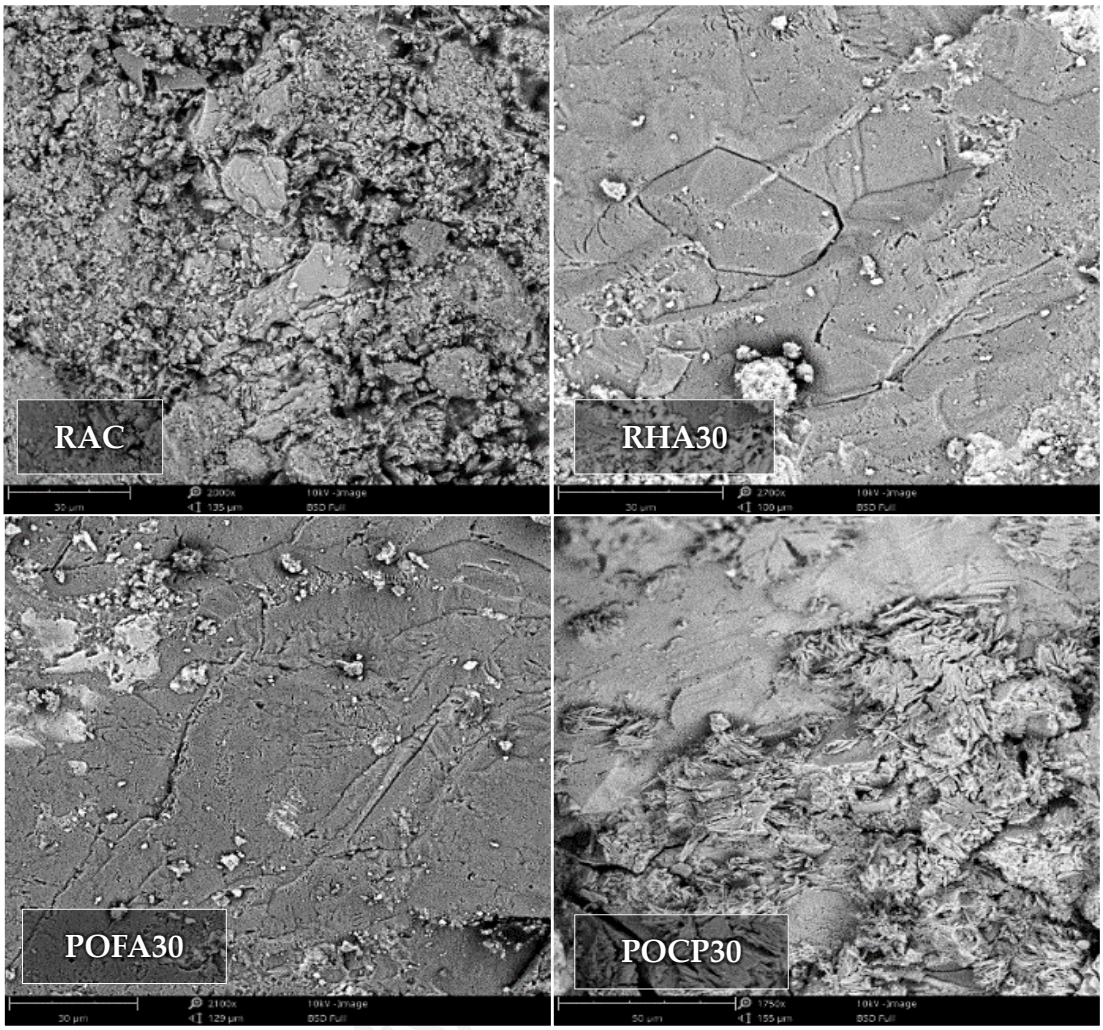

Figure 4.48: SEM images of concrete samples cured in water

4.6.2.2 Acid attack condition

Figure 4.49 shows SEM images of RA concrete exposed to HCl solution for 75 days. The SEM images indicate that the microstructure of RAC specimens exposed to HCl acid solution has a tenuous surface texture and considerable amounts of precipitated salts compared with concrete specimens blended with RHA, POFA and POCP, which indicates better performance of the RA concrete containing SCMs against acid attack. Additionally, it is observed that the acid attack on cement matrix of RAC mix results in detachment of sand grains from the cement matrix and a producing a loosened microstructure. On the other hand, precipitated salts were formed near the aggregates of samples containing SCMs.

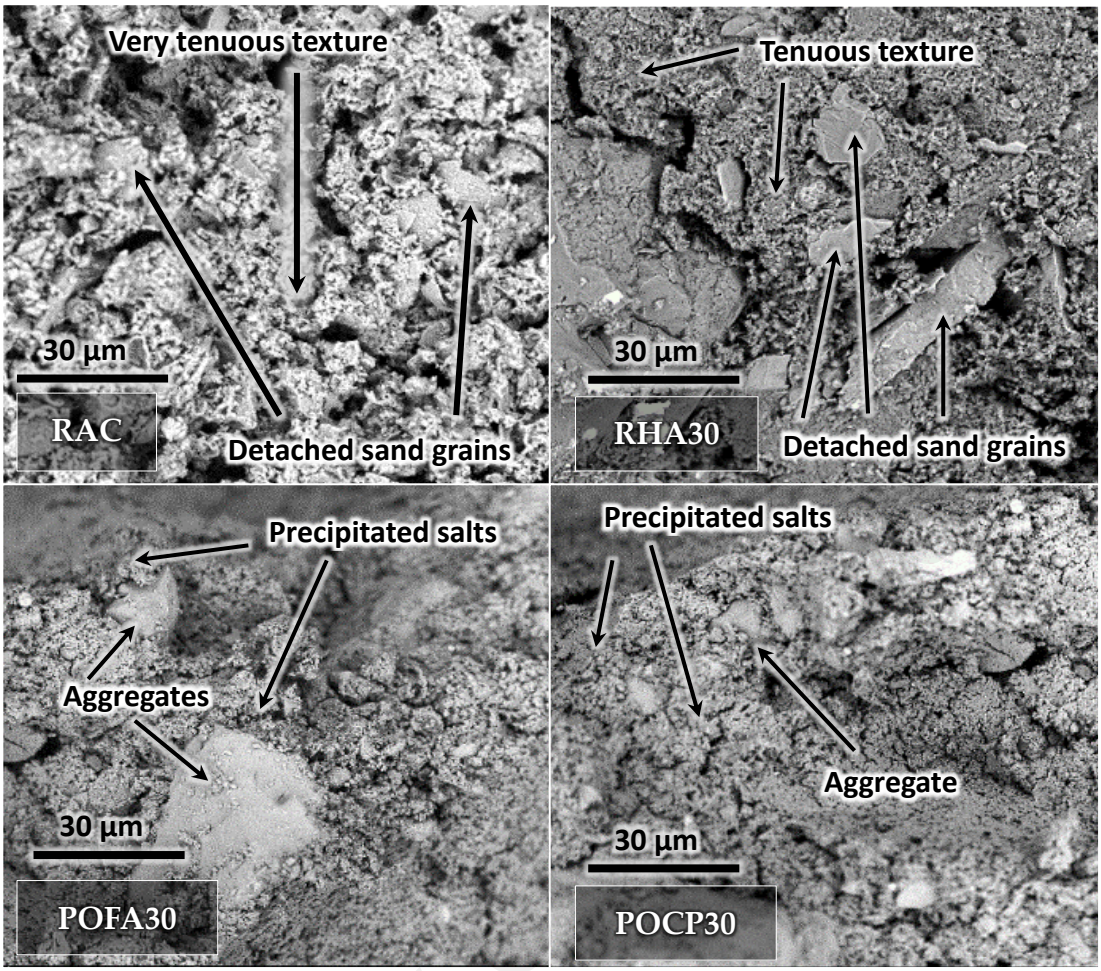

Figure 4.49: SEM images of concrete samples exposed to HCl solution

4.6.2.3 Sulfate attack condition

In the case of sulfate attack, the SEM images in Figure 4.50 show a propagation of micro-cracks in the cement matrix with dissimilar degrees from concrete to another, due to the formation of expansive ettringite (a needle-like crystals shown in Figure 4.51). Nevertheless, the concrete specimens blended with RHA showed superior capability of resisting the propagation of the micro-cracks, even though very few cracks were observed; this enhancement could be attributed to the improved pore structure of RHA-based concretes that prevents the ingress of sulfate ions, which in turn prohibit the formation of gypsum and ettringite. Moreover, the concrete specimens blended with POFA and POCP showed improvement against micro-cracks propagation, but at lower levels than that of RHA-based concretes.

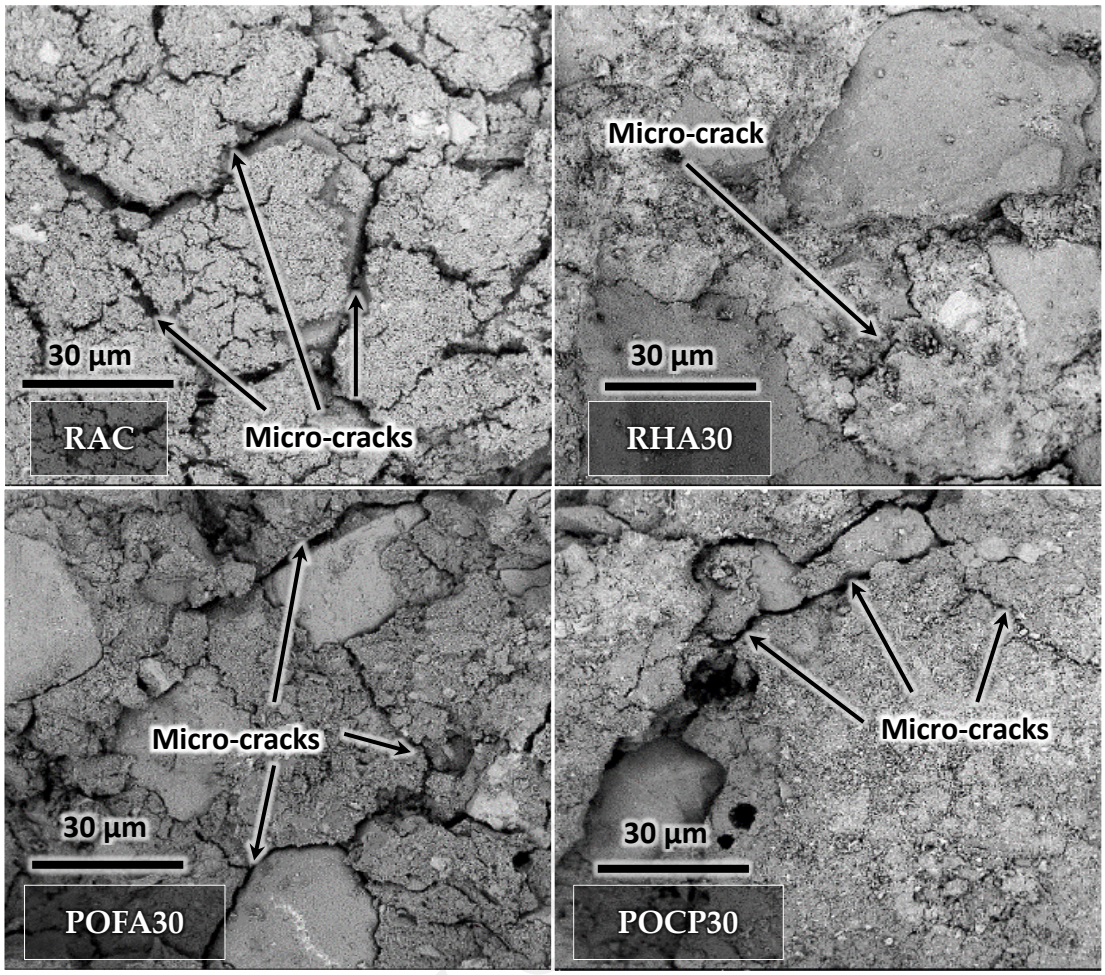

Figure 4.50: SEM images of concrete samples exposed to $MgSO_4$ solution

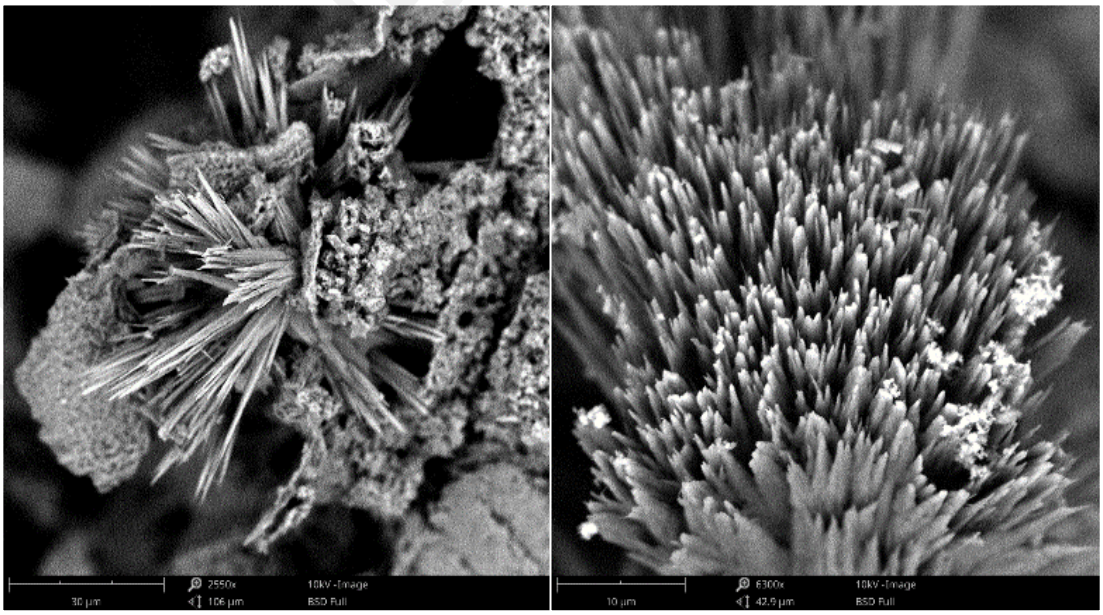

Figure 4.51: SEM image of ettringite needles growing inside the pores of concrete exposed to sulfate solution

4.6.3 X-ray diffraction analysis

The X-ray diffraction (XRD) analysis was performed on concrete samples containing RHA, POFA and POCP at replacement level of 30% for comparison with RAC samples. The samples were extracted from concrete exposed to HCl solution for 75 days and $MgSO_4$ solution for 120 days, and was compared to those cured in water. All samples ground into powder after being extracted from the surface layer of concretes that showed superior performance against chemical attacks, i.e. RHA30, POFA30 and POCP30, for comparison with RAC. Figures 4.52-4.55 show the pattern of the peaks for selected concretes.

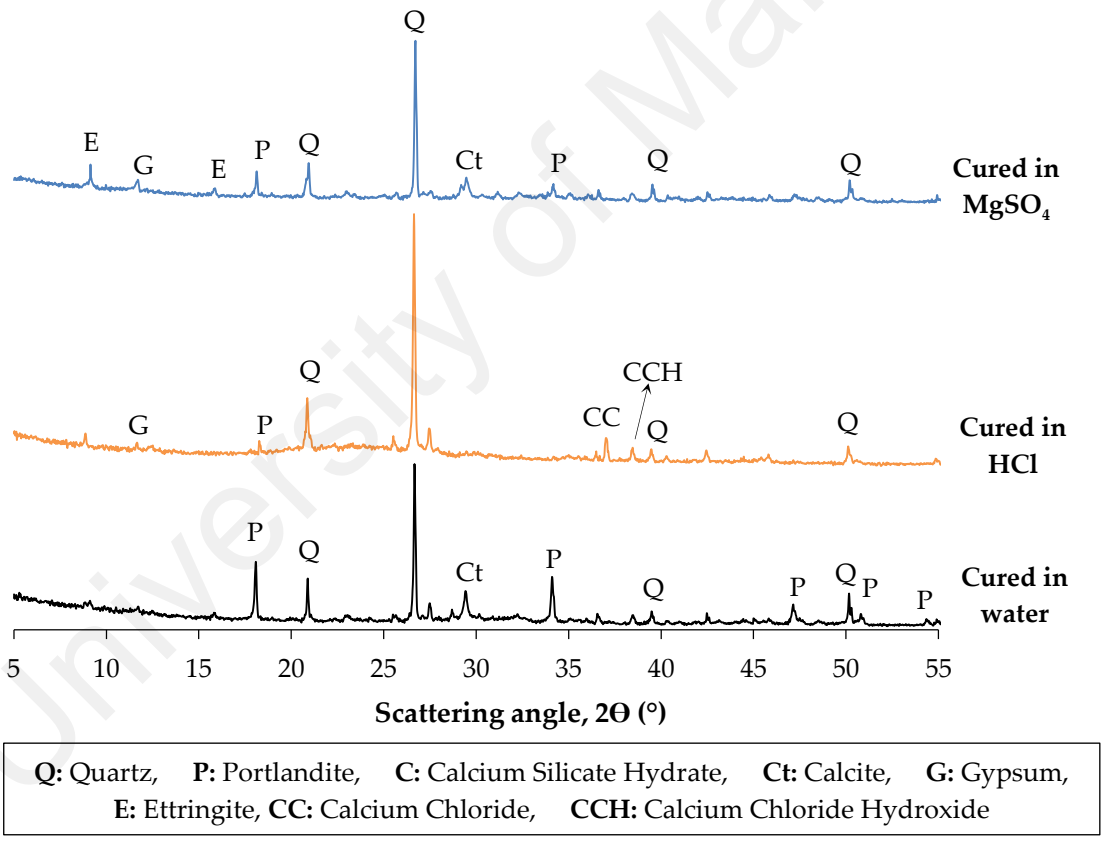

Q: Quartz, **P:** Portlandite, **C:** Calcium Silicate Hydrate, **Ct:** Calcite, **G:** Gypsum, **E:** Ettringite, **CC:** Calcium Chloride, **CCH:** Calcium Chloride Hydroxide

Figure 4.52: XRD patterns of RAC mix

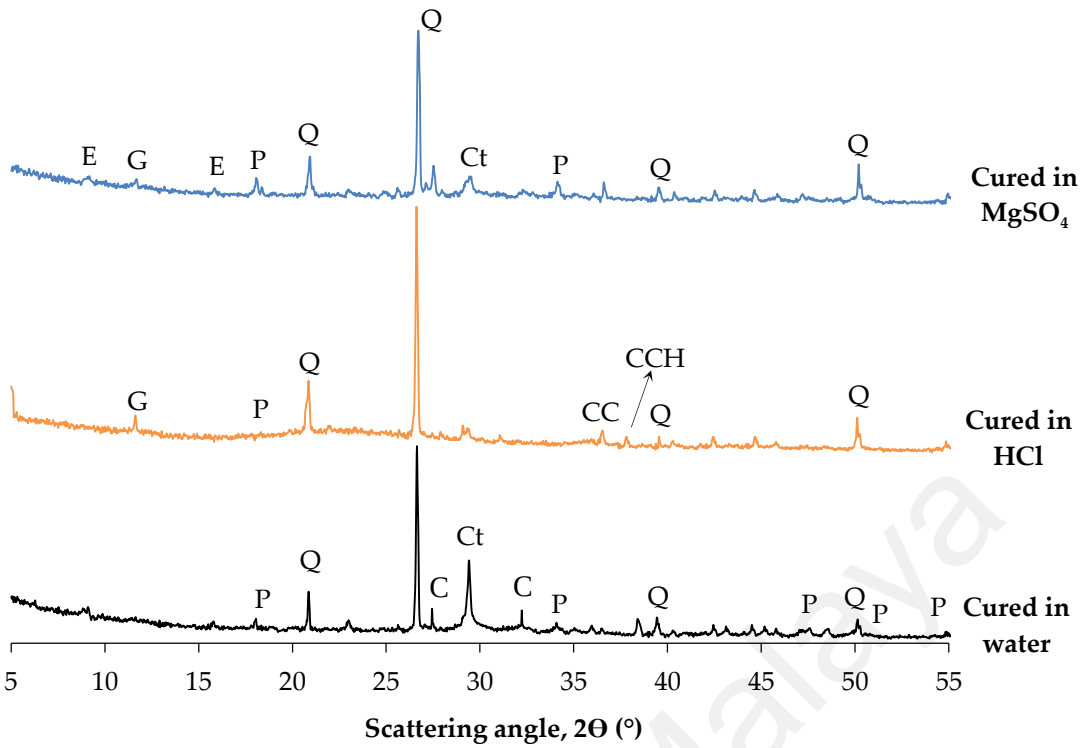

Q: Quartz, **P:** Portlandite, **C:** Calcium Silicate Hydrate, **Ct:** Calcite, **G:** Gypsum, **E:** Ettringite, **CC:** Calcium Chloride, **CCH:** Calcium Chloride Hydroxide

Figure 4.53: XRD patterns of RHA30 mix

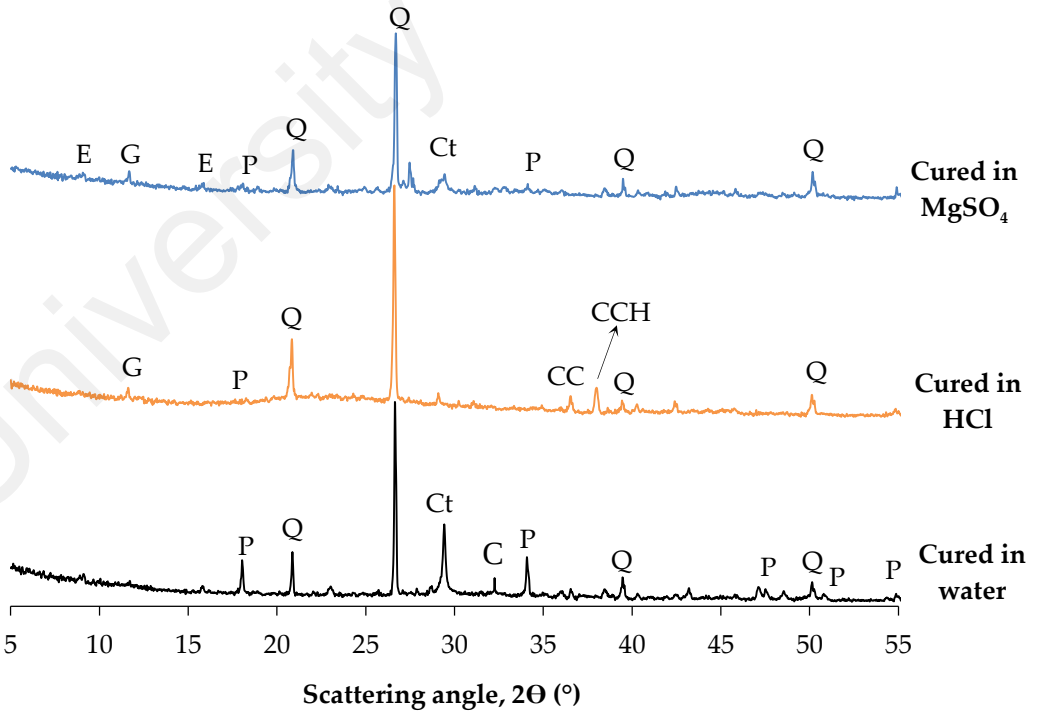

Q: Quartz, **P:** Portlandite, **C:** Calcium Silicate Hydrate, **Ct:** Calcite, **G:** Gypsum, **E:** Ettringite, **CC:** Calcium Chloride, **CCH:** Calcium Chloride Hydroxide

Figure 4.54: XRD patterns of POFA30 mix

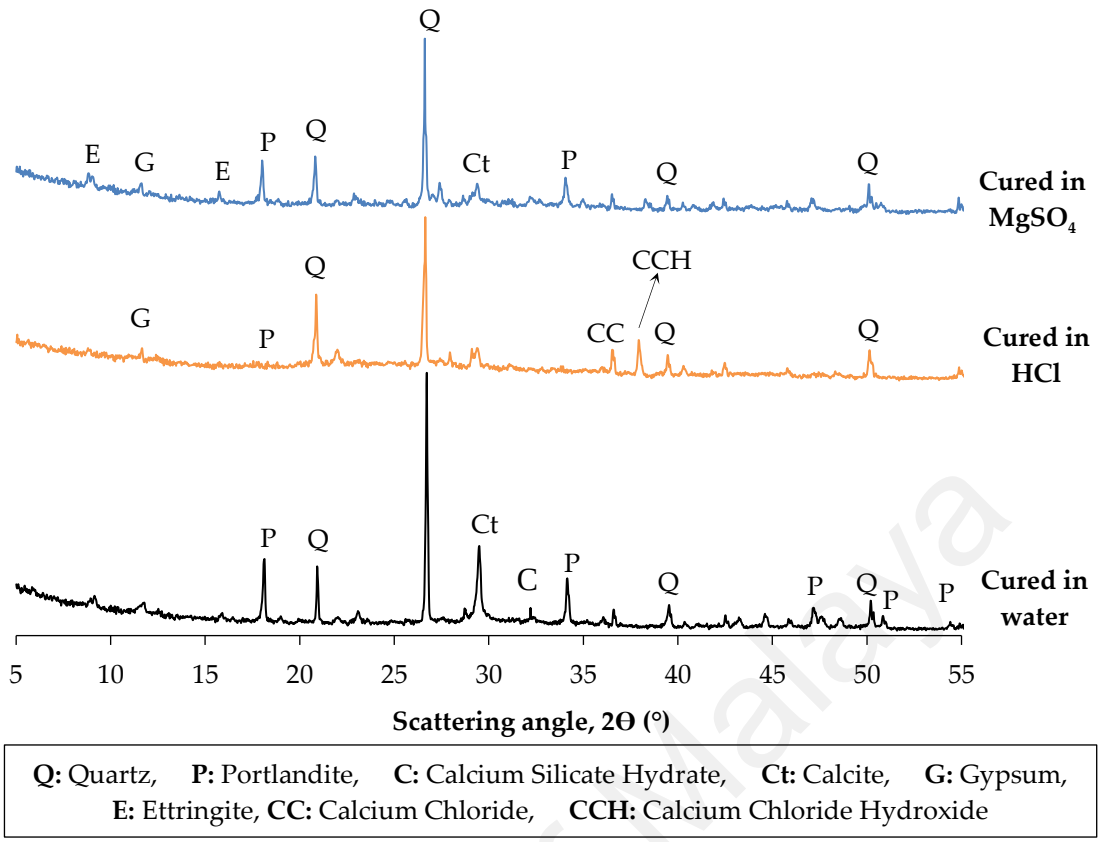

Q: Quartz, **P:** Portlandite, **C:** Calcium Silicate Hydrate, **Ct:** Calcite, **G:** Gypsum, **E:** Ettringite, **CC:** Calcium Chloride, **CCH:** Calcium Chloride Hydroxide

Figure 4.55: XRD patterns of POCP30 mix

Evidently, all concrete samples cured in water showed similar peaks with different intensities for the main phases of portlandite, C–S–H and calcite, irrespective of the type of material used. For instance, the salient peaks at 2Θ of 18.1°, 34.2°, 47.3° and 50.9°, which represent the phase of portlandite (Jo et al., 2017), are more intense in the case of RAC, while lower intensity peaks of portlandite were observed in RHA30, POFA30 and POCP30. The C–S–H peaks are more prominent in samples of RHA30, POFA30 and POCP30 at 2Θ of 31.92° (Jo et al., 2017) as portlandite is used to produce extra C–S–H during the pozzolanic reaction. The XRD results indicate that RHA is more effective as pozzolanic additive than POFA and POCP, where RHA30 showed the lowest trace of portlandite, followed by POFA30 and POCP30. It should be noted that the peaks of quartz could be due to the presence SiO_2 in sand particles, and it does not reflect any of hydration products (Ranjbar et al., 2016).

In the case of specimens immersed in HCl acid solution, the XRD results showed peaks of gypsum, calcium chloride and calcium chloride hydroxide at 2Θ of 11.6°, 37.1° and 38.3°, respectively. The low intensity peak of calcium chloride is due to its high solubility in water. Nevertheless, it can be seen that the portlandite peaks disappeared from all samples due to the penetration of HCl ions, which decompose the hydration products (Gutberlet et al., 2015).

The XRD patterns of the specimens exposed to $MgSO_4$ solution show peaks of gypsum and ettringite with different intensities, depending on the type of material incorporated, due to the reaction between $MgSO_4$ ions and portlandite. The high intensity peaks of gypsum and ettringite observed in RAC samples indicate a high possibility of deterioration, while these peaks were hardly detected in samples of RHA30, POFA30 and POCP30. Table 4.13 summarizes the main phases detected in specimens cured in water, acid and sulfate solutions.

Table 4.13: The main phases detected in specimens cured in water, HCl solution and $MgSO_4$ solution

Phase	Peaks at 2Θ	Remarks
Quartz (SiO_2)	20.9°, 26.6°, 39.5° and 50.1°	The quartz phase does not reflect one of the hydration products as it might be due to the presence of SiO_2 that can be found in the sand particles.
Portlandite ($Ca(OH)_2$)	18.1°, 34.2°, 47.3°, 50.9° and 54.5°	Blended concretes with RHA, POFA and POCP showed lower intensity peaks of portlandite than RAC.
Calcium silicate hydrate ($3CaO{\cdot}2SiO_2{\cdot}4H_2O$)	31.92°	This peak more prominent in specimens containing RHA, POFA and POCP.
Calcite ($CaCO_3$)	29.4°	This peak was greatly reduced after exposure to HCl and $MgSO_4$ solutions.
Calcium chloride ($CaCl_2$)	37.1°	Due to HCl attack, these peaks were recorded in all samples but with low intensities due to their high solubility in water.
Calcium chloride hydroxide (CaClHO)	38.3°	
Tricalcium aluminates (C_3A) ($3CaO{\cdot}Al_2O_3$)	33.2° and 47.7°	Due to $MgSO_4$ attack, these peaks were found in very low intensity as expected, due to their conversion to ettringite when reacted with gypsum.
Gypsum ($CaSO_4{\cdot}2H_2O$)	11.6°	Gypsum peaks were more prominent in samples immersed in sulfate solution as a result of the reaction between portlandite and $MgSO_4$.
Ettringite ($3CaO{\cdot}Al_2O_3{\cdot}3CaSO_4{\cdot}32H_2O$)	9.1° and 15.8°	Due to $MgSO_4$ attack, high intensity peaks were detected in the control RAC sample, while they are hardly noticed in the samples containing RHA, POFA and POCP.

4.7 Chemical composition effect of concrete mixtures

4.7.1 Effect of chemical composition on compressive strength

The pozzolanicity and ability of the SCM to consume $Ca(OH)_2$ and form more C–S–H is influenced by different parameters, such as chemical composition, SiO_2 content and particle size of the SCM (Juenger & Siddique, 2015). Consequently, the level of reactivity depends on the replacement ratio of OPC by SCM to attain sufficient strength. For instance, mixes RHA30 and POFA10 resulted in similar strength at the age of 90 days, even though the replacement level was different. Table 4.14 shows the comparison of the major oxide compositions of all mixes. For those containing 10% SCM, i.e. RHA10, POFA10 and POCP10, the ratio of CaO/SiO_2 was 2.08, 2.32, and 2.35, respectively. Thus, RHA10 contains less CaO and more SiO_2 than POFA10 and POCP10, which led to the formation of more C–S–H, and subsequent higher strength. On the contrary, the addition of more SiO_2 by increasing the replacement level by more than 10%, the CaO content will also decrease, where CaO plays a significant role in the development of compressive strength, especially in the early age (Islam et al., 2014). As a consequence of the surplus SiO_2, the hydration process will be prolonged, which is evident in RHA30 that contains the maximum content of SiO_2 among all mixes, but the CaO/SiO_2 ratio of 1.08 was very low, making its compressive strength lower than that of RHA10 and RHA20.

Table 4.14: Chemical composition and compressive strength of concrete mixes

Mix	Chemical composition (%)					Compressive strength (MPa)	
	CaO	SiO_2	Al_2O_3	Fe_2O_3	CaO/SiO_2	28-d	90-d
NAC	64.7	21.0	5.9	3.4	3.08	45.4	48.3
RAC	64.7	21.0	5.9	3.4	3.08	35.8	38.4
RHA10	58.3	28.0	5.4	3.1	2.08	38.9	46.2
RHA20	51.9	35.0	4.8	2.8	1.48	37.0	43.3
RHA30	45.4	42.0	4.2	2.5	1.08	33.3	38.0
POFA10	58.8	25.3	5.7	3.7	2.32	31.0	39.3
POFA20	52.9	29.6	5.5	4.0	1.79	28.5	36.5
POFA30	47.0	34.0	5.3	4.3	1.39	26.1	32.5
POCP10	58.6	25.0	5.9	3.5	2.35	29.7	37.4
POCP20	52.4	28.9	5.9	3.7	1.82	30.4	36.7
POCP30	46.3	32.8	5.9	3.8	1.41	26.5	32.1

Figure 4.56 represents the layout of all concrete mixtures in $CaO–SiO_2–Al_2O_3$ ternary diagram. Qualitatively, it can be seen that the incorporation of SiO_2-rich SCMs leads to decrease the amount of portlandite and increase the formation of more C–S–H. Nevertheless, Lothenbach et al. (2011) outlined that at excessive replacement levels, the reaction rate decreases as the pH of the pore solution reduces due to the reduction of dissolved calcium and increases uptake of the alkaline compounds, e.g. portlandite, which slows down the rate of reaction when the pH is below 12. The solubility of amorphous silica is extremely sensitive to increases in pH between 12 and 14. The higher the pH, the faster the rate of reaction. In Portland cement–SCM blends, the high pH is provided by alkali hydroxides and calcium hydroxide, with pore solution pH increasing rapidly in the first few hours of hydration as sulfate ions are removed from pore solution due to reaction with aluminates. To maintain electro-neutrality, hydroxyl ions replace the sulfate ions in solution, and pH levels are usually maintained between 13 and 14 after about 24 h. These hydroxyl ions allow the secondary reactions to occur with the amorphous silica-rich

phases in SCMs. Provided that sufficient hydroxyl ions remain in solution to maintain the pH of the pore solution, the SCM reactions will continue. If the SCM replacement level is too high, the pH will drop, reducing the solubility of the amorphous silicates and thus slowing the rate of reaction (Lothenbach et al., 2011).

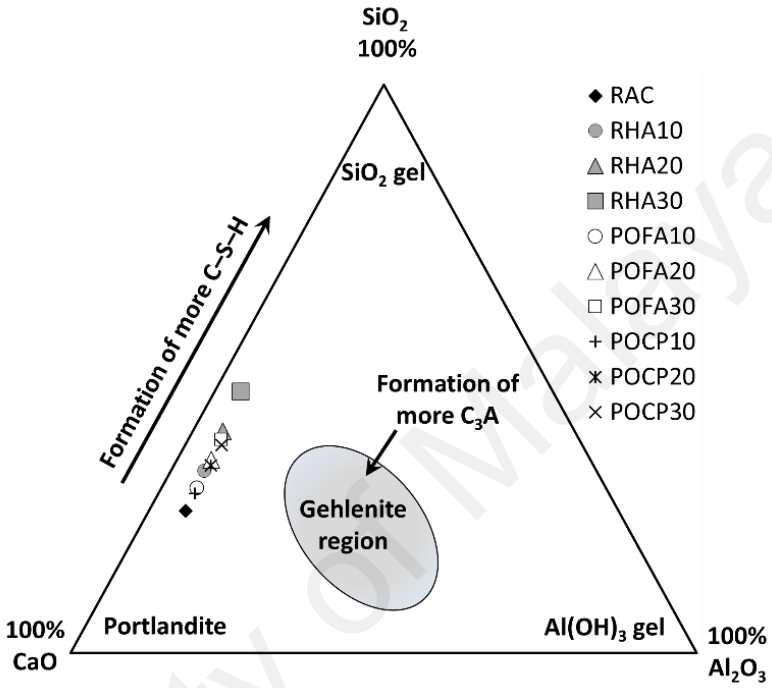

Figure 4.56: Concrete mixtures in the $CaO–Al_2O_3–SiO_2$ ternary diagram

4.7.2 Effect of chemical composition on acid resistance

Generally, the chemical composition of hydration products for SCM-based concrete with SiO_2-rich content is characterized by lower calcium content than 100% OPC-based concrete. The decomposition of cement matrix attacked by acid is primarily due to the release of calcium from the hydration products and, only at very low pH values, due to the release of aluminum and iron (Gutberlet et al., 2015). Bassuoni and Nehdi (2007) revealed that the C–S–H structure with high CaO/SiO_2 ratio is more vulnerable to acid attacks, and on the contrary, the decomposition of C–S–H with low CaO/SiO_2 ratio occurs at slower rate. Additionally, Chatveera and Lertwattanaruk (2011) concluded that the chemical composition and the CaO/SiO_2 ratio in concrete mixture are important factors for evaluating the effect of acid attacks. Consequently, the C–S–H that produced with low

CaO/SiO_2 ratio is less susceptible to decompose (release of calcium), since it has a crystalline structure with low amounts of calcium. These observations also support the results of this study, where the superior performance was recorded for concretes containing low CaO/SiO_2 ratios.

4.7.3 Effect of chemical composition on sulfate resistance

The position of concrete mixture on the $CaO–Al_2O_3–SiO_2$ ternary diagram could be useful to determine its sulfate resistance. For instance, if the concrete mixture falls within the gehlenite region as shown in Figure 4.56, it typically has a low resistance against sulfate attacks (Kruse, 2012). This could be related to the high C_3A content in this region, where C_3A is considered as the reactive compound responsible for ettringite formation. However, the results of this study showed that the SCM-based concretes have lower CaO content than that of RAC, and thus, the resulting content of reactive C_3A will be reduced. Therefore, in this ternary diagram, one would expect to see a shift of the SCM-based concrete mixtures away from the gehlenite region. Donatello et al. (2013) revealed that the CaO content of pastes incorporating high volume fly ash is much lower as a direct consequence of the lower OPC content and higher fly ash content. They stated that the substantially higher C_3A content in the OPC paste made it more susceptible to sulfate attacks.

4.8 Carbon dioxide (CO_2) emissions

4.8.1 Assumptions for CO_2 emissions due to the manufacture of major concrete materials

This section illustrates the CO_2 emission factors for the major ingredients that used in all concrete mixtures of this study including OPC, RHA, POFA, POCP, recycled coarse aggregate, normal coarse aggregate and mining sand.

4.8.1.1 CO_2 emissions due to manufacture of OPC

Numerous researchers have estimated the emission factor due to the activities associated to the manufacture of OPC. One of the most recent studies, which belongs to Collins (2010), reported an emission factor of 0.82 kg CO_2/kg of OPC. The manufacture of OPC shows high emission factor as a result of the high energy consumed during production process starting from the extraction of raw materials, then the calcination of limestone at a temperature of 1500 °C, and finally packing and transportation to concrete batching plants.

4.8.1.2 CO_2 emissions due to treatment of SCMs

In this research, RHA, POFA and POCP were used as SCMs. The CO_2 emission factors were determined by calculating the emissions during their preparation, including transportation, grinding and treatment process. The total energy that was consumed to improve the reactivity of RHA, POFA and POCP was 0.160, 0.175 and 0.211 kWh/kg, respectively. Additionally, to estimate the emission factor during transportation, the diesel that was consumed over 100 km by truck with engine size of 2,000cc was calculated during the delivery of one ton for each of RHA, POFA and POCP for treatment and processing. According to the United Kingdom's Department for Energy and Climate Change (DECC, 2011), the assumed emission factors due to electricity generation and transportation are 0.521 kg CO_2/kWh and 0.192 kg CO_2/km, respectively. Based on these assumptions, the total emission factors caused by electricity required for treatment and

fuel (diesel) used for transportation to prepare RHA, POFA and POCP are 0.1032, 0.1102 and 0.1292 kg CO_2/kg, respectively.

4.8.1.3 CO_2 emissions during coarse and fine aggregate extraction

The CO_2 emission factors that arose from preparation of crushed granite aggregate and mining sand were assumed based on the estimated data by Flower and Sanjayan (2007). The amount of CO_2 was calculated by considering the fuel, electricity and explosives that were used during the extraction process of coarse and fine aggregates. The CO_2 emission factors were found to be 0.0459 and 0.0139 kg CO_2/kg for crushed granite and mining sand, respectively.

4.8.1.4 CO_2 emissions during demolition and recycling of built structure

According to García-Segura et al. (2014), the CO_2 amount arise due to the recycling process of a built structure was 3.81 kg CO_2/m^3 for demolishing stage and 0.59 kg CO_2/m^3 for crushing and screening stage, which is equivalent to 0.002 kg CO_2 per kg of recycled concrete aggregate (RA). Therefore, the total CO_2 emissions due to treatment and transportation of RA is 0.0212 kg CO_2/kg. Table 4.15 and Figure 4.57 show the CO_2 emission factors for the major ingredients used in all concrete mixes

Table 4.15: CO_2 emission factors for SCMs

Item	Energy requirements for 1000 kg SCM			Transportation of 1000 kg SCM		Total emission (kg CO_2/kg SCM)
	Consumption (kWh)		Emission factor (kg CO_2/ kWh)[c]	Distance (km)[d]	Emission factor (kg CO_2/km)[e]	
	Drying [a]	Sieving and grinding[b]				
RHA	00	160	0.521	100	0.192	0.1032
POFA	25	160	0.521	100	0.192	0.1102
POCP	25	186	0.521	100	0.192	0.1292

[a]The energy consumed by laboratory oven during 24 hours with consumption rate of 1041.67 W/h.
[b]The energy consumed by sieving and grinding machines.
[c]Emission factor due to electricity generation (DECC, 2011).
[d]The distance from rice mill/palm-oil mill to the laboratory in the University of Malaya.
[e]The emission factor of the lorry used to transport the materials (DECC, 2011).

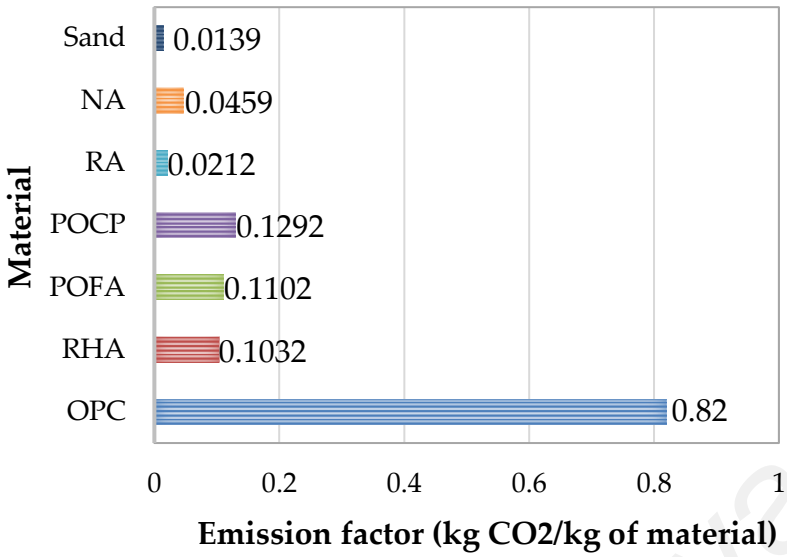

Figure 4.57: CO_2 emission factors for the major ingredients used in all concrete mixes

4.8.2 Comparison of CO_2 emissions for concrete mixtures

Table 4.16 and Figure 4.58 summarize the CO_2 emissions for one cubic meter of concrete. The results showed that NAC mix with 100% OPC and crushed granite aggregate has the highest emission value of 369 kg CO_2/m^3, while the lowest value of 260 kg CO_2/m^3 recorded for RHA30 mix with 30% reduction when compared to NAC mix. In addition, the whole replacement of crushed granite aggregate by RA decreased the CO_2 emissions by about 7% at 342 kg CO_2/m^3 for RAC when compared to NAC. Hanif et al. (2017) reported that the substitution of conventional aggregate by RA leads to reduce the CO_2 emissions by about 2%. However, the benefit of using RA is summed up in conserving the natural resources despite their meagre contribution in reducing the CO_2 emissions. When SCMs was incorporated, it can be observed that the reduction of CO_2 emissions increases as the substitution level of SCMs increases. Alsubari et al. (2016) reported a reduction in CO_2 emissions of up to 32-45% when POFA was used to partially replace OPC. According to the results of this study, it can be seen from Figure 4.58 that the binder (cement + SCMs) was by far the most significant contributor to CO_2 emissions at rates ranging from 84% to 90% of the total emissions of 1 m^3, depending on the replacement ratio and type of SCMs, followed by the extraction process of coarse

aggregate as second highest source of CO_2 emissions. Although RA-based concretes containing POFA and POCP beyond 20% replacement level have inferior properties in terms of compressive strength, they could attain sufficient reduction level of CO_2 emissions alongside achieving ecological balance.

Table 4.16: CO_2 emissions for one cubic meter of concrete

Mix	CO_2 emissions for one cubic meter of concrete (kg CO_2/m^3)							
	Binders				Coarse aggregate		Fine aggregate	Total
	OPC	RHA	POFA	POCP	Normal	Recycled		
NAC	311.6	0	0	0	46.8	0	10.43	369
RAC	311.6	0	0	0	0	20.0	10.43	342
RHA10	280.4	3.9	0	0	0	20.0	10.43	314
RHA20	249.3	7.8	0	0	0	20.0	10.43	287
RHA30	218.1	11.8	0	0	0	20.0	10.43	260
POFA10	280.4	0	4.2	0	0	20.0	10.43	315
POFA20	249.3	0	8.4	0	0	20.0	10.43	288
POFA30	218.1	0	12.6	0	0	20.0	10.43	261
POCP10	280.4	0	0	4.9	0	20.0	10.43	315
POCP20	249.3	0	0	9.8	0	20.0	10.43	289
POCP30	218.1	0	0	14.7	0	20.0	10.43	263

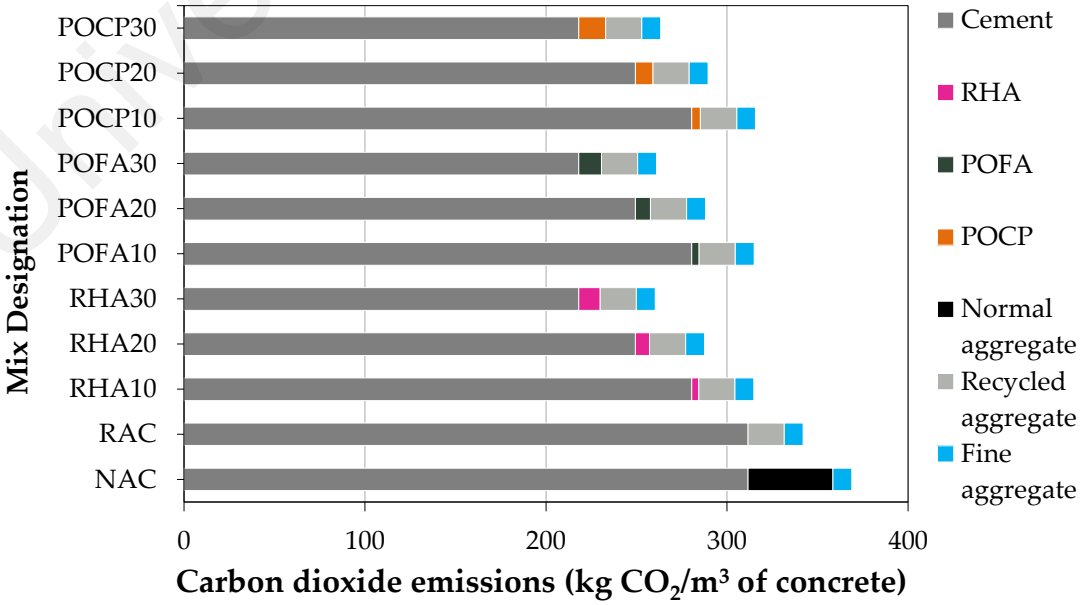

Figure 4.58: Comparison of CO_2 emissions of RA-based concrete containing SCMs

4.8.3 Eco-strength efficiency

Figure 4.59 illustrates the efficiency of all concrete mixtures by comparing the ratio of compressive strength to CO_2 emissions at the ages of 28 and 90 days. Generally, it can be seen that the 20% replacement ratio has the highest efficiency value for each SCM. In addition, the efficiency value of NAC and RHA10 was similar at the age of 28 days with 0.123 MPa/kg $CO_2.m^{-3}$ even though NAC has higher compressive strength than RHA10. Further, at the age of 90 days, the efficiency value for RHA10 was 0.147 MPa/kg $CO_2.m^{-3}$ which is 13% higher than NAC value of 0.130 MPa/kg $CO_2.m^{-3}$, although they have similar compressive strength. Similar concept observed by García-Segura et al. (2014) when they concluded that the replacement of cement by RHA together with fly ash in concrete reduced CO_2 emissions without considerable reduction in compressive strength. After 90 days, RHA20 showed superior performance among all mixtures with 0.150 MPa/kg $CO_2.m^{-3}$ or 34% higher than RAC which has the lowest efficiency value of 0.112 MPa/kg $CO_2.m^{-3}$; despite the least contribution of RA towards CO_2 emissions coupled with its negative effect on the compressive strength, the mix RHA 20 showed excellent eco-efficiency. In addition, POFA and POCP concretes exhibited efficiency values in the range between 0.092 and 0.110 MPa/kg $CO_2.m^{-3}$ at the age of 28 days, while the efficiency improved to be in the range between 0.118 and 0.127 MPa/kg $CO_2.m^{-3}$ at the age of 90 days. Overall, it can be observed that the efficiency values of concretes containing SCMs were considerably improved at the age of 90 days due to the enhancement of the compressive strength at this age.

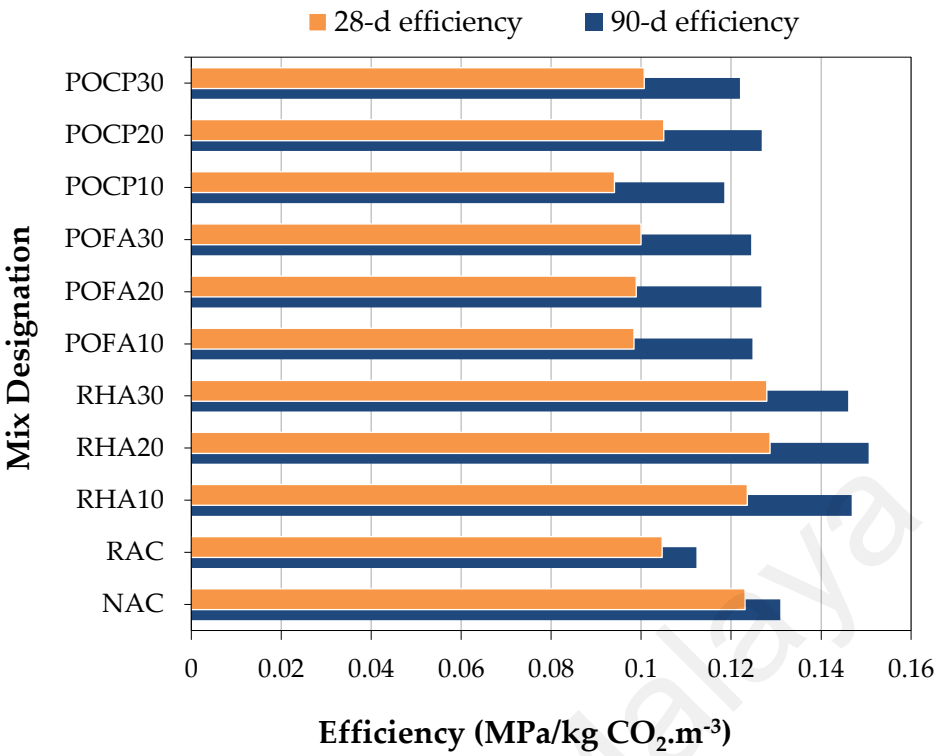

Figure 4.59: Efficiency of concrete with respect to CO_2 emissions and compressive strength

4.9 Summary

This section presents the summary based on the results of using agricultural by-products from different industries as sustainable SCMs in RA-based concrete.

1. The hardened properties of RA based concrete decreased by about 21%, 7%, 14% and 21% for compressive strength, splitting tensile strength, flexural strength and modulus of elasticity, respectively, when the normal aggregates were wholly replaced by recycled aggregates.
2. The splitting tensile and flexural strengths of RA-based concrete improved by utilization of RHA up to 20% and POFA at a replacement level of 10%.
3. The modulus of elasticity was largely influenced when the crushed granite aggregate was wholly replaced by RA, while the use of RHA, POFA and POCP in RA-based concrete has no significant effect as the elastic properties of the aggregate has more significant effect than the strength of cement matrix on the concrete's modulus of elasticity.

4. Generally, the strength evolution between 28 and 90 days was more prominent for concretes containing SCMs. For instance, the increments of compressive, splitting tensile and flexural strengths for concretes containing SCMs were found in the ranges of 12%–22%, 6%–15% and 16%–23%, respectively, regardless of the type and ratio of SCM used, in contrast to the corresponding increments of 6%, 8% and 14% for RAC mix without SCMs; this indicates that the pozzolanic reaction between SiO_2 and $Ca(OH)_2$ to form additional C-S-H gel takes place after 28 days of curing period.
5. The capillary water absorption (sorptivity) of RA-based concrete was decreased significantly after long curing period of 90 days using RHA, POFA and POCP at replacement levels of up to 30%, 20% and 10%, respectively. The effect of the aforementioned SCMs on the sorptivity was via the formation of additional C–S–H gel which has the potential of infilling the existing micro-voids and refining the pore structure.
6. After exposure to HCl acid solution, the RA-based concrete containing RHA, POFA and POCP showed superior performance against deterioration, weight loss and strength loss due to low amount of $Ca(OH)_2$, which is very weak in resisting acid attack.
7. The SEM images showed that the incorporation of RHA, POFA and POCP was able to minimize the deterioration of RA-based concrete exposed to $MgSO_4$ solution due to the formation of dense microstructure that inhibits the ingress of sulfate ions and reduces the formation of expansive ettringite, which in turn leads to less propagation of micro-cracks.
8. The XRD results showed that incorporation of SiO_2-rich SCMs decreases the amount of portlandite and forms more C–S–H.

9. The RCPT results showed that the risk of corrosion of RAC mix is classified as "high" due to the increase in volume of the paste (old mortar found in RA particles + new mortar), which considered as the weakest point for penetration of chloride ions. On the other hand, the resistance to the penetration of chloride ions of RA-based concrete significantly enhanced with the use of SCMs after 90 days of water curing. The superior performance of RA-based concrete incorporated with SCMs explained by the enhancement in impermeability of the pore structure.
10. The electrical resistivity values for both NAC and RAC indicated a "high" possibility of corrosion. Nevertheless, an improvement of resistivity for RA-based concretes containing SCMs especially for those incorporated with RHA was noticed. For instance, the resistivity of RHA-based concrete indicated a "very low" possibility of corrosion. Further, the resistivity of POFA and POCP-based concretes indicated a "low to medium" possibility of corrosion.
11. The CO_2 emissions resulting from the manufacture of concrete clearly reduced when the substitution level of SCMs was increased, and the compressive strength with respect to CO_2 emissions showed the highest efficiency values at 20% cement replacement level for all RA based SCM concretes.

CHAPTER 5: CONCLUSIONS AND RECOMMENDATIONS

5.1 Introduction

A research program was undertaken to determine the microstructure, mechanical and durability of RA-based concrete with the research emphasized on cement replacement materials from agricultural by-products as they have had limited attention in the literature. The objective of the study was to investigate the use of supplementary cementitious materials (SCMs), namely, RHA, POFA and POCP that are available in Malaysia, to improve the properties of RA-based concrete and to reduce the dependency on cement as a standalone binder. This was achieved by conducting experiments on concrete mixtures, evaluating the performance of the materials that were incorporated and comparing them to a control mixture.

5.2 Conclusions

Based on the results of using agricultural wastes from different industries as sustainable SCMs in RA-based concrete, the following conclusion can be drawn according to the objectives of the study:

1. The effect of recycled concrete aggregate on the engineering performance of concrete.

The results indicated that the mechanical properties of the concrete made with the recycled aggregate derived from parent concrete with compressive strength of 50 MPa was decreased in the range of 7% - 21%. However, adequate compressive strength of the concrete made with 100% RA was achieved at the age of 28 days. Additionally, The concrete made from RA produced lower modulus of elasticity compared with the normal concrete due to the presence of old mortar with a relatively low modulus of elasticity; the RA, due to its porosity, affects the modulus of elasticity of concrete, as its inability to resist the deformation directly influences the modulus of elasticity of concrete.

Nevertheless, RA-based concrete with a low modulus of elasticity is less susceptible to cracking due to its ability to sustain more deformation. Thus, there may be a beneficial effect in minimizing the cracks when RA is incorporated in concrete.

2. The effect of supplementary cementitious materials on the fresh and hardened properties of RA concrete.

It can be concluded that the RHA, POFA and POCP with high fineness are reactive pozzolanic materials and can be utilized to achieve the required 30 MPa compressive strength for RA concrete after 90 days of water curing by replacing the ordinary Portland cement at levels up to 30%. The RHA improved the compressive strength of the concrete at all ages, whereas the beneficial effect of POFA and POCP has been noticed only after a relatively long curing time (>28 days).

3. The durability performance of RA-based concrete incorporated with supplementary cementitious materials and exposed to aggressive environments.

In this study, the effect of SCMs on the acid and sulfate resistance of RA concrete is investigated. The results revealed that the incorporation of RHA, POFA and POCP up to 30% minimizes concrete deterioration and loss in compressive strength when the specimens were exposed to aggressive solutions. In addition, although the early age performance of the RA-based concrete containing SCMs was low, a significant enhancement observed for the durability-related properties, namely water absorption, chloride-ion penetration and electrical resistivity at later stages when RA-based concrete incorporated with up to 30% RHA or up to 20% POFA and POCP. The proportion of chemical compositions in concrete mixture is a significant factor affecting the performance of concrete attacked by aggressive chemicals. SCM-based concrete with SiO2-rich content is characterized by lower calcium content than 100% OPC-based

concrete. Thus, the hydration products are less susceptible to decompose (release of calcium) when exposed to acid. In addition, the content of reactive C3A will be reduced, where the latter is considered as reactive compound responsible for the formation of ettringite.

4. The microstructure characteristics of RA-based concrete containing supplementary cementitious materials.

The scanning electron microscopy image showed less propagation of micro-cracks caused by expansive ettringite in the case of $MgSO_4$ attack. Further, the X-ray diffraction analysis indicated that RHA is more effective as pozzolanic additive than POFA and POCP, due to the higher amount of reactive SiO_2 found in RHA compared to POFA and POCP.

Based on the findings of this study, the utilization of agricultural wastes as cement replacement material to conventional cement is feasible in 100% RA-based concrete. Further, the benefits of sustainable SCMs are not only constrained to the technical effects on the concrete, but also through their vital impact on the economic and environmental aspects. The incorporation of such products serves as an avenue to reduce the volume of waste dumped in the vicinity of factories and at the same time would reduce the exploitation of natural resources. Therefore, minimizing the deleterious impact of the construction industry on the environment and keeping the movement towards more environmentally-conscientious building materials would pave the way for achieving sustainability in the concrete industry. The cost-benefits of incorporating sustainable materials into concrete differ for each application and depend on the availability of these materials. The widespread acceptance of waste materials and agricultural by-products by the concrete industry can be facilitated by filling the knowledge gaps that currently exist with respect to the myriad of potential alternatives.

5.3 Recommendations

Based on this investigation, a few recommendations for future research can be made:

- Different w/b ratios should be considered to evaluate if the proposed optimum replacement content works with RA-based concrete.
- Further research should also be done on the treatment of POFA since it has a high LOI value. Hence, the heat treatment is recommended to remove the high carbon content exists in POFA.
- The behavior of concrete mixes incorporating RA and high volumes of SCMs should be studied.
- This research focused only on the mechanical, durability and microstructure properties of concrete at material levels. Future work would include testing the RA-based concrete incorporating SCMs in a full scale structural applications. Possible composite components that could be tested include concrete filled tubes for structural columns and dual skin composite shear walls to resist gravity and seismic loadings. An advantage of using a high-volume SCM concrete in these applications is that early strength is not required from the concrete, since the steel jacket is capable of supporting the initial construction load and formwork is not removed (as would be required for a reinforced concrete component). Therefore, RA-based concrete containing SCMs can be more readily used in composite construction, even though a low early strength (< 28 days) is often associated with such concrete.
- Additional durability studies can be undertaken to further the knowledge of SCMs being used to mitigate concrete deterioration.
- Life cycle assessment is needed for the agricultural wastes that are being used in concrete to evaluate the environmental impacts associated with all the stages

of their life from production stage and disposal as waste to the stage of recycling, processing and use in concrete.

REFERENCES

ACI 222R-01. (2001). Protection of Metals in Concrete Against Corrosion. *American Concrete Institute*.

ACI 318-14. (2014). Building code requirements for structural concrete and commentary *American Concrete Institute*.

Adams, M. P., Fu, T., Cabrera, A. G., Morales, M., Ideker, J. H., & Isgor, O. B. (2016). Cracking susceptibility of concrete made with coarse recycled concrete aggregates. *Construction and Building materials, 102*, 802-810.

Ahmmad, R., Alengaram, U. J., Jumaat, M. Z., Sulong, N. R., Yusuf, M. O., & Rehman, M. A. (2017). Feasibility study on the use of high volume palm oil clinker waste in environmental friendly lightweight concrete. *Construction and Building materials, 135*, 94-103.

Akça, K. R., Çakır, Ö., & İpek, M. (2015). Properties of polypropylene fiber reinforced concrete using recycled aggregates. *Construction and Building materials, 98*, 620-630.

Alexander, M., Bertron, A., & De Belie, N. (2013). *Performance of cement-based materials in aggressive aqueous environments* (Vol. 10): Springer.

Alsubari, B., Shafigh, P., & Jumaat, M. Z. (2015). Development of Self-Consolidating High Strength Concrete Incorporating Treated Palm Oil Fuel Ash. *Materials, 8*(5), 2154-2173.

Alsubari, B., Shafigh, P., & Jumaat, M. Z. (2016). Utilization of high-volume treated palm oil fuel ash to produce sustainable self-compacting concrete. *Journal of Cleaner Production, 137*, 982-996.

Anderson, K., Uhlmeyer, W., & Russell, M. (2009). Use of recycled concrete aggregate in PCCP. *Literature Search WA-RD, 726*.

Andreu, G., & Miren, E. (2014). Experimental analysis of properties of high performance recycled aggregate concrete. *Construction and Building materials, 52*, 227-235.

ASTM C143/C143M−15. (2015). Standard Test Method for Slump of Hydraulic-Cement Concrete. *ASTM International, West Conshohocken, PA*.

ASTM C192/C192M−15. (2015). Standard Practice for Making and Curing Concrete Test Specimens in the Laboratory. *ASTM International, West Conshohocken, PA*.

ASTM C267 – 01. (2001). Standard Test Methods for Chemical Resistance of Mortars, Grouts, and Monolithic Surfacings and Polymer Concretes. *ASTM International, West Conshohocken, PA*.

ASTM C469/C469M−14. (2014). Standard Test Method for Static Modulus of Elasticity and Poisson's Ratio of Concrete in Compression. *ASTM International, West Conshohocken, PA*.

ASTM C494/C494M−15. (2015). Standard Specification for Chemical Admixtures for Concrete. *ASTM International, West Conshohocken, PA*.

ASTM C496/C496M−11. (2011). Standard Test Method for Splitting Tensile Strength of Cylindrical Concrete Specimens. *ASTM International, West Conshohocken, PA*.

ASTM C597−09. (2009). Standard test method for pulse velocity through concrete. *ASTM International, West Conshohocken, PA*.

ASTM C618−12a. (2012). Standard Specification for Coal Fly Ash and Raw or Calcined Natural Pozzolan for Use in Concrete. *ASTM International, West Conshohocken, PA*.

ASTM C1012/C1012M−13. (2013). Standard Test Method for Length Change of Hydraulic-Cement Mortars Exposed to a Sulfate Solution. *ASTM International, West Conshohocken, PA*.

ASTM C1760. (2012). Standard Test Method for Bulk Electrical Conductivity of Hardened Concrete. *ASTM International, West Conshohocken, PA*.

Bamaga, S., Hussin, M. W., & Ismail, M. A. (2013). Palm oil fuel ash: promising supplementary cementing materials. *KSCE Journal of Civil Engineering, 17*(7), 1708-1713.

Baroghel-Bouny, V., Kinomura, K., Thiery, M., & Moscardelli, S. (2011). Easy assessment of durability indicators for service life prediction or quality control of concretes with high volumes of supplementary cementitious materials. *Cement and Concrete Composites, 33*(8), 832-847.

Bassuoni, M., & Nehdi, M. (2007). Resistance of self-consolidating concrete to sulfuric acid attack with consecutive pH reduction. *Cement and Concrete Research, 37*(7), 1070-1084.

Beddoe, R. E. (2016). Modelling acid attack on concrete: Part II. A computer model. *Cement and Concrete Research, 88*, 20-35.

Beddoe, R. E., & Dorner, H. W. (2005). Modelling acid attack on concrete: Part I. The essential mechanisms. *Cement and Concrete Research, 35*(12), 2333-2339.

Begum, R. A., Siwar, C., Pereira, J. J., & Jaafar, A. H. (2006). A benefit–cost analysis on the economic feasibility of construction waste minimisation: the case of Malaysia. *Resources, Conservation and Recycling, 48*(1), 86-98.

Behera, M., Bhattacharyya, S., Minocha, A., Deoliya, R., & Maiti, S. (2014). Recycled aggregate from C&D waste & its use in concrete–A breakthrough towards sustainability in construction sector: A review. *Construction and Building materials, 68*, 501-516.

Benhelal, E., Zahedi, G., Shamsaei, E., & Bahadori, A. (2013). Global strategies and potentials to curb CO 2 emissions in cement industry. *Journal of Cleaner Production, 51*, 142-161.

Bizzozero, J., Gosselin, C., & Scrivener, K. L. (2014). Expansion mechanisms in calcium aluminate and sulfoaluminate systems with calcium sulfate. *Cement and Concrete Research, 56*, 190-202.

Brundtland, G. H. (1985). World commission on environment and development. *Environmental policy and law, 14*(1), 26-30.

BS EN 206-1:2000. (2000). Concrete – Specification, performance, production and conformity. *BSI Standard Publications, London, UK,*.

BS EN 12390-2. (2009). Testing hardened concrete. Making and curing specimens for strength tests. *BSI Standard Publications, London, UK,*.

Çakır, Ö. (2014). Experimental analysis of properties of recycled coarse aggregate (RCA) concrete with mineral additives. *Construction and Building materials, 68*, 17-25.

Cao, Z., Shen, L., Zhao, J., Liu, L., Zhong, S., Sun, Y., & Yang, Y. (2016). Toward a better practice for estimating the CO 2 emission factors of cement production: An experience from China. *Journal of Cleaner Production, 139*, 527-539.

Celik, K., Meral, C., Gursel, A. P., Mehta, P. K., Horvath, A., & Monteiro, P. J. (2015). Mechanical properties, durability, and life-cycle assessment of self-consolidating concrete mixtures made with blended portland cements containing fly ash and limestone powder. *Cement and Concrete Composites, 56*, 59-72.

Chao-Lung, H., Le Anh-Tuan, B., & Chun-Tsun, C. (2011). Effect of rice husk ash on the strength and durability characteristics of concrete. *Construction and Building materials, 25*(9), 3768-3772.

Chatveera, B., & Lertwattanaruk, P. (2011). Durability of conventional concretes containing black rice husk ash. *Journal of environmental management, 92*(1), 59-66.

Chatveera, B., & Lertwattanaruk, P. (2014). Evaluation of nitric and acetic acid resistance of cement mortars containing high-volume black rice husk ash. *Journal of environmental management, 133*, 365-373.

Chen, G., He, Y., Yang, H., Chen, J., & Guo, Y. (2014). Compressive behavior of steel fiber reinforced recycled aggregate concrete after exposure to elevated temperatures. *Construction and Building materials, 71*, 1-15.

Chindaprasirt, P., Kanchanda, P., Sathonsaowaphak, A., & Cao, H. (2007). Sulfate resistance of blended cements containing fly ash and rice husk ash. *Construction and Building materials, 21*(6), 1356-1361.

Collins, F. (2010). Inclusion of carbonation during the life cycle of built and recycled concrete: influence on their carbon footprint. *The International Journal of Life Cycle Assessment, 15*(6), 549-556.

Cordeiro, G. C., Toledo Filho, R. D., & Fairbairn, E. d. M. R. (2009). Use of ultrafine rice husk ash with high-carbon content as pozzolan in high performance concrete. *Materials and structures, 42*(7), 983-992.

Corinaldesi, V., & Moriconi, G. (2009). Influence of mineral additions on the performance of 100% recycled aggregate concrete. *Construction and Building materials, 23*(8), 2869-2876.

Cultrone, G., Sebastian, E., & Huertas, M. O. (2005). Forced and natural carbonation of lime-based mortars with and without additives: Mineralogical and textural changes. *Cement and Concrete Research, 35*(12), 2278-2289.

Damtoft, J., Lukasik, J., Herfort, D., Sorrentino, D., & Gartner, E. (2008). Sustainable development and climate change initiatives. *Cement and Concrete Research, 38*(2), 115-127.

De Brito, J., & Saikia, N. (2013). Recycled aggregate in concrete, green energy and technology. *Springer-Verlag London DOI, 10*, 978-971.

De Juan, M. S., & Gutiérrez, P. A. (2009). Study on the influence of attached mortar content on the properties of recycled concrete aggregate. *Construction and Building materials, 23*(2), 872-877.

Debieb, F., Courard, L., Kenai, S., & Degeimbre, R. (2010). Mechanical and durability properties of concrete using contaminated recycled aggregates. *Cement and Concrete Composites, 32*(6), 421-426.

DECC. 2011. Guidelines to Defra/DECC's GHG Conversion Factors for Company Reporting. Department for Environment, Food and Rural Affairs and Department for Energy and Climate Change, Defra London.

Delhomme, F., Ambroise, J., & Limam, A. (2012). Effects of high temperatures on mortar specimens containing Portland cement and GGBFS. *Materials and structures, 45*(11), 1685-1692.

Department of the Environment. (1997). Design of normal concrete mixes. *Building Research Establishment, Watford, U.K.*

Dhir, R., Limbachiya, M., & Leelawat, T. (1999). Suitability of recycled concrete aggregate for use in BS 5328 designated mixes. *Proceedings of the Institution of Civil Engineers. Structures and buildings, 134*(3), 257-274.

Dilbas, H., Şimşek, M., & Çakır, Ö. (2014). An investigation on mechanical and physical properties of recycled aggregate concrete (RAC) with and without silica fume. *Construction and Building materials, 61*, 50-59.

Donatello, S., Palomo, A., & Fernández-Jiménez, A. (2013). Durability of very high volume fly ash cement pastes and mortars in aggressive solutions. *Cement and Concrete Composites, 38*, 12-20.

Etxeberria, M., Vázquez, E., Marí, A., & Barra, M. (2007). Influence of amount of recycled coarse aggregates and production process on properties of recycled aggregate concrete. *Cement and Concrete Research, 37*(5), 735-742.

FAOSTAT. (2012). Food and Agriculture Organization of the United Nations Statistic Division (FAOSTAT) Domains e Crops: Rice paddy, Production Quantity, World Total.

Flower, D. J., & Sanjayan, J. G. (2007). Green house gas emissions due to concrete manufacture. *The international Journal of life cycle assessment, 12*(5), 282-288.

Fonseca, N., De Brito, J., & Evangelista, L. (2011). The influence of curing conditions on the mechanical performance of concrete made with recycled concrete waste. *Cement and Concrete Composites, 33*(6), 637-643.

García-Segura, T., Yepes, V., & Alcalá, J. (2014). Life cycle greenhouse gas emissions of blended cement concrete including carbonation and durability. *The International Journal of Life Cycle Assessment, 19*(1), 3-12.

Givi, A. N., Rashid, S. A., Aziz, F. N. A., & Salleh, M. A. M. (2010). Assessment of the effects of rice husk ash particle size on strength, water permeability and workability of binary blended concrete. *Construction and Building materials, 24*(11), 2145-2150.

Guo, Y.-c., Zhang, J.-h., Chen, G.-m., & Xie, Z.-h. (2014). Compressive behaviour of concrete structures incorporating recycled concrete aggregates, rubber crumb and reinforced with steel fibre, subjected to elevated temperatures. *Journal of Cleaner Production, 72*, 193-203.

Gursel, A. P., Maryman, H., & Ostertag, C. (2016). A life-cycle approach to environmental, mechanical, and durability properties of "green" concrete mixes with rice husk ash. *Journal of Cleaner Production, 112*, 823-836.

Gutberlet, T., Hilbig, H., & Beddoe, R. (2015). Acid attack on hydrated cement—Effect of mineral acids on the degradation process. *Cement and Concrete Research, 74*, 35-43.

Hall, C. (1989). Water sorptivity of mortars and concretes: a review. *Magazine of concrete research, 41*(147), 51-61.

Hanif, A., Kim, Y., Lu, Z., & Park, C. (2017). Early-age behavior of recycled aggregate concrete under steam curing regime. *Journal of Cleaner Production, 152*, 103-114.

Hassan, M., Yusoff, M., Sulaiman, W., & Rahman, R. A. (1998). Issues and problems of solid waste management in Malaysia. *Proceedings on national review on environmental quality management in Malaysia: towards the nest two decades*.

Heikal, M., Radwan, M., & Al-Duaij, O. (2015). Physico-mechanical characteristics and durability of calcium aluminate blended cement subject to different aggressive media. *Construction and Building materials, 78*, 379-385.

Hornbostel, K., Larsen, C. K., & Geiker, M. R. (2013). Relationship between concrete resistivity and corrosion rate–A literature review. *Cement and Concrete Composites, 39*, 60-72.

Hwang, J. P., Shim, H. B., Lim, S., & Ann, K. Y. (2013). Enhancing the durability properties of concrete containing recycled aggregate by the use of pozzolanic materials. *KSCE Journal of Civil Engineering, 17*(1), 155-163.

Islam, A., Alengaram, U. J., Jumaat, M. Z., & Bashar, I. I. (2014). The development of compressive strength of ground granulated blast furnace slag-palm oil fuel ash-fly ash based geopolymer mortar. *Materials & Design, 56*, 833-841.

Islam, M. M. U., Mo, K. H., Alengaram, U. J., & Jumaat, M. Z. (2016a). Durability properties of sustainable concrete containing high volume palm oil waste materials. *Journal of Cleaner Production, 137*, 167-177.

Islam, M. M. U., Mo, K. H., Alengaram, U. J., & Jumaat, M. Z. (2016b). Mechanical and fresh properties of sustainable oil palm shell lightweight concrete incorporating palm oil fuel ash. *Journal of Cleaner Production, 115*, 307-314.

Jain, N., Garg, M., & Minocha, A. (2015). Green Concrete from Sustainable Recycled Coarse Aggregates: Mechanical and Durability Properties. *Journal of Waste Management, 2015*.

Jaturapitakkul, C., Tangpagasit, J., Songmue, S., & Kiattikomol, K. (2011). Filler effect and pozzolanic reaction of ground palm oil fuel ash. *Construction and Building materials, 25*(11), 4287-4293.

Jo, B. W., Sikandar, M. A., Chakraborty, S., & Baloch, Z. (2017). Investigation of the acid and sulfate resistance performances of hydrogen-rich water based mortars. *Construction and Building materials, 137*, 1-11.

Johari, M. M., Zeyad, A., Bunnori, N. M., & Ariffin, K. (2012). Engineering and transport properties of high-strength green concrete containing high volume of ultrafine palm oil fuel ash. *Construction and Building materials, 30*, 281-288.

Juenger, M. C., & Siddique, R. (2015). Recent advances in understanding the role of supplementary cementitious materials in concrete. *Cement and Concrete Research, 78*, 71-80.

Kanadasan, J., & Abdul Razak, H. (2015). Utilization of palm oil clinker as cement replacement material. *Materials, 8*(12), 8817-8838.

Kanadasan, J., & Razak, H. A. (2015). Engineering and sustainability performance of self-compacting palm oil mill incinerated waste concrete. *Journal of Cleaner Production, 89*, 78-86.

Kannan, V., & Ganesan, K. (2014). Chloride and chemical resistance of self compacting concrete containing rice husk ash and metakaolin. *Construction and Building materials, 51*, 225-234.

Karim, M. R., Hashim, H., & Razak, H. A. (2016). Assessment of pozzolanic activity of palm oil clinker powder. *Construction and Building materials, 127*, 335-343.

Khalaf, F. M., & DeVenny, A. S. (2004). Recycling of demolished masonry rubble as coarse aggregate in concrete: review. *Journal of materials in civil engineering, 16*(4), 331-340.

Kou, S. C., & Poon, C. (2012). Enhancing the durability properties of concrete prepared with coarse recycled aggregate. *Construction and Building materials, 35*, 69-76.

Kou, S. C., & Poon, C. S. (2013). Long-term mechanical and durability properties of recycled aggregate concrete prepared with the incorporation of fly ash. *Cement and Concrete Composites, 37*, 12-19.

Kou, S. C., & Poon, C. S. (2015). Effect of the quality of parent concrete on the properties of high performance recycled aggregate concrete. *Construction and Building materials, 77*, 501-508.

Kou, S. C., Poon, C. S., & Agrela, F. (2011). Comparisons of natural and recycled aggregate concretes prepared with the addition of different mineral admixtures. *Cement and Concrete Composites, 33*(8), 788-795.

Kruse, K. A. (2012). *Characterization of high-calcium fly ash for evaluating the sulfate resistance of concrete.* (MSc thesis), The University of Texas at Austin.

Kutchko, B. G., Strazisar, B. R., Hawthorne, S. B., Lopano, C. L., Miller, D. J., Hakala, J. A., & Guthrie, G. D. (2011). H 2 S–CO 2 reaction with hydrated Class H well cement: Acid-gas injection and CO 2 Co-sequestration. *International Journal of Greenhouse Gas Control, 5*(4), 880-888.

Kwan, W. H., Ramli, M., Kam, K. J., & Sulieman, M. Z. (2012). Influence of the amount of recycled coarse aggregate in concrete design and durability properties. *Construction and Building materials, 26*(1), 565-573.

Li, L., Poon, C. S., Xiao, J., & Xuan, D. (2017). Effect of carbonated recycled coarse aggregate on the dynamic compressive behavior of recycled aggregate concrete. *Construction and Building materials, 151*, 52-62.

Li, X., Zhang, Y., Shen, X., Wang, Q., & Pan, Z. (2014). Kinetics of calcium sulfoaluminate formation from tricalcium aluminate, calcium sulfate and calcium oxide. *Cement and Concrete Research, 55*, 79-87.

Lima, C., Caggiano, A., Faella, C., Martinelli, E., Pepe, M., & Realfonzo, R. (2013). Physical properties and mechanical behaviour of concrete made with recycled aggregates and fly ash. *Construction and Building materials, 47*, 547-559.

Limbachiya, M., Meddah, M. S., & Ouchagour, Y. (2012). Use of recycled concrete aggregate in fly-ash concrete. *Construction and Building materials, 27*(1), 439-449.

López-Gayarre, F., Serna, P., Domingo-Cabo, A., Serrano-López, M., & López-Colina, C. (2009). Influence of recycled aggregate quality and proportioning criteria on recycled concrete properties. *Waste management, 29*(12), 3022-3028.

Lothenbach, B., Scrivener, K., & Hooton, R. (2011). Supplementary cementitious materials. *Cement and Concrete Research, 41*(12), 1244-1256.

Ma, Q., Guo, R., Zhao, Z., Lin, Z., & He, K. (2015). Mechanical properties of concrete at high temperature—a review. *Construction and Building materials, 93*, 371-383.

Mahayuddin, S., Pereira, J. J., Badaruzzaman, W. H. W., & Mokhtar, M. (2008). Construction waste management in a developing country: case study of Ipoh, Malaysia. *WIT Transactions on Ecology and the Environment, 109*.

Malešev, M., Radonjanin, V., & Marinković, S. (2010). Recycled concrete as aggregate for structural concrete production. *Sustainability, 2*(5), 1204-1225.

Matias, D., De Brito, J., Rosa, A., & Pedro, D. (2013). Mechanical properties of concrete produced with recycled coarse aggregates–Influence of the use of superplasticizers. *Construction and Building materials, 44*, 101-109.

McNeil, K., & Kang, T. H.-K. (2013). Recycled concrete aggregates: A review. *International Journal of Concrete Structures and Materials, 7*(1), 61-69.

Meyer, C. (2009). The greening of the concrete industry. *Cement and Concrete Composites, 31*(8), 601-605.

Mo, K. H., Alengaram, U. J., Jumaat, M. Z., Liu, M. Y. J., & Lim, J. (2016). Assessing some durability properties of sustainable lightweight oil palm shell concrete incorporating slag and manufactured sand. *Journal of Cleaner Production, 112*, 763-770.

Mo, K. H., Ling, T.-C., Alengaram, U. J., Yap, S. P., & Yuen, C. W. (2017). Overview of supplementary cementitious materials usage in lightweight aggregate concrete. *Construction and Building materials, 139*, 403-418.

Mohammadhosseini, H., Yatim, J. M., Sam, A. R. M., & Awal, A. A. (2016). Durability performance of green concrete composites containing waste carpet fibers and palm oil fuel ash. *Journal of Cleaner Production*.

Mohammed, M., Salmiaton, A., Azlina, W. W., Amran, M. M., Fakhru'l-Razi, A., & Taufiq-Yap, Y. (2011). Hydrogen rich gas from oil palm biomass as a potential source of renewable energy in Malaysia. *Renewable and Sustainable Energy Reviews, 15*(2), 1258-1270.

Mujah, D. (2016). Compressive strength and chloride resistance of grout containing ground palm oil fuel ash. *Journal of Cleaner Production, 112*, 712-722.

Müllauer, W., Beddoe, R. E., & Heinz, D. (2013). Sulfate attack expansion mechanisms. *Cement and Concrete Research, 52*, 208-215.

Nagaratnam, B. H., Rahman, M. E., Mirasa, A. K., Mannan, M. A., & Lame, S. O. (2016). Workability and heat of hydration of self-compacting concrete incorporating agro-industrial waste. *Journal of Cleaner Production, 112*, 882-894.

Nuaklong, P., Sata, V., & Chindaprasirt, P. (2016). Influence of recycled aggregate on fly ash geopolymer concrete properties. *Journal of Cleaner Production, 112*, 2300-2307.

Pacheco-Torgal, F., Castro-Gomes, J., & Jalali, S. (2008). Alkali-activated binders: A review: Part 1. Historical background, terminology, reaction mechanisms and hydration products. *Construction and Building materials, 22*(7), 1305-1314.

Padmini, A., Ramamurthy, K., & Mathews, M. (2009). Influence of parent concrete on the properties of recycled aggregate concrete. *Construction and Building materials, 23*(2), 829-836.

Poon, C., Shui, Z., Lam, L., Fok, H., & Kou, S. (2004a). Influence of moisture states of natural and recycled aggregates on the slump and compressive strength of concrete. *Cement and Concrete Research, 34*(1), 31-36.

Poon, C. S., Shui, Z., & Lam, L. (2004b). Effect of microstructure of ITZ on compressive strength of concrete prepared with recycled aggregates. *Construction and Building materials, 18*(6), 461-468.

Ranjbar, N., Behnia, A., Alsubari, B., Birgani, P. M., & Jumaat, M. Z. (2016). Durability and mechanical properties of self-compacting concrete incorporating palm oil fuel ash. *Journal of Cleaner Production, 112*, 723-730.

Rao, M. C., Bhattacharyya, S., & Barai, S. (2011). Influence of field recycled coarse aggregate on properties of concrete. *Materials and structures, 44*(1), 205-220.

Rashad, A. M. (2015). An investigation of high-volume fly ash concrete blended with slag subjected to elevated temperatures. *Journal of Cleaner Production, 93*, 47-55.

RILEM. (1995). Test Methods for Mechanical Properties of Concrete at High Temperatures. *Materials and structures, 28*, 410-414.

Rozainee, M., Ngo, S., Salema, A. A., & Tan, K. (2008). Fluidized bed combustion of rice husk to produce amorphous siliceous ash. *Energy for Sustainable Development, 12*(1), 33-42.

Rukzon, S., Chindaprasirt, P., & Mahachai, R. (2009). Effect of grinding on chemical and physical properties of rice husk ash. *International Journal of Minerals, Metallurgy and Materials, 16*(2), 242-247.

Sabet, F. A., Libre, N. A., & Shekarchi, M. (2013). Mechanical and durability properties of self consolidating high performance concrete incorporating natural zeolite, silica fume and fly ash. *Construction and Building materials, 44*, 175-184.

Sadati, S., Arezoumandi, M., Khayat, K. H., & Volz, J. S. (2016). Shear performance of reinforced concrete beams incorporating recycled concrete aggregate and high-volume fly ash. *Journal of Cleaner Production, 115*, 284-293.

Safiuddin, M., Alengaram, U. J., Rahman, M. M., Salam, M. A., & Jumaat, M. Z. (2013). Use of recycled concrete aggregate in concrete: A review. *Journal of Civil Engineering and Management, 19*(6), 796-810.

Safiuddin, M., Alengaram, U. J., Salam, A., Jumaat, M. Z., Jaafar, F. F., & Saad, H. B. (2011). Properties of high-workability concrete with recycled concrete aggregate. *Materials Research, 14*(2), 248-255.

Sagoe-Crentsil, K. K., Brown, T., & Taylor, A. H. (2001). Performance of concrete made with commercially produced coarse recycled concrete aggregate. *Cement and Concrete Research, 31*(5), 707-712.

Saint-Pierre, F., Philibert, A., Giroux, B., & Rivard, P. (2016). Concrete Quality Designation based on Ultrasonic Pulse Velocity. *Construction and Building materials, 125*, 1022-1027.

Sata, V., Jaturapitakkul, C., & Kiattikomol, K. (2004). Utilization of palm oil fuel ash in high-strength concrete. *Journal of Materials in Civil Engineering, 16*(6), 623-628.

Sata, V., Jaturapitakkul, C., & Kiattikomol, K. (2007). Influence of pozzolan from various by-product materials on mechanical properties of high-strength concrete. *Construction and Building materials, 21*(7), 1589-1598.

Seara-Paz, S., González-Fonteboa, B., Eiras-López, J., & Herrador, M. F. (2014). Bond behavior between steel reinforcement and recycled concrete. *Materials and structures, 47*(1-2), 323-334.

Shafigh, P., Nomeli, M. A., Alengaram, U. J., Mahmud, H. B., & Jumaat, M. Z. (2016). Engineering properties of lightweight aggregate concrete containing limestone powder and high volume fly ash. *Journal of Cleaner Production, 135*, 148-157.

Sheen, Y. N., Wang, H. Y., Juang, Y. P., & Le, D. H. (2013). Assessment on the engineering properties of ready-mixed concrete using recycled aggregates. *Construction and Building materials, 45*, 298-305.

Shi, C., Jiménez, A. F., & Palomo, A. (2011). New cements for the 21st century: the pursuit of an alternative to Portland cement. *Cement and Concrete Research, 41*(7), 750-763.

Shi, C., Li, Y., Zhang, J., Li, W., Chong, L., & Xie, Z. (2016). Performance enhancement of recycled concrete aggregate–a review. *Journal of Cleaner Production, 112*, 466-472.

Shi, X., Xie, N., Fortune, K., & Gong, J. (2012). Durability of steel reinforced concrete in chloride environments: An overview. *Construction and Building materials, 30*, 125-138.

Silva, R. V., de Brito, J., & Dhir, R. K. (2016). Establishing a relationship between modulus of elasticity and compressive strength of recycled aggregate concrete. *Journal of Cleaner Production, 112*, 2171-2186.

Siwar, C. (2008). *Solid waste management: recycling, green jobs and challenges in Malaysia.* Paper presented at the ILO Research Conference on Green Jobs for Asia & Pacific, Nigata, Japan.

Snellings, R., Mertens, G., & Elsen, J. (2012). Supplementary cementitious materials. *Reviews in Mineralogy and Geochemistry, 74*(1), 211-278.

Somna, R., Jaturapitakkul, C., & Amde, A. M. (2012). Effect of ground fly ash and ground bagasse ash on the durability of recycled aggregate concrete. *Cement and Concrete Composites, 34*(7), 848-854.

Tabsh, S. W., & Abdelfatah, A. S. (2009). Influence of recycled concrete aggregates on strength properties of concrete. *Construction and Building materials, 23*(2), 1163-1167.

Tangchirapat, W., Buranasing, R., Jaturapitakkul, C., & Chindaprasirt, P. (2008). Influence of rice husk–bark ash on mechanical properties of concrete containing high amount of recycled aggregates. *Construction and Building materials, 22*(8), 1812-1819.

Tangchirapat, W., Jaturapitakkul, C., & Chindaprasirt, P. (2009). Use of palm oil fuel ash as a supplementary cementitious material for producing high-strength concrete. *Construction and Building materials, 23*(7), 2641-2646.

Tangchirapat, W., Khamklai, S., & Jaturapitakkul, C. (2012). Use of ground palm oil fuel ash to improve strength, sulfate resistance, and water permeability of concrete containing high amount of recycled concrete aggregates. *Materials & Design, 41*, 150-157.

Thomas, C., Setién, J., Polanco, J., Alaejos, P., & De Juan, M. S. (2013). Durability of recycled aggregate concrete. *Construction and Building materials, 40*, 1054-1065.

Trtnik, G., Kavčič, F., & Turk, G. (2009). Prediction of concrete strength using ultrasonic pulse velocity and artificial neural networks. *Ultrasonics, 49*(1), 53-60.

USDA. (2014). Census of Agriculture: United States Summary and State Data. Volume 1, Geographic Area Series, Part 51.

Wang, X., Yang, Z., Yates, J., Jivkov, A., & Zhang, C. (2015). Monte Carlo simulations of mesoscale fracture modelling of concrete with random aggregates and pores. *Construction and Building materials, 75*, 35-45.

Wong, H., Zhao, Y., Karimi, A., Buenfeld, N., & Jin, W. (2010). On the penetration of corrosion products from reinforcing steel into concrete due to chloride-induced corrosion. *Corrosion Science, 52*(7), 2469-2480.

Xiao, J.-Z., Li, J.-B., & Zhang, C. (2006). On relationships between the mechanical properties of recycled aggregate concrete: an overview. *Materials and structures, 39*(6), 655-664.

Yehia, S., Helal, K., Abusharkh, A., Zaher, A., & Istaitiyeh, H. (2015). Strength and durability evaluation of recycled aggregate concrete. *International Journal of Concrete Structures and Materials, 9*(2), 219-239.

Yuan, H., Dangla, P., Chatellier, P., & Chaussadent, T. (2013). Degradation modelling of concrete submitted to sulfuric acid attack. *Cement and Concrete Research, 53*, 267-277.

Yuan, H., & Shen, L. (2011). Trend of the research on construction and demolition waste management. *Waste management, 31*(4), 670-679.

Yusoff, S. (2006). Renewable energy from palm oil–innovation on effective utilization of waste. *Journal of Cleaner Production, 14*(1), 87-93.

LIST OF PUBLICATIONS AND PAPERS PRESENTED

The following publications will cover the objectives of this research

Alnahhal, M. F., Alengaram, U. J., Jumaat, M. Z., Alqedra, M. A., Mo, K. H., & Sumesh, M. (2017). Evaluation of Industrial By-Products as Sustainable Pozzolanic Materials in Recycled Aggregate Concrete. *Sustainability*, 9(5), 767. ***(Published)***

Alnahhal, M. F., Alengaram, U. J., Jumaat, M. Z., Alsubari, B., Alqedra, M. A., Mo, K. H. (2017). Effect of aggressive chemicals on durability and microstructure properties of recycled aggregate concrete containing non-traditional supplementary cementitious materials. *Construction and Building Materials*. ***(Reviewed with minor correction)***

Alnahhal, M. F., Alengaram, U. J., Jumaat, M. Z. (2017). Comparison of performance and CO_2 emissions of recycled aggregate concrete incorporating waste products as supplements to Portland cement. *Journal of Cleaner Production*. ***(Comments received)***